

Old Dominion University

ODU Digital Commons

Mechanical & Aerospace Engineering Theses & Dissertations

Mechanical & Aerospace Engineering

Spring 1997

Input Design for Systems Under Identification Using Indirect and Direct Methods

Marco P. Schoen
Old Dominion University

Follow this and additional works at: https://digitalcommons.odu.edu/mae_etds



Part of the [Mechanical Engineering Commons](#), [Structures and Materials Commons](#), and the [Systems Engineering and Multidisciplinary Design Optimization Commons](#)

Recommended Citation

Schoen, Marco P. "Input Design for Systems Under Identification Using Indirect and Direct Methods" (1997). Doctor of Philosophy (PhD), Dissertation, Mechanical & Aerospace Engineering, Old Dominion University, DOI: 10.25777/x66b-sj35
https://digitalcommons.odu.edu/mae_etds/191

This Dissertation is brought to you for free and open access by the Mechanical & Aerospace Engineering at ODU Digital Commons. It has been accepted for inclusion in Mechanical & Aerospace Engineering Theses & Dissertations by an authorized administrator of ODU Digital Commons. For more information, please contact digitalcommons@odu.edu.

INPUT DESIGN FOR SYSTEMS UNDER IDENTIFICATION USING INDIRECT AND DIRECT METHODS

by

Marco P. Schoen
M.E. May 1993, Widener University
B.Sc. November 1989, Swiss College of Engineering

A Dissertation submitted to the Faculty of Old Dominion University in Partial Fulfillment
of the Requirement for the Degree of

**DOCTOR OF PHILOSOPHY
ENGINEERING MECHANICS**

Old Dominion University
May 1997

Approved by:

Jen-Kuang Huang (Director)

Sebastian Bawah (Member)

David Cox (Member)

Gene Hou (Member)

ABSTRACT

INPUT DESIGN FOR SYSTEMS UNDER IDENTIFICATION, USING INDIRECT AND DIRECT METHODS

Marco P. Schoen
Old Dominion University, 1997
Director: Dr. Jen-Kuang Huang

The motivation for system identification can be manifold. In this work, the provocation to identify unknown system characteristics is derived from the control engineering point of view. That is, one intends to design a control strategy based on the identified system properties. The used system identification methods are the Open-Loop Kalman filter System Identification method (OKID) and the Closed-Loop System Identification method (CLID). It is shown that the quantitative largest error of the system identification is given by its model representation, that is the attempt to describe a system with model parameters which poses a linear relationship with the input/output data. Parameter identifiability is reduced to the problem of consistent estimation. The identifiability is largely determined by the way the system is excited, and in addition by the output of the system for the indirect system identification. A quantitative comparison between the indirect and direct system identification method is given, where indirect system identification showed to be slightly superior in accuracy if a suitable controller is selected. The example models used in the comparison are a heat-mass transfer model, a macro economical model, a structural model, NASA's Large-Angle Magnetic Suspension Test Facility (LAMSTF), and a human respiratory system. The problem of defining the input data such that accuracy and identifiability are increased is addressed and controller design criteria can be developed from it. The excitation input is calculated from input/output data and substituted into the current input. Simulation indicate that only a few substitution are necessary to successfully identify the system. The new input design results in very accurate identification with reduced noise influence and data length requirement. Controller design criteria can be formed based on the input design, such that identification leads to more accurate and more reliable results.

To
Herbert Schoen

ACKNOWLEDGEMENTS

I would like to express my sincerest gratitude to my advisor, Dr. Jen-Kuang Huang for his thoughtful guidance, care and motivation. The members of my doctoral committee, Dr. Sebastian Bawab, Dr. Gene Hou and Mr. David Cox are especially appreciated for all the help they gave me.

This dissertation will not be possible without my parent's love, understanding and support. I would also like to thank my wife, Renata, for her constant love, patience and encouragement. A special thanks to my siblings Gerhard and Claudia for their sincere care and advice.

This work was supported partially by NASA Langley Research Center (NAS1-19858, No. 30). This support is gratefully acknowledged.

TABLE OF CONTENTS

	Page
ACKNOWLEDGMENT	v
LIST OF TABLES	x
LIST OF FIGURES	x
LIST OF SYMBOLS	xiv
 CHAPTER	
I. INTRODUCTION	1
1.1 Background and Problem Statement.	1
1.2 Objective	2
1.3 Dissertation Outline	3
II. EXAMPLE SYSTEMS UNDER IDENTIFICATION	5
2.1 Introduction	5
2.2 Chemical Processing Systems	5
2.2.1 Distillation Process	6
2.2.2 Williams-Otto Process	
a fourth Order Time Delay System	6
2.3 Heat and Mass Transfer based Systems	8
2.3.1 Lyophilization Process	9
2.3.2 Mathematical Model of the Primary Stage of	
a Lyophilization Process	10
2.4 Structural Systems	11
2.4.1 Beam-Like Structure	12
2.5 Large-Gap Magnetic Suspension System	13
2.5.1 System Specifications	14
2.5.2 System Model	15
2.6 Biomedical Systems	16
2.6.1 Respiratory System: CO ₂ Concentration	18
2.6.2 Controlled System	19

	Page
2.6.3 The Controlling System	22
2.6.4 Closed-Loop System	22
2.6.5 Linearized Model and State-Space Representation	23
2.7 Econometric Systems	24
2.7.1 Investment Mechanism Model	24
2.7.2 Deterministic fourth order macro economic model	27
III. SYSTEM IDENTIFICATION METHODS AND ALGORITHMS	29
3.1 Introduction	29
3.2 Model Structures	31
3.2.1 AR-Model	32
3.2.2 ARX-Model	32
3.2.3 MA-Model	33
3.2.4 ARMA and ARMAX-Models	33
3.3 Parameter Estimation	33
3.3.1 Least-Squares Method	34
3.3.2 Recursive Least-Squares Method	35
3.3.3 Maximum Likelihood Method	35
3.3.4 Comparison and Applicability of Parameter Estimators	36
3.4 Direct System Identification	37
3.4.1 Calculation of Observer and System Markov Parameters	38
3.4.2 Eigensystem Realization	40
3.4.3 Step-by-Step Procedure for System Identification using OKID	41
3.5 Indirect System Identification	41
3.5.1 Relationship between the State-Space and ARX Models	42
3.5.2 Open and Closed-Loop System and Kalman Filter Markov Parameters	44

	Page
3.5.3 Step-by-Step Procedure for System Identification with Output Feedback	47
3.5.4 Closed-Loop Identification with Full-State Feedback	47
3.6 Coordinate Transformation	48
IV. ACCURACY MEASURES OF SYSTEM IDENTIFICATION PROCESSES	51
4.1 Introduction	51
4.2 ARX Model Representation	51
4.3 Error Development during the System Identification Process	56
4.3.1 Closed-Loop Markov Parameters	57
4.3.2 Open-Loop Markov Parameters	59
4.4 Accuracy of the ARX Parameterization	60
4.4.1 Output Description	61
4.4.2 Quantification of the Truncation Error of the ARX Model	62
4.5 Influence of the Process Noise to the System Identification	63
V. A NOTE ON IDENTIFIABILITY	72
5.1 Introduction	72
5.2 System Identifiability	73
5.3 Parameter Identifiability	74
5.3.1 Canonical Forms and Identifiability	75
5.3.2 Process Identification of Linear Time Invariant Deterministic Systems, with Single Output: the Role of the Initial Condition	75
5.3.3 Identifiability of the ARX Model Coefficients	78
5.3.4 Experimental Condition for Identifiability	81
5.4 Numerical Example	86
VI. COMPARISON BETWEEN DIRECT AND INDIRECT SYSTEM IDENTIFICATION	91
6.1 Introduction	91

	Page
6.2 Identification with Constant Reference Input	91
6.3 Loss of Identifiability due to Feedback	94
6.4 Data Length Comparison for different Systems	95
VII. INPUT DESIGN FOR SYSTEMS UNDER IDENTIFICATION	113
7.1 Introduction	113
7.2 Input Design for ARX Model Representation	113
7.3 Feedback Controller Design for System under Identification	119
VIII. CONCLUSIONS	131
8.1 Contributions	131
8.2 Further Extension of Research	133
BIBLIOGRAPHY	134
APPENDIX	141

LIST OF TABLES

	Page
Table 2.1 Human Respiratory System Description	21
Table 3.1 Nonparametric Identification Methods	30
Table 4.1 Error Percentage of the Closed-Loop System Markov Parameters	59
Table 4.2 Error Percentage of the Open-Loop System Markov Parameters	60
Table 4.3 Correlation Coefficient for the Outputs	61
Table 5.1 System Characteristics with and without Controller	86

LIST OF FIGURES

	Page
Figure 2.1 Wiliams-Otto Process	7
Figure 2.2 The simulated lumped-mass beam like structure	12
Figure 2.3 The six DOF Magnetic Suspension System Configuration	14
Figure 2.4 Simplified model of CO ₂ concentration on ventilation	19
Figure 2.5 Closed Loop Chemostat	22
Figure 2.6 Macro Economic System	26
Figure 2.7 Theoretical ventilation transient for nonlinear system	28
Figure 2.8 Theoretical ventilation transient for linearized system	28
Figure 4.1 Identification schematic	56
Figure 4.2 Closed-Loop Markov Parameters	58
Figure 4.3 Contour plot of the percentage of error deviation of the system Markov Parameters for a variable ARX model order and noise level, using 5000 data points	66
Figure 4.4 Contour plot of the percentage of error deviation of the system Markov Parameters for a variable ARX model order and noise level, using 5000 data points	66

Figure 4.5 Contour plot of the error percentage of the system Markov parameters for a variable data length and noise level, using an ARX model order of 14	67
Figure 4.6 Contour plot of the error percentage of the system Markov parameters for a variable data length and noise level, using an ARX model order of 14	67
Figure 4.7 Closed-loop system Markov parameters, (1,1) element, using the LAMSTF 6 d.o.f. system and 5% measurement and process noise (variance)	68
Figure 4.8 Open-loop system Markov parameters, (1,1) element, using the LAMSTF 6 d.o.f. system and 5% measurement and process noise (variance)	68
Figure 4.9 Coherence Function Estimate for y_{arx} , y_{arx_id} , y_{an} , using the LAMSTF 6 d.o.f. system and 5% measurement and process noise (variance)	69
Figure 4.10 $C\bar{A}^q\eta_{k-q}$ and ϵ_k for the first output of the LAMSTF 6 d.o.f. system	70
Figure 4.11 $C\bar{A}^q\eta_{k-q}$ and ϵ_k for the first output using 100 data points	79
Figure 4.12 Coherence Function Estimate for y_{an} , $C\bar{A}^q\eta_{k-q}$ and ϵ_k for 5% noise	71
Figure 4.13 Coherence Function Estimate for y_{an} and ϵ_k for 5% noise (variance)	71
Figure 5.1 F-Norm of error covariance for compensated (dashed line) and uncompensated (dot-dashed line)	88
Figure 5.2 Open-loop Markov parameters of uncompensated system. Markov parameters computed from ARX model in dotted line, true Markov parameters are plotted in dashed line and identified Markov parameter are given in dot-dashed line	89

	Page
Figure 5.3 Open-loop Markov parameters of compensated system. Markov parameters computed from ARX model in dotted line, true Markov parameters are plotted in dashed line and identified Markov parameter are given in dot-dashed line	89
Figure 5.4 Estimated and true output of the first state for uncompensated system	90
Figure 5.5 Estimated and true output of the first state for uncompensated system	90
Figure 6.1 Situation for identification with constant reference input	99
Figure 6.2 Magnitude of the norm of the error covariance vs. noise level	99
Figure 6.3 Error percentage of the open-loop Markov parameters vs. noise level	100
Figure 6.4 Error percentage of open-loop Markov parameters for the indirect identification	101
Figure 6.5 Error percentage of Markov parameters for the direct and indirect identification	102
Figure 6.6 Magnitude of error covariance for the direct and indirect identification	103
Figure 6.7 Magnitude of the percentage of error deviation of the open-loop system Markov parameters in relation to the ARX model order and the noise level	104
Figure 6.8 Error percentages of the 30 first open-loop Markov parameters for the direct and indirect system identification method	105
Figure 6.9 Magnitude of the percentage of error deviation of the open-loop system Markov parameters in relation to the number of data points and the noise level	106
Figure 6.10 Magnitude of the percentage of error deviation of the open-loop system Markov parameters in relation to the ARX model order and the data length	107

	Page
Figure 6.11 Error percentages of the 30 first open-loop Markov parameters for the direct and indirect system identification method	108
Figure 6.12 Error percentages of the 30 first open-loop Markov parameters for the direct and indirect system identification method	109
Figure 6.13 Error percentages of the 30 first open-loop Markov parameters for the direct and indirect system identification method	110
Figure 6.14 Error percentages of the 30 first open-loop Markov parameters for the direct system identification method	111
Figure 6.15 Error percentages of the 30 first open-loop Markov parameters for the direct and indirect system identification method	112
Figure 7.1 Two-step system identification with proposed input design	121
Figure 7.2 Input signal design with repeated substitution of new input data	122
Figure 7.3 System output of original simulation and simulation with input design	123
Figure 7.4 System input of original simulation and simulation with input design	124
Figure 7.5 Original system input and corrected input for respiratory system	125
Figure 7.6 System output of original simulation and simulation with input design	126
Figure 7.7 System input of original simulation and simulation with input design	127
Figure 7.8 Error percentages of open-loop Markov parameters for identification of the system operating in open-loop, with and without input design and different noise levels	128
Figure 7.9 Error percentages of open-loop Markov parameters for identification of the system operating in closed-loop, with and without input design and different noise levels	129
Figure 7.10 Possible iterative controller design schematic with input design	130

LIST OF SYMBOLS

Unless otherwise stated the listed symbols are specified as follows.

A, B, C, D	open-loop system matrices
A_c, B_c, C_c, D_c	closed-loop system matrices
A_d, B_d, C_d, D_d	system matrices of dynamic controller
a_i, b_i	coefficient matrices of ARX model
$E[\]$	expectation operator
H	Hankel matrix
I	identity matrix
K	Kalman filter gain
l	data length
m	number of outputs
N	open-loop Kalman filter Markov parameters
N_c	closed-loop Kalman filter Markov parameters
n	number of states
q	order of ARX model
q_2	new order of ARX model
r	reference input
u	control input
\bar{V}	data matrix
v	measurement noise
w	process noise
x	system state
Y	system Markov parameter
y	system output

Greek Letters

ε	residual
Φ	input/output information matrix
η	augmented state of open-loop system and controller
Θ	augmented coefficient matrix of ARX model
ξ	output data

Subscripts

k	k-th time step
i, j	discrete numbers

Superscripts

T	matrix transpose
-1	matrix inverse

Notation above a Symbol

\wedge	estimate
\cdot	time derivative

CHAPTER I

INTRODUCTION

1.1 Background and Problem Statement

The field of system identification has been developed for a multitude of purposes. As each discipline gives its motivation there is a common goal: one wants to infer the characteristics of a particular system from its input/output data. Suppose one has a space structure, on which an antenna is installed. This antenna is pointing to a particular ground station to transmit and/or receive information. Space structures have relatively little mass distributed over a large volume, which causes the system to be lightly damped, or from a control point of view, to be marginally stable. The mathematical modeling of the system was done on earth, using physical laws, assumptions, and simplifications. The controller design for the positioning of the antenna and its vibration compensation are based upon the mathematical model. During the deployment of the structure in space, the characteristics changes continuously, and other disturbances occur which are not accounted for by the controller. Changes in material properties develop due to ever changing heat radiation from the sun and thermal stresses. New or altered equipment noises transpire. Though the task of the antenna to point accurately to the ground station does remain. To compensate these alterations, the controller has to be updated constantly based on the new system characteristics. System identification proves to be a very useful tool in this and related problems. One can automatically update, or compute the system equations, using the input/output data and a system identification method. Though, the identification problems investigated in this work is driven by the controls engineering point of view. The goal is to identify an unknown or partially known system such that a controller can be designed for that particular system.

There exists a great multitude of proposed and developed identification methods for stochastic, linear, autonomous systems¹⁻¹⁴. The main concern of this work is the

The journal mode adapted for this dissertation is AIAA

parametric system identification methods, in particular the Open-loop Kalman filter Identification method (OKID) and the Closed-Loop system Identification method (CLID)¹⁵⁻¹⁷. The latter one can be used for direct and for indirect system identification. These methods compute the Markov parameters of the identified system, which are the same as its pulse response history. Both identification methods use an observer for the identification, which makes it possible to identify not only the open-loop system, but also an associated observer which can be later used for possible controller design.

In general, one seeks to obtain a system representation as accurate and close to the original system as possible. The system identification methods used here, employ ARX model representations and least-squares estimation for the determination of its parameters. Comparing system performances from identified models with the characteristics of the true systems, one can always detect some differences. If the source of the inaccuracy is known, the quality of the identification result can be improved by addressing or by-passing the origination of the inaccuracy.

Parameter identifiability concerns the ability of deducing the model parameters from the input/output data. This is an extensively studied field for the closed-loop system identification method. However, direct usable or practical methodologies or formulas are not available. In the literature this problem is treated in a very abstract way^{3,18} or the identifiability is computable if the system is known¹⁹.

The closed-loop system identification method uses the controller dynamics to compute the open-loop system Markov parameters. The controller normally serves to generate bounded input and output data from the system. The effect on the system identification results are not known. For example it is desirable to design a controller which produces inputs such that the identification results are improved in accuracy, speed of computation and/or data length.

1.2 Objective

The objective of this dissertation is to develop a new input design which improves the accuracy of the identification results compared to the true system. First the source of the identification error is determined. Each step of the identification algorithm is investigated of possible error sources. The investigation is done numerically using the direct and

indirect identification method. Also, the influence of the controller to limit the process noise is investigated.

Second, identifiability criteria in general are surveyed and then developed particularly for the two system identification methods. The identifiability for the ARX model parameters are given in terms of the input/output data for practical use. From these results, the experimental condition for the identification is derived.

Third, the two identification methods are compared numerically using several different example systems. These systems are a structural system, a heat and mass transfer system, a magnetic suspension test facility, a biomedical system and an economical system. The identifiability, data length and accuracy of the identification results from the two methods are used as criteria. In particular, system identification with a constant reference input is studied. These situations occur when the plant has to be identified on-line. The problem of loss of identifiability due to the feedback signal is explored.

Fourth, a new input design is elaborated. This design consists of computing the ARX model parameters first and then using this information to update the current input. The identification is performed either in two steps, or on-line. The acquired data points are windowed for substitution of the new input data points. Some of the current inputs are kept to guarantee identifiability.

1.3 Dissertation Outline

Chapter II introduces the example systems used in this work. In particular the characteristics of heat and mass transfer systems and its problematic for system identification are given. A structural system in form of NASA's minimast represents another system for the class of marginal, lightly damped systems. NASA's Large Angle Magnetic Suspension Test Facility (LAMSTF) is a highly unstable system, where a specimen is suspended and its six degree of freedom are controlled. Other system used are a macro economical system, a freeze-drying system and a human respiratory system.

The direct and indirect system identification methods used in this work are given in Chapter III. Next introducing the two methods used in this work, a general overview of parametric and nonparametric system identification methods is presented. Then, for the direct system identification method and indirect system identification method, the model representation is given, its parameter estimation and the open-loop Kalman filter system

identification (OKID) and the closed-loop system identification (CLID) algorithm is described in detail.

Chapter IV develops the ARX model for a finite-dimensional system with and without state controller. It is shown that the ARX models for the direct and the indirect system identification are of the same type, and poses the same accuracy problematic. Inaccuracies occurring during the system identification process are located. Also the influence of the process noise to the system identification accuracy is investigated.

Chapter V presents an introduction to the problematic of identifiability. In particular, parameter identifiability is distinguished from system identifiability and from structural identifiability. The focus is given to parameter identifiability since the model structure of the system identification is fixed. The importance of the canonical representation in system identification for identifiability is outlined and the role of the initial condition to the problem of process identification of linear time invariant deterministic systems is derived. From the parameter identifiability, the experimental conditions are obtained and with numerical examples validated.

Chapter VI provides a comparison between the direct and the indirect system identification methods. In particular, identification with constant reference input is studied. The problem of the loss of parameter identifiability due to feedback is deliberated. Also the required data length for achieving a certain accuracy for both method is investigated, using the described systems given in Chapter 2 as numerical examples.

Finally, Chapter VII proposes a new input design for systems under identification. The input design addresses the problematic of identifiability and accuracy. The system identification is performed in two steps, or on-line. In the first step, a normal excitation signal is given to the system, which is in most cases a random or binary random signal. This input along with the output of the system is then windowed and some of the inputs are substituted by calculated input data. The calculation of the new inputs is based on the estimated model parameters.

CHAPTER II

EXAMPLE SYSTEMS UNDER IDENTIFICATION

2.1 Introduction

In this chapter several example systems and their descriptions are given. The example systems are being used in the subsequent chapters for numerical validation of the obtained theory. The different dynamical models distinguish themselves from each other by some relevant characteristics, which may or may not have an influence on the identification process or controller design problem. The first system is a distillation column, where rather large time delays are expected, in this particular case a time delay of 10 minutes. The second system describes a lyophilization process for pharmaceuticals. The special characteristic of heat and mass transfer systems is the large time constants used to describe the dynamics of the system. The interest in structural system is based on the fact that many such systems have rather low damping ratios and their stability is marginal. An example of an highly unstable system is described in Section 2.5. Also of interest are biomedical systems, discussed in Section 2.6 and economical systems, in particular macro economical systems, in Section 2.7.

2.2 Chemical Processing Systems

System identification is a useful tool for processes which are difficult to model from basic physical laws only. Industrial processes, such as chemical processes, often are structured in a complex way and therefore pose great difficulties for developing models, from physical and chemical laws. System identification represents a logical approach for obtaining a suitable model for control purposes. A big obstacle for the identification problem is the existence of large disturbances and severe measurement problems that exist for many of the chemical processes. In general there are several processes which can be defined as chemical processes. In this work, a distillation process is being used to present

the numerical results, as well as to indicate the problematic of system identification in chemical processes. In Section 2.3 a heat and mass transfer based system is being introduced, which can also be classified as a chemical process, but due to the distinct difference in its characteristic, the heat and mass transfer systems are treated separately. Another concern is the slow dynamical behavior of chemical processes. Its slow response to manual inputs represents a danger, since the stability can not be guaranteed. Yet another problem in modeling and designing controllers for chemical processes is the large number of variables, which are used to describe the system.

2.2.1 Distillation Process

The study of distillation processes with the intent of applying and designing control laws is quite popular, Gustavsson²⁰. The problem of excitation of the to be identified plant, the distillation column, is solved by using perturbations in power supply, feed composition etc. The excitation of the system has to be handled carefully, since the process itself can not be altered too much, unless the security of the plant or the quality of the product is jeopardized. Quite often, the experiments were carried out using pseudo-random binary sequences as the input signal. This input is especially suitable for the cross correlation analysis, which is preferred when high signal to noise ratio of the data is expected. Cross correlation is also considered to be useful for estimation of time delays and model orders. Hence, parametric identification methods yield more accurate results. Maudsley and Anderson²¹.

2.2.2 Williams-Otto Process, a fourth Order Time Delay System:

The detailed description of this process can be found in Williams and Otto²². The diagram in Figure 2.1 depicts the schematics of the process.

The raw materials are fed and mixed in the chemical reactor. The feed rates of the raw materials are F_A and F_B . Upon leaving the reactor, the product is being cooled in the heat exchanger and an undesirable by-product is removed in the decanter. The product enters at this stage the distillation column. At this point the product contains besides of the desired material also impurities, some remaining raw materials and some undesirable by-products of the chemical reaction. The desired product F_p is extracted in the overhead of the distillation column.

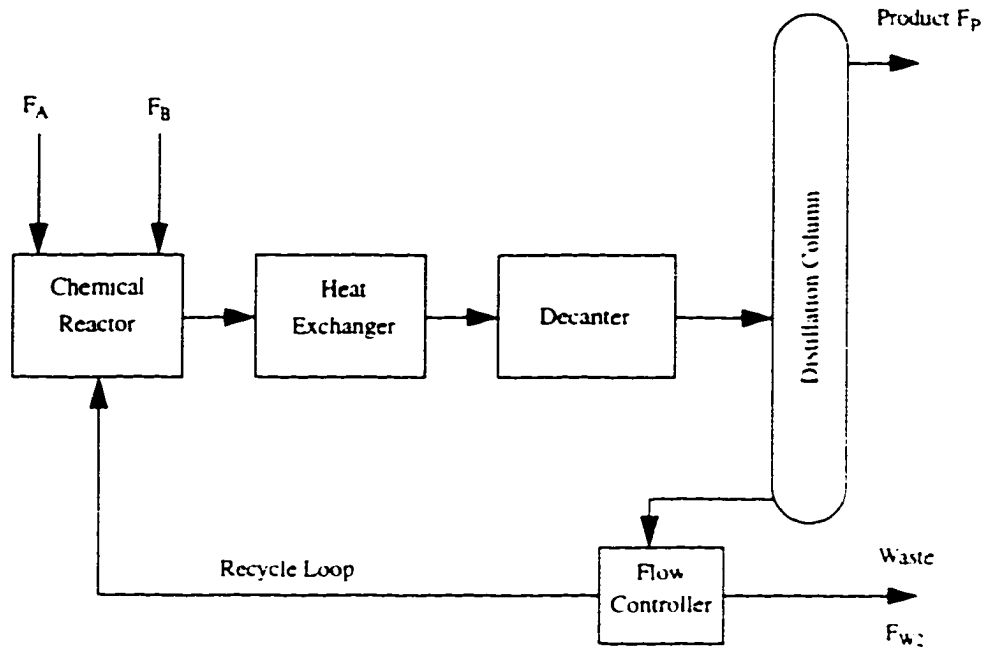


Figure 2.1 Williams-Otto Process.

The purge F_{w2} is removed at the bottom of the distillation column, and the remaining raw material with the by-products is recycled back to the reactor. This feed back of unprocessed raw material and other by-products represents a significant time delay into the described process. A whole cycle can take up to 10 min. The product is transported from the chemical reactor to the heat exchanger, the decanter, the distillation column, and the recycle loop back to the reactor.

The system given by Ross²³ comprises four states, that is the deviation in the weight composition of reactant A from its nominal value (dimensionless), the deviation in the weight composition of reactant B , the deviation in the weight composition of an intermediate product C , and the deviation in the weight composition of the desired product P . The time unit in this particular example is 10 min. Given δF_A as the deviation of the feed rate of material A from the nominal value, V_R as the pound-volume of the chemical reactor and δF_B as the deviation of the feed rate of material B , then the input vector $u = [u_1 \ u_2]^T$ is

defined as $u_1 = \frac{\delta F_A}{\delta V_R}$ and $u_2 = \frac{\delta F_B}{\delta V_R}$ and the system can be given as

$$x(t) = A_0 x(t) + A_1 x(t-1) + B u(t) \quad (2.1)$$

where

$$A_0 = \begin{bmatrix} -4.93 & -1.01 & 0 & 0 \\ -3.20 & -5.30 & -12.8 & 0 \\ 6.40 & 0.347 & -32.5 & -1.04 \\ 0 & 0.833 & 11.0 & -3.96 \end{bmatrix}, A_1 = \begin{bmatrix} 1.92 & 0 & 0 & 0 \\ 0 & 1.92 & 0 & 0 \\ 0 & 0 & 1.87 & 0 \\ 0 & 0 & 0 & 0.724 \end{bmatrix} \text{ and } B = \begin{bmatrix} 1 & 0 \\ 0 & 1 \\ 0 & 0 \\ 0 & 0 \end{bmatrix} \quad (2.2)$$

2.3 Heat and Mass Transfer based Systems

The durability of many pharmaceutical and biological products such as serum, blood plasma, vaccines, antibiotics, hormones, enzymes, vitamins, proteins etc. is governed by bacterial degradation if they are subjected to moisture. The technology and financial expenditure in processing and manufacturing of such products is nowadays immense. A major factor in this display is found in the lyophilization process, where the water content is reduced to guarantee biological stability. Lyophilization takes place as a batch freeze drying operation. The dehydration in this case occurs in a closed low pressurized chamber, where the frozen liquid, filled in vials, is subjected to a heat flux from the shelf through the frozen product to the ice front, which is also known as backface heating. The frozen water content of the product sublimates at this ice front and evaporates, following the declining pressure gradient, into the chamber and then to the condenser wall, where the water vapor crystallizes into ice again. This process claims a lot of time due to the small pressure differences. The energy to maintain vacuum and refrigeration at the condenser and the latent heat supply for the sublimation over a long period of time all represent major cost factors.

Extensive efforts by industry and research centers are made to predict and predetermine the course of freeze drying cycles in order to control the quality of the product and to minimize costs. Many different strategies for operating freeze dryers have been proposed in order to optimize the process. Most of them are based on mathematical models. In this work, a mathematical model for the primary drying cycle of a lyophilization process is used to present the problematic expected by using system identification to develop

a mathematical representation of this process. The basic relationship of the drying cycle is given as a mass and heat transfer process. The expected time constant describing this process are normally quite large. In the following, the lyophilization process is described in some more detailed.

2.3.1 Lyophilization Process

The lyophilization process can be partitioned into four stages: product preparation and freezing, primary drying, secondary drying, stoppering and removal. In the first stage, the pharmaceuticals are filled into vials along with so called additives for protection. The vials are placed into the freeze dryer and the product is being frozen. During the freezing stage, a boundary, where phase change occurs, moves from the vial bottom upwards to the top of the product. The unconstrained water crystallizes while the remaining water turns into a higher concentration with the product. The latter typically represents either an eutectic or an amorphous solution. The crystallization of the water normally occurs in such a way, that the ice crystals grow in a shape of little cylinders or fingers perpendicular to the moving ice front. During the second stage, the primary drying cycle, the chamber of the freeze dryer is evacuated in order to increase the partial water vapor pressure difference between the frozen ice zone and the chamber. The shelf heating system is turned on and starts to provide the enthalpy for the sublimation process. The sublimation takes place at a moving ice front, which proceeds from the top of the frozen material downwards. The participating ice is the unconstrained water accumulated in the cylindrical tubes. Throughout the primary drying, the product, which consists of the dried layer on the top and the frozen core at the bottom of the product, stays below a certain temperature to insure that no melting occurs. The secondary drying circumcises the third stage of the lyophilization process. At the end of the primary drying, all the unconstrained water has been removed and what remains is the water which is bound in the solution. At this point, the product could be removed, but in practice the water content is still too high to guarantee biological stability. The secondary drying is responsible for lowering the bounded water content to an acceptable level, which depends on the product. This stage is less crucial and can be performed at a higher shelf temperature. The last stage is the stoppering of the product and the removal from the freeze dryer. The freeze dried product can normally be stored at room temperature.

2.3.2. Mathematical Model of the Primary Stage of a Lyophilization Process

The mathematical model used in this work is taken from Schoen et al.²⁴. The model describes a nonlinear fourth order system, where the states are the interface position of the ice front, the temperature in the frozen part of the product, the temperature in the dried portion of the product and the chamber gas temperature. The following improvements are made to the original system: inclusion of the inert gas inside the pores of the product; subtraction of the heat, carried by the evaporating water molecules from the dried product mass instead of subtracting it from the frozen product layer; and incorporation of top and bottom heat radiation. The improved nonlinear set of equations and the corresponding nomenclature for this system is given in the Appendix.

The model is based on data taken from an *Edwards Lyoflex 1.0 Special Freeze Dryer*, installed at Glaxo Inc. in Raleigh, North Carolina. The product formulation used were composed of 15 mg glycine and 2 mg active product. The pilot freeze dryer has a shelf area of 12 ft.², which can be regarded as the shelf temperature control surface. The other control inputs are the nitrogen pressure in the chamber and the condenser coil temperature. A more detailed discussion of the model and its foundation can be found in Schoen et al.²⁴. The linearization of the model was done at the operating point of $t = 450$ min in total process time (that is about 30 minutes into the primary drying time). The states are the interface position of the dried and frozen product layer, the temperature in the frozen product layer, the temperature in the dried product layer and the chamber temperature. The state-space representation of the linearized model is given as follows:

$$A = \begin{bmatrix} -0.1222659 & 0.0 & -0.5784 \times 10^{-4} & 0.5358 \times 10^{-4} \\ 256.6889971 & -0.85449787 & 0.62666897 & 0.05339573 \\ -3539.317452 & 0.29782521 & -1.8745728 & 1.4601441 \\ 4706423.195 & 0.0 & 2243.724818 & -1971710.996 \end{bmatrix} \quad (2.3)$$

$$B = \begin{bmatrix} 0 & 0 & 0.15028643 \times 10^{-9} \\ 0.22737876 & 0 & 0.01627583 \\ 0.00053678 & 0 & 0.00409832 \\ 0 & 1969657.94 & 2.88764861 \end{bmatrix} \quad (2.4)$$

2.4 Structural Systems

Examples for structural systems can be found in space structures, building structures, chassis of automobiles, antennas, etc. The problematic of controlling such kind of structures can be easily visualized on space antennas. These structures have a distinct characteristic, since they are normally light weighted and have large dimensions. The objective of a space antenna is to point with very high accuracy to a specified point on the surface of the earth, that is for example a ground station. The antenna and the satellite on which it is mounted is exposed to various changing influences, such as thermal changes or changes in the material property of which the structure is built etc. The structure has some natural vibration, which is to be neutralized by some control algorithm, so that the pointing accuracy is not affected by the movements. The space antenna also has to deal with the problem to maintain the shape of its reflector accurately.

The original controller design for solving this problem was based on some mathematical formulations, which employed the original characteristics of the material used and some assumed describing laws. During the course of the satellites deployment in space, it is exposed to continued thermal changes, alteration of its material properties etc., such that the controller requires a steady adaptation. This can be done using system identification, where the most recent characteristic changes are detected and passed on to update the controller.

In general, two different approaches are being used to describe structural systems mathematically. One way is to use infinite dimensional distributed parameter models, the other way is to use ordinary differential equations, which results in finite dimensional models. The controller design is then based on the particular mathematical representation. A major error introduced into the design process is then the truncation of the model, such that the mathematical description is more practical. Another model error is, as mentioned above, the lack of exact values for the model parameters.

Identification of such systems are rather popular. There are two types of methods deriving a mathematical representation of the system from input/output data. One type is the modal testing approach, the other is the system identification method. Modal testing of a structures can yield the values of the damping ratios, the frequencies, the mode shapes and the modal participation factors of the system, using suitable measurements. System

identification uses also suitable measurements of some input/output signals and processes them to develop a mathematical representation of the system.

Structural systems, such as large space structures, possess quite often very low frequencies, lightly damped modes and sometimes their natural frequencies are located closely to each other. Some natural frequencies may even be lower than the rigid body spacecraft controller bandwidth. The induced problems are treated by using specially design controllers, Joshi²⁵. In this work, a simple structure will be used. This structure represents a beam like mast, which is introduced in the following section.

2.4.1 Spring-Mass System

Figure 2.4.1 depicts the schematic of the spring-damper-mass system. Chen et al.¹⁵. The lumped mass system has three modes (six states). The modal frequency and the damping ratio of each mode are listed as follows:

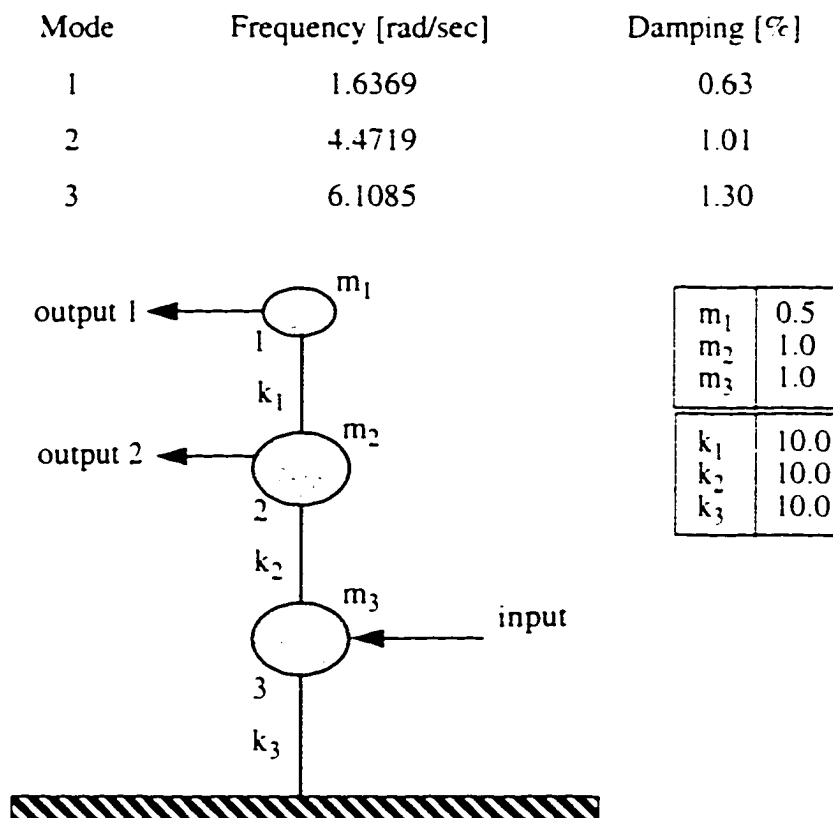


Figure 2.2 The simulated lumped-mass beam-like structure.

The system is excited by a random force at node 3, and the output is measured at nodes 1 and 2. The state-space model is given as follows:

$$A = \begin{bmatrix} 0.9856 & 0.1628 & 0 & 0 & 0 & 0 \\ -0.1628 & 0.9856 & 0 & 0 & 0 & 0 \\ 0 & 0 & 0.8976 & 0.4305 & 0 & 0 \\ 0 & 0 & -0.4305 & 0.8976 & 0 & 0 \\ 0 & 0 & 0 & 0 & 0.8127 & 0.5690 \\ 0 & 0 & 0 & 0 & -0.5690 & 0.8127 \end{bmatrix} \quad (2.5)$$

$$B = [0.0011 \ 0.0134 \ -0.0016 \ -0.0072 \ 0.0011 \ 0.0034]^T \quad (2.6)$$

$$C = \begin{bmatrix} 1.5119 & 0.0 & 2.0 & 0.0 & 1.5119 & 0.0 \\ 1.3093 & 0.0 & 0.0 & 0.0 & -1.3093 & 0.0 \end{bmatrix} \quad (2.7)$$

2.5 Large-Gap Magnetic Suspension Systems

At NASA-Langley Research Center in Hampton, VA, a magnetic suspension system has been developed. The objectives of this testbed are to develop and evaluate the technology for magnetic suspension at large gaps, accurate position sensing at large gaps, accurate suspended element control at large gaps and suspended element control over large angles. Possible applications include magnetic suspension systems for wind tunnels, microgravity and vibration isolation systems, magnetically suspended pointing mounts and large-angle magnetic suspension systems for advanced actuators.

Unstable systems represent an additional difficulty for applying system identification. In order to obtain bounded input and bounded output signals, the system has to operate in closed-loop. The identification uses therefore either the closed-loop input/output data, or the bounded input/output from the system. Both methods, the direct and indirect system identification methods can be applied.

The system, which is currently under development, is capable to control all six degrees of freedom of the suspended specimen, that is, three displacements (x , y and z) and three rotations (pitch, yaw and roll). A total of eight electromagnets are arranged in a planar array to control the suspended element as depicted in Figure 2.3.

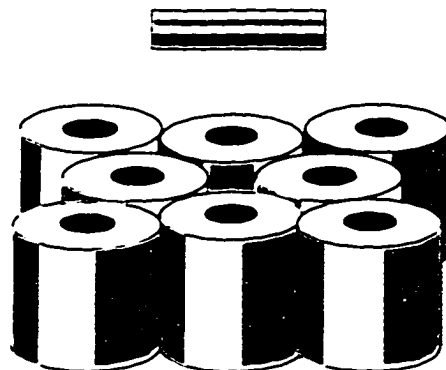


Figure 2.3 The six DOF Magnetic Suspension System Configuration.

The measurement of the position and motion of the suspended element are performed using a total of six pairs of laser sensors. The outputs are the amount of light blocked along a thin laser sheet and the inputs consists of eight currents into the eight electromagnets. The details of the suspended specimen, the coils and power amplifiers and the position sensors are described in the following sections.

2.5.1 System Specifications

The suspended element consist of a nylon outer shell and a Neodymium-Iron-Boron core, which is permanently magnetized. The dimensions of the specimen are determined by a diameter of 1.27 cm and a length of 5.08 cm. The total weight of the suspended element is 51.9 g, with the inertias $I_{xx} = 1.11\text{e-}6 \text{ kgm}^2$ and $I_{yy} (=I_{zz}) = 1.25\text{e-}5 \text{ kgm}^2$. The suspended height is 100 cm.

The arrangement of the coils is an eight coil planar array with iron cores, which consists of two concentric arrays of four coils each. The primary coil array location radius is 11.43 cm, while the secondary coil array location radius is 21.59 cm. Each coil has a height of 10.3 cm and has an outer radius of 7.62 cm with an iron core radius of 5.08 cm and an inner radius of 3.25 cm. The maximum current density of the electromagnets is $333.5\text{e+}6 \text{ A/m}^2$.

2.5.2 System Model

The analytical state-space representation of the suspension system is given as follows:

$$\begin{aligned}
 A_1 &= 1.0e+05 \times \begin{bmatrix} 0 & 0 & 0 & 0 & 0 & 0 \\ 0 & 0 & 0 & 0 & 0 & 0 \\ 0 & 0 & 0 & 0 & 0 & 0 \\ 0 & 0 & 0 & 0 & 0 & 0 \\ 0 & 0 & 0 & 0 & 0 & 0 \\ 0 & 0 & 0 & 0 & 0 & 0 \\ 0.67147458 & 0 & 0.00022199 & 2.4092417 & 0.0 & 0 \\ 0 & 0.05952476 & 0.0 & -0.21357518 & -0.1968 \times 10^{-4} & -0.0 \\ 0 & 0 & 0 & 0 & 0 & 0 \\ 0 & -0.00015005 & 0 & 0 & 0 & 0 \\ 0.00015005 & -0 & 0.0 & 0 & 0 & 0 \\ 0 & 0 & 0 & 0 & 0 & 0.00121139 \end{bmatrix} \\
 A_2 &= 1.0e+05 \times \begin{bmatrix} 0.00001 & 0 & 0 & 0 & 0 & 0 \\ 0 & 0.00001 & 0 & 0 & 0 & 0 \\ 0 & 0 & 0.00001 & 0 & 0 & 0 \\ 0 & 0 & 0 & 0.00001 & 0 & 0 \\ 0 & 0 & 0 & 0 & 0.00001 & 0 \\ 0 & 0 & 0 & 0 & 0 & 0.00001 \\ 0 & 0 & 0 & 0 & 0 & 0 \\ 0 & 0 & 0 & 0 & 0 & 0 \\ 0 & 0 & 0 & 0 & 0 & 0 \\ 0 & 0 & 0 & 0 & 0 & 0 \\ 0 & 0 & 0 & 0 & 0 & 0 \\ 0 & 0 & 0 & 0 & 0 & 0 \end{bmatrix} \\
 B &= 1.0e+03 \times \begin{bmatrix} 0 & 0 & 0 & 0 & 0 & 0 & 0 & 0 \\ 0 & 0 & 0 & 0 & 0 & 0 & 0 & 0 \\ 0 & 0 & 0 & 0 & 0 & 0 & 0 & 0 \\ 0 & 0 & 0 & 0 & 0 & 0 & 0 & 0 \\ 0 & 0 & 0 & 0 & 0 & 0 & 0 & 0 \\ 0 & 0 & 0 & 0 & 0 & 0 & 0 & 0 \\ 0 & 1.0834 & 0 & -1.0834 & 0.2774 & 0.2774 & -0.2774 & -0.2774 \\ -0.0960 & 0 & 0.0960 & 0 & -0.0246 & 0.0246 & 0.0246 & -0.0246 \\ 0 & 0 & 0 & 0 & 0.0021 & -0.0021 & 0.0021 & -0.0021 \\ 0.0003 & 0 & -0.0003 & 0 & 0.0 & -0.0 & -0.0 & 0.0 \\ 0 & 0.0003 & 0 & -0.0003 & 0.0 & 0.0 & -0.0 & 0.0 \\ -0.0001 & -0.0001 & -0.0001 & -0.0001 & 0.0001 & 0.0001 & 0.0001 & 0.0001 \end{bmatrix}
 \end{aligned}
 \tag{2.8}$$

$$A = \begin{bmatrix} A_1 & A_2 \end{bmatrix} \tag{2.9}$$

$$C = \begin{bmatrix} -0.0 & -24.1544 & 0 & 0 & 0 & 754.8250 & 0 & 0 & 0 & 0 & 0 \\ -0.0 & 6.4160 & 0 & 0 & 0 & 754.8250 & 0 & 0 & 0 & 0 & 0 \\ 0 & 0 & -20.2853 & 533.8225 & -533.8225 & 0 & 0 & 0 & 0 & 0 & 0 \\ 0 & 0 & -20.2853 & -533.8225 & 533.8225 & 0 & 0 & 0 & 0 & 0 & 0 \\ 0 & 0 & 20.2853 & -533.8225 & -533.8225 & 0 & 0 & 0 & 0 & 0 & 0 \\ 0 & 0 & 20.2853 & 533.8225 & 533.8225 & 0 & 0 & 0 & 0 & 0 & 0 \\ 20.0535 & -0.0 & 0 & 0 & 0 & 0.0 & 0 & 0 & 0 & 0 & 0 \end{bmatrix}, D = \text{zeros}(7 \times 8)$$

(2.10) (2.11)

2.6 Biomedical Systems

Biomedical engineering is a rapidly growing field, where more and more control and system identification tools are utilized to maximize performance and ensure safety. System identification and controls are applied to broad area of physiological kinetics, which contains characterization of metabolism, compartments and movement of materials through compartments within the organism. The two major fields where controls and system identification in biomedical engineering are applied are the cardiovascular system and the respiratory system of organisms. The identification problem concerns the characterization of biological systems where the modeling approach fails to address the characteristics of the system under investigation and enables the application of the developed model to clinical problems. Most physiological investigators still favor the direct measurement approach of biological parameters and the physical model derivation whenever possible over the identification approach. The systems are normally represented by compartment models. The basic equations of compartmental systems are mass balance equations since the models are assumed to consist of interconnected compartments where each has a homogeneous characteristic.

As for the cardiovascular systems, attention is given to systems arteries, to the heart and to capillary fluid exchange, since the variables describing these systems possess a high degree of information content. Arteries systems, such as for leg or arms, are normally realized as lumped systems or so called segments. The measured signals of the system are the pressures at various locations such as at knee or foot etc. System descriptions of the heart use phenomena and variables such as electric signals, volume changes, pump characteristics and heart muscle mechanics. Also of much interest is the relationship of the heart rate and the respiration of a subject.

In the present work, the interest on biomedical system will be constrained to the respiratory system, the other major application field for controls and system identification besides of the cardiovascular system. The simplest representation of the respiratory system is by assigning values to the airway resistant and the lung compliance. Uhl and Lewins et al.²⁶ used least squares techniques to obtain those values for a simple description of a respiratory system. Some studies used more complex models of the lung. Ferguson et al.²⁷ employed a two compartment model of CO_2 transport between alveoli and the tissues. The parameter vector to be identified contains of the cardiac output, the lung volume, the metabolic production rate of CO_2 of the tissues and the initial concentration of CO_2 in the tissues. These models were general description of respiratory systems. In this work, the focus is on the human respiratory control system, which is somewhat more involved and its modeling is based on the later application.

For the mathematical model of human control systems, there exists two types of control systems in the human body. The first is called the servo system, which is responsible for example for the positioning of body parts to a cerebral signal, where the motor cortex initiate a step input for movement of the body part. With internal damping, this part reaches its final position. The other control type is the regulator. The internal respiratory control system belongs to the class of regulator. Here the disturbance is considered as a step input of inhaled CO_2 and the regulator forces the respiration to increase its ventilation in order to decrease the CO_2 content to a new steady-state level.

Several studies attack the modeling problem of the human respiratory system and its biological regulator. The model given by Grodins et al.²⁸, considers CO_2 as the only controlling variable of the ventilation. The tissues were considered as a single lumped system. The model was expanded by Horgan and Lange²⁹, where circulation time and oxygen control were included, such that periodic breathing could be investigated. Milhorn Jr. et al.³⁰ divided the tissue reservoir into two compartments, the brain and the body tissue and considered cerebral blood flow as a function of arterial CO_2 . Also the effect of oxygen as a controller of ventilation, and the effect of time delays in the transport of gases from the lungs to both tissue reservoirs, were included into the model. Grodins et al.³¹ expanded the

model to include a variety of other effects, such as hypoxia at sea level or altitude, metabolic disturbances in acid-based buffering, the dependence of time delay on cardiac outputs, concentration equilibria etc. The present work will use the somewhat more simple but efficient model by Grodins et al.²⁸.

The application of respiratory systems, its identification and the application to control systems is manifold. The model given by Grodins et al.³¹ was slightly altered by Sano et al.³² to introduce an adaptive feedback control system for incubator oxygen treatments. The controller determines the optimum oxygen concentration of the mixed gas, which is forced into the incubator so that the partial oxygen pressure in the arterial blood flow is kept in a certain range. This is a necessary treatment for newborns who suffer from respiratory distress. In general, system identification in biomedical engineering is very helpful wherever modeling is difficult due to the lack of physical information or describing laws. Indirect identification for closed loop system is especially interesting in this field, since biological system can not always be excited over the whole range of frequency spectrum without destruction of the biological system.

2.6.1 Respiratory System: CO₂ Concentration

The basic analogy is that while inhaling, the lung receives besides of the necessary oxygen also a CO₂ mixture. This CO₂ is passed on into the blood through diffusion membranes and to the tissues. The body has an internal control mechanism to keep the CO₂ concentration at a certain level. The controlling quantity is the pulmonary ventilation, that is the increase of CO₂ concentration in the tissues and the blood, causes an increase of the ventilation. The purpose of the ventilation, in this context, is to minimize the rise in CO₂ concentration in blood and tissues. The process is also true in the opposite direction, the pulmonary ventilation controls the CO₂ concentration, but also the CO₂ concentration controls the ventilation. Therefore we have a closed loop system, where the controlling quantity is the pulmonary ventilation, the controlled quantity is the CO₂ concentration and the disturbing quantity is the concentration of CO₂ in inspired gas. The model given by Grodins et al. describes the system by controlling system equations, which characterize the dependence of the ventilation on body CO₂ concentration, and controlled system

equations, which describe the dependency of the CO_2 concentration on ventilation and in the inspired gas. Grodins et. al. calls therefore the whole system as the respiratory chemostat.

2.6.2 Controlled System

As mentioned above, the controlled system represents the dependency of the CO_2 concentration on ventilation and the inspired gas. The model describes a simplified lung-blood-tissue CO_2 exchanger model. The diagram in Figure 2.4 depicts the major elements of this system.

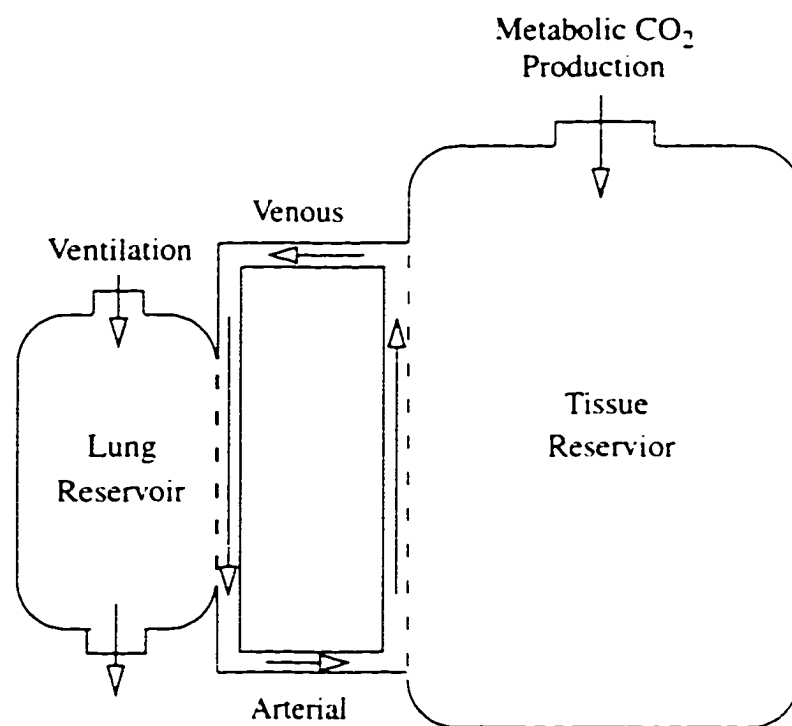


Figure 2.4 Simplified model of CO_2 concentration on ventilation.

The ventilation depicted symbolically in Figure 2.4 is a cyclic process, where the volume of the lung is periodically changed. A variable portion of the total ventilation is ineffective

because of the dead air, whose volume is a function of tidal volume. The oxygen and CO_2 is exchanged across the alveolar membrane. If the alveolar $R.Q.$ is not unity, dry inspired and expired gas volume will differ (which is normally the case, $R.Q. \approx 0.875$). The tissues consists of a number of individual elements connected in parallel. Each has its own characteristic, such as rate of metabolism, blood flow, buffer capacity for CO_2 etc. Also each element is connected by an arterial and a venousal blood flow to the lung. The time for a blood element from the lung to the tissue element differs for each tissue element as well as for the time a blood element needs to reach a particular tissue element differs in the arterial blood flow from the time a blood element needs to reach the lung in the venousal blood flow from that particular tissue element.

The model given by Grodins et al.²⁸ includes a number of simplification in order to model the process. It is assumed that the events of the respiratory cycle are ignored, where the lung has a constant volume and zero dead space. The oxygen exchange across the alveolar membrane is set equal to the CO_2 exchange (opposite direction) at every instant ($R.Q. = 1.0$). The CO_2 tension in the lung is assumed to be uniform. All tissues are combined into a tissue reservoir, whose rate of CO_2 production becomes the total CO_2 production and whose rate of blood flow becomes the cardiac output. To convert the CO_2 tension to total CO_2 concentration, approximated CO_2 absorption curves are used. No time delays occur in the blood flow, that is the circulation time is infinitely short. Gas diffusion across alveolar and capillary membranes occur at an infinitely fast rate at any tension other than zero.

Using the above mentioned simplification, the controlled system equation, that is the description of the dependency of the ventilation on body CO_2 concentration, is derived using continuity analogy. As for the lung reservoir, the difference between the rates of CO_2 inflow and outflow is equal to the rate of change of the quantity of CO_2 in the reservoir and the CO_2 fraction in the expired gas is the same as in the lung reservoir. The tissue reservoir balance equations involve the tissue CO_2 production, the CO_2 flow rate in arterial blood, the CO_2 flow rate in venous blood and the volume rate of CO_2 in the tissue reservoir. For the equations, the following symbols and units were used.

Table 2.1 Human Respiratory System Description

K_1 ... tissue CO_2 production, 0.2632 [l(BTPD)/min].
K_2 ... tissue fluid volume, 40.0 [l].
K_3 ... cardiac output, 6.0 [l/min].
K_4 ... controller sensitivity, 2.0 [-].
K_5 ... modified controller intercept setting, 246.24 [-].
K_6 ... lung volume, 3.0 [l].
K_7 ... fraction of CO_2 in inspired gas, (0.047)[-].
G_1 ... barometric pressure, 760 [mmHg].
G_2 ... slope of CO_2 absorption curve, 0.00425 [l(BTPD) CO_2 /l.blood].
G_3 ... extrapolated intercept of CO_2 absorption curve, 0.32 [l(BTPD) CO_2 /l.blood 38°C].
V ... pulmonary ventilation, [l(BTPD)/min].
q_1 ... CO_2 flow rate in expired gas, [l(BTPD)/min].
q_2 ... CO_2 flow rate in arterial blood, [l(BTPD)/min].
q_3 ... CO_2 flow rate in venous blood, [l(BTPD)/min].
q_4 ... volume of CO_2 in tissue reservoir, [l(BTPD)].
q_5 ... volume of CO_2 in lung reservoir, [l(BTPD)].

And introducing two new variables:

$$\Theta_T = \frac{\text{Volume of } \text{CO}_2 \text{ in tissue reservoir}}{\text{tissue fluid volume}} \quad (2.12)$$

$$\Theta_A = \frac{\text{Volume of } \text{CO}_2 \text{ in lung reservoir}}{\text{lung volume}} \quad (2.13)$$

By using an equation which defines the equilibrium between tissue and venous CO_2 tension and an equation which represents a linearized absorption curve for the CO_2 content in arterial blood, the controlled system equation are formulated as follows:

$$\frac{K_2 K_6}{K_1 V} \Theta_T + \left\{ \frac{K_6}{V} + \frac{G_1 G_2 K_2}{V} + \frac{K_2}{K_1} \right\} \Theta_T + \Theta_T = \frac{K_1}{K_1} + \frac{K_1 G_1 G_2}{V} + G_3 + G_1 G_2 K_4 \quad (2.14)$$

2.6.3 The Controlling System

The controlling system comprises all those physiological elements through which body CO_2 concentration operates upon pulmonary ventilation. It includes elements such as the motor nerves to the respiratory muscles or the motor nerves to the ventilatory pump, etc. This system is very difficult to model, since of lack of physical informations and describing laws. The used model is based on empirical relationships. The authors of the present model show that the effective input to the described system is the CO_2 tissue concentration and not the arterial - or alveolar - CO_2 concentration. The controlling system equation is given as follows:

$$V(t) = \frac{K_4}{G_2} \Theta_T(t) - K_5 \quad (2.15)$$

It is noteworthy that the controlling system is of the type of a proportional controller.

2.6.4 Closed-Loop System

Figure 2.5 represents several interesting closed loop situations of the respiratory system.

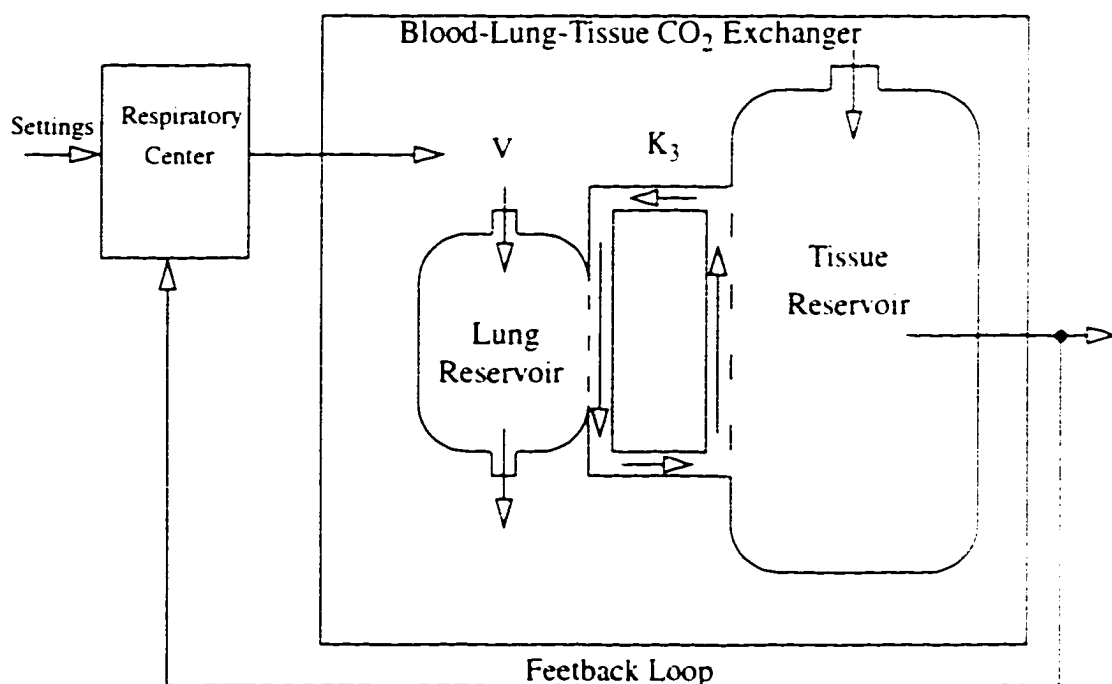


Figure 2.5 Closed Loop Chemostat²⁸.

The equation where the system is regarded as a regulator of tissue CO_2 concentration is obtained by implementing Equation (2.15) into (2.14), so that V is eliminated:

$$\begin{aligned} \frac{K_2 K_6 G_2}{K_4} \Theta_T + \frac{K_2}{K_1} \Theta_T \Theta_T + \frac{K_3 K_6 G_2 + K_2 K_3 G_1 G_2^2 - K_2 K_5 G_2}{K_1 K_4} \Theta_T + \Theta_T^2 - \left\{ \frac{K_5 G_2}{K_4} + \frac{K_1}{K_1} + K_4 G_1 G_2 + G_1 \right\} \Theta_T = \\ = \left(\frac{G_2}{K_4} \right)^2 \left\{ K_1 K_4 G_1 + K_5 \left(K_5 - K_4 K_2 G_1 - \frac{G_1 K_4}{G_2} - \frac{K_1 K_4}{K_1 G_2} \right) \right\} \quad (2.16) \end{aligned}$$

Other interests can be investigated by deriving closed loop equations from (2.14) and (2.15) for alveolar (arterial) CO_2 concentration and for pulmonary ventilation. The former is rather complex and is therefore not given here. The latter, relationship for pulmonary ventilation, is of the same form as Equation (2.16), but its constants possess different values. The pulmonary ventilation description is given as follows:

$$AV + BVV + CV + V^2 + DV = E \quad (2.17)$$

where

$$A = K_2 \frac{K_6}{K_1}, B = \frac{K_2}{K_1}, C = K_6 + K_2 G_1 G_2, D = K_5 - K_4 K_2 G_1 - \frac{G_1 K_4}{G_2} - K_1 \frac{K_4}{K_1 G_2} \text{ and } E = K_1 K_4 G_1.$$

2.6.5. Linearized Model and State-Space Representation

Since both equations, for the tissue CO_2 regulator and for the pulmonary ventilation differ only by the value of their constants, and the characteristics are similar, only the pulmonary ventilation description is being linearized and used in this work.

The linearization was done with the values given in Table 2.1. The input variable is K_7 , the fraction of CO_2 in inspired gas. The linearization point was taken at $V=15.65$ [l/min]. Figure 2.6 and Figure 2.7 depict the theoretical ventilation transient for the nonlinear and the linear system. The linear system describes the nonlinear event quite well. The state-space description for the pulmonary ventilation is given as follows:

$$A = \begin{bmatrix} 0 & 1 \\ -1.8861 & -11.826145 \end{bmatrix}, B = \begin{bmatrix} 0 \\ 760 \end{bmatrix}, C = \begin{bmatrix} 1 & 0 \end{bmatrix} \quad (2.18)$$

2.7 Econometric Systems

Economics is a social science. It can be divided into macro and micro economics. We shall discuss only macro economic systems. Macro economic is the dynamic behavior of consumption, investment and employment driven by private and public activities. The model building of economic systems is not as straight forward as the one to describe a physical system, since there exists a vagueness about some of the functional relationships, particularly those including variables of a psychological nature. Another problem is the measurement, unlike a physical system, the economy is not well suited either to specialized measurement instrumentation or planned experiments. Econometric theory is concerned with the deterministic relationship between economical variables, for example between consumption and disposable income. In the following sections, the economical relationships are introduced.

2.7.1 Investment Mechanism Model

In this section, we are concerned with the macro economic modeling, at a fairly elementary level, of a capitalist economy. The state variables are not decomposed, for example so that one can also model effects of international trade. Thus the model is a single sector model, also called closed capitalist economy model. The states of the model are called aggregates. Defining the aggregate Z as the demand, resulting from the plans of consumers, businesses and government to spent their incomes. It is composed of consumer purchases C , investment purchases I , and government expenditure G :

$$Z = C + I + G \quad (2.19)$$

This demand will eventually lead to an output Y . There will be obviously a lag between demand and output, because of the time it takes to translate demands for goods and services into actual outputs. In economics, this lag is called the *Lundbergian* lag. For simple models one can assume that this lag can be approximated by a first order lag with time constant T_y , in years.

$$Y = \frac{Z}{1 + T_y s} \quad (2.20)$$

where s is the Laplace operator.

The disposable income Y_d is the income Y left after taxation T .

$$Y_d = Y - T \quad (2.21)$$

It is assumed that some portion c of the total disposable income is used for making consumer purchases. This proportion c is defined in economics as propensity to consume. Using again a first order approximation for the relationship of the receipt of income and its use for the purchase of consumer goods:

$$C = \frac{c}{1 + T_c s} \quad (2.22)$$

where T_c is called the *Robertsonian* consumption lag.

It is generally known that the problem of modeling the investment is rather complex and difficult. Many different models and approaches have been suggested. In general it can be considered as a function of changes in the output. Allen³³ described the investment modeling as a linear function of the time derivative of the output, and a lag time constant T_I .

$$I = \frac{k s Y}{1 + T_I s} \quad (2.23)$$

where k is a proportional coefficient. The private capital investment comes from that proportion of the disposable income not used for direct consumption, i.e. $(1-c)Y_d$, where the term $(1-c)$ is called the *propensity to save*. In general the investment is a function of the output Y , output rate of change, interest rate and marginal efficiency of investment:

$$I = f(Y, Y, r, r_m) \quad (2.24)$$

The governmental expenditure can be modeled on a similar way as the investment problem. The government makes its expenditure decisions, u , based on the level of public expenditure, which leads to the government expenditure G . The relationship between u and G is again to be assumed of a first order lag with the time constant T_g :

$$G = \frac{u}{1 + T_g s} \quad (2.25)$$

The total model can be symbolized in a block diagram as follows:

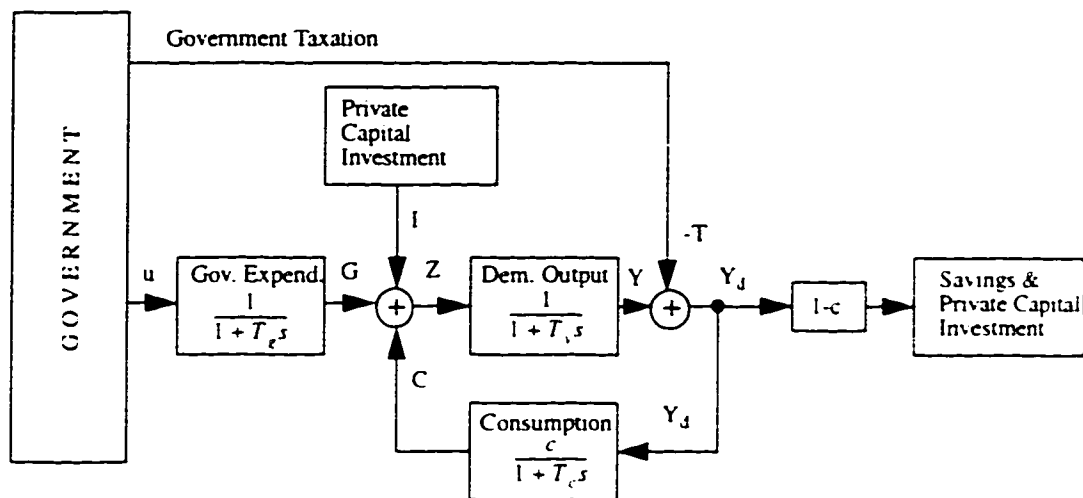


Figure 2.6 Macro Economic System.

The described model is extremely simple and for example, there is no mentioning about any accumulation and economic growth, and can be classified as a perturbation model. In spite of its simplicity, it does illustrate most of the important economical factors, such as the multiplier effect, where investment is rewarded by increases in the output, or reduction in taxation. The steady state gain from the investment, using this model, can be found to be $1/(1-c)$, where $c \leq 1.0$. The steady state gain from the reduction in taxation is somewhat smaller, $c/(1-c)$. The question now arises, how can one apply control theory to develop rules for government economic policy decisions. This problem has been extensively studied by numerous authors, such as Noton³⁴, Desai et. al.³⁵ etc. In general, it is quit straight forward to apply control theory, for example one can transform the above model easily into state space form and apply any control law required to achieve the desired output. The interpretation of this control law to economical actions is somewhat more involving and will not be treated here.

2.7.2 Deterministic fourth order macroeconomic model

There exists a vast amount of macro economical models in the literature, i.e. Livesey³⁶, Klein et al.³⁷ etc. Many models are deterministic in their forms, although more and more research is being done with stochastic models. In this dissertation, a simple deterministic fourth order macro economical model will be used. The model is given in Mahmoud³⁸, where also a brief description about the model is given. The aggregates (states) are as follows:

- total personal consumption expenditure
- gross private domestic investment in durable goods
- new construction
- effective interest rate

The model is similar to the one above described, although is based on actual empirical data from 1966 to 1974 from the Egyptian economy.

The basic equations which form the model are given as follows:

$$C_k = \alpha_1 Y_k + \alpha_2 C_{k-1} \quad (2.26)$$

$$K_k = b_0 + b_1 Y_k + b_2 R_k + b_3 K_{k-1} \quad (2.27)$$

$$I_k = K_k - (1 - \delta) K_{k-1} \quad (2.28)$$

$$M_k = \gamma_0 + \gamma_1 Y_k + \gamma_2 R_k + \gamma_3 M_{k-1} \quad (2.29)$$

$$Y_k = -e_0 + (1 - g)[C_k + I_k + G_k] \quad (2.30)$$

where C_k represents the consumption rate, Y_k is the disposable personal income, K_k denotes the actual stock of capital goods, I_k accounts for the gross investment expenditure, M_k is the stock of money. The lower case letters represent suitable coefficients. In state space form the model is given as follows:

$$A = \begin{bmatrix} 0.5021 & 0.3083 & 0.3083 & 0 \\ 0.2806 & -0.3819 & 0.2806 & 0 \\ 0.1406 & 0.1406 & 0.4403 & -0.2198 \\ 0.1109 & 0.1109 & 0.1109 & 0 \end{bmatrix}, B = \begin{bmatrix} 0.4079 & 0.0783 \\ 0.1683 & 0 \\ 0 & 0 \\ -0.7389 & 0.1872 \end{bmatrix} \quad (2.31)$$

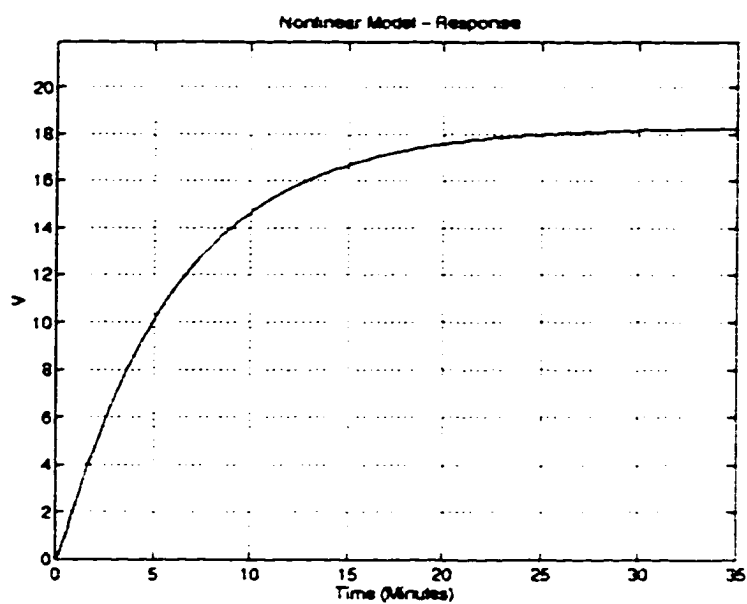


Figure 2.7 Theoretical ventilation transient for the nonlinear system.

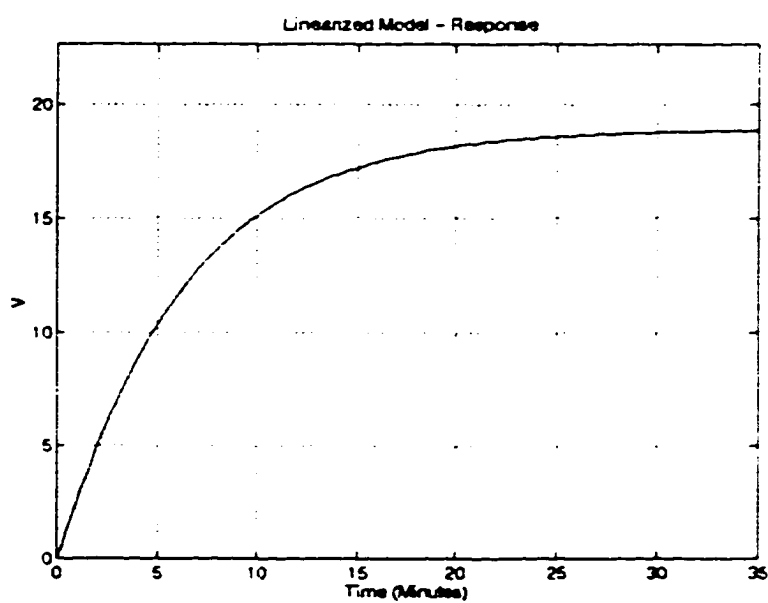


Figure 2.8 Theoretical ventilation transient for the linearized system.

CHAPTER III

SYSTEM IDENTIFICATION METHODS AND ALGORITHMS

3.1 Introduction

As has been seen in the previous chapter, there is a definite need by engineers and researchers in various fields to obtain a better knowledge of their systems, plants, structures etc. The motivation, in this work, for performing system identification is derived from the control engineering point of view. That is, one intends to design a control strategy based on the identified system characteristics. There are basically two classes of system identification methods, the nonparametric system identification methods and the parametric system identification methods. The nonparametric system identification methods were developed from the classical control theory. The frequency analysis technique played a dominant role of this development. This methodology made it possible to determine the transfer function accurately, in a format which could be used for the controls design. The modern control theory introduced an other kind of system representation, and with a few expectations, they all were of parametric form. The problem introduced with these parametric models was, that the identification process had to solve parameter estimation and related techniques. This development introduced a renewed interest in the field of parameter estimation techniques.

In general, an identification process can be characterized by a class of models, by the set of input/output data and a criterion for the determination of the goodness of the results. Zadeh³⁹ (1962) gives the following definition for system identification:

Definition 3.1:

Identification is the determination, on the basis of input and output, of a system within a specified class of systems, to which the system under test is equivalent.

In Table 3.1 some of the more popular nonparametric identification methods are listed, including a brief statement of its principal on which the method is based and its characteristics.

Table 3.1: Nonparametric Identification Methods

Method	Domain	Principle	Characteristics
Correlation	Time	Correlation of output with input, and solve for the impulse response	Approximation of the covariance matrix R_{yu}
Frequency Response	Frequency	Apply a sine wave, and determine amplitude and phase graphically	- Sinusoid inputs only - Long experiment periods necessary
Frequency Response and correlation	Frequency	Apply a sine wave, correlate with sine and cosine to suppress noise	- Sinusoid inputs only - Long experiment periods necessary
Fourier Analysis	Frequency	The empirical transfer function estimate = discrete fourier transformation of the output divided by the discrete fourier transform of the input	- Fast - Noise-sensitive

There are many other nonparametric identification methods available, though the interest in this work is on parametric system identification methods, and we shall therefore concentrate on those methods. Parametric system identification methods^{1,2,3} can be characterized on what model structure their algorithm is based, what estimation method is utilized to determine the model parameters and, if the identification process is performed on-line or off-line. The different model structures are introduced in Section 3.2, while some of the popular estimation methods are briefly described in Section 3.3. A different classification can be made based on the inclusion of a feedback controller and the availability of the input data. That is, some systems do not require feedback control, and the identification can be performed based on the input/output data of the actual system. However, for unstable and marginal stable systems, most identification methods fail to characterize such

a system. In these cases, feedback controllers are used, and the input data to the closed loop system is used for identification. Though, some systems, such as biological systems, a feedback controller is inherent, and the only choice is the identification of the closed loop system. In general, based on the inclusion of the feedback dynamics, one can distinguish between the direct system identification methods⁴⁻¹¹, where an open-loop system is identified, indirect system identification methods¹², where the closed-loop dynamics of a system is identified, and the jointly input-output identification methods¹³, where the controller dynamics is unknown and the output of the system is driven by noise only. One specific direct system identification method is introduced in Section 3.3, while a particular indirect system identification method is given in Section 3.4.

The identification methods are based on “real-live” experiments, which have to be carefully designed. For example, the input signals have to excite all the system modes, but should be restricted such that they do not destroy the system. The portion of input design in the experimental design is widely studied¹⁴, and includes issues such as parameter sensitivity, limitations on instruments, parameter identifiability, model assumptions, etc. Also of much interest is the overall experimental design, for example which output and with what frequency shall they be measured, open-loop or closed-loop dynamics etc. Some of these issues will be treated in later chapters.

3.2 Model Structures

A crucial point in the process of identifying a system is the selection of a candidate model. The choice of the model structure will greatly influence the identification process and its results. In practice, sometimes a wide variety of different models are tested and evaluated upon which delivers the best description of the actual process. The different model structures differ from each other by what they try to include of the description of the real process, that is where one sets the system boundaries, what will be taken into account as the system, and what will be neglected. Closely related to this decision is the experimental design, the determination of which signals actually should be measured at what sampling time and with what input signals. Once the experimental conditions are fixed, the choices for the candidate model structures are reduced to satisfy the requirements given by the intended application of the identified model.

In the following, four different model structures will be briefly discussed. although, only one will be used later on in this work, it is worthwhile to introduce the differences and characteristics of the other models.

3.2.1 AR-Model

Yule⁴⁰ (1927) proposed to represent a stochastic process by parametric models, in specific by an Auto-Regressive model (AR-model). This model proved to be very efficient in fitting time series data in many different fields. In general, the AR-model is a linear discrete-time filter, which is excited by random impulses. The model can be given as follows:

$$y_k = \sum_{i=1}^q w_i u_{k-i} + e_k \quad (3.1)$$

where w_i are the filter tap weights or in this case the AR-model parameters, u_{k-i} is the observed time series and e_k is a random, white noise process. Equation (3.2) satisfies the time series with the order q

$$u_n + a_1 u_{n-1} + a_2 u_{n-2} + \dots + a_q u_{n-q} = e_n \quad (3.2)$$

Than, it is easy to see that

$$u_n = w_1 u_{n-1} + w_2 u_{n-2} + \dots + w_q u_{n-q} + e_k$$

where $a_k = -w_k$. The term autoregressive stems from the fact that the current value of the process is the convolution of the past values of the process with some tap weight and some random error. The variable u is the regressor and the output of the process is therefor regressed on itself.

3.2.2 ARX-Model

The Auto-Regressive with eXogenous (ARX) input model is an extension of the AR-model by an additional, the exogenous, input. The term exogenous stems from the economical system representation, where ARX-models are quite often used. The model description includes therefore two convolution terms, the linear combination of the autoregressor and the one from the exogenous variable. The model can be given as follows:

$$y_k = \sum_{i=1}^q a_i y_{k-i} + \sum_{i=1}^q b_i u_{k-i} + e_k \quad (3.3)$$

Note, that the described model is of the form of a transversal filter. A more detailed discussion of this model and in particular its relationship with the state-space model will be given in Chapter IV.

3.2.3 MA-Model

The general difference between the AR-model and the Moving Average (MA) - model is that the former concerns the problem of solving a set of linear equations and the latter of solving a set of nonlinear equations for its model parameters. The model can be given as follows:

$$u_k = e_k + \sum_{i=1}^q b_i e_{k-i} \quad (3.4)$$

where b_i are the moving average parameters, and e_k are the white, gaussian noise terms with variance σ_e^2 . One may compute u_k by constructing a weighted average of sample values e_k, e_{k-1}, \dots , from which the name *moving average* arose.

3.2.4 ARMA and ARMAX-Models

The autoregressive moving average model (ARMA) and the autoregressive moving average with exogenous input model (ARMAX) are models composed of the above discussed models. The ARMA-model is given as follows:

$$u_k + \sum_{i=1}^q a_i u_{k-i} = e_k + \sum_{i=1}^q b_i e_{k-i} \quad (3.5)$$

where a_k and b_k are the ARMA parameters. Note that the AR-model and the MA-model are special cases of the ARMA-model.

The ARMAX-model includes the same extension as the AR-model to an ARX-model. Here, one includes the convolution of an exogenous variable to the ARMA model.

3.3 Parameter Estimation

In system identification, one is constantly confronted by the problem of inferring consistent data from measured random data. The random nature of the measurement defines the need for a suitable estimator. It also implies that the estimator should yield estimates that are reasonable, for example the estimator should deliver efficient and unbiased

estimates. Estimation theory is an intensively studied subject and known for centuries. Astronomers around 300 B.C. dealt with the problem to estimate parameters of observed data. Legendre and Gauss are credited with the popular method of least-squares around 1795. In the following, the least-squares method, the on-line least squares method and the maximum likelihood method will be briefly introduced using the following definitions:

Given the an unknown parameter set $\Theta = [a_1 \ b_1 \ a_2 \ b_2 \ \dots \ a_q \ b_q]$ and an output sequence $\xi = [y_{q+1} \ y_{q+2} \ \dots \ y_l]$, where l is the data length and q the model order. Then one can form the information matrix from the input r , and the output y

$$\Phi = \begin{bmatrix} y_q^T & r_q^T & y_{q-1}^T & r_{q-1}^T & \dots & y_1^T & r_1^T \\ y_{q+1}^T & r_{q+1}^T & y_q^T & r_q^T & \dots & y_2^T & r_2^T \\ y_{q+2}^T & r_{q+2}^T & y_{q+1}^T & r_{q+1}^T & \dots & y_3^T & r_3^T \\ \dots & \dots & \dots & \dots & \dots & \dots & \dots \\ \dots & \dots & \dots & \dots & \dots & \dots & \dots \\ y_{l-1}^T & r_{l-1}^T & y_{l-2}^T & r_{l-2}^T & \dots & y_{l-q}^T & r_{l-q}^T \end{bmatrix}$$

and the following relationship is true:

$$\xi = \Phi\Theta + \varepsilon \quad (3.6)$$

where ε is a random white, gaussian data vector.

3.3.1 Least-Squares Method

Least-squares estimation methods do employ a quadratic functional, where the objective is to minimize this function, also called cost function or loss function. The scalar cost function is composed of the estimation error; for example of the actual output and the estimated output:

$$\varepsilon_k = \xi - \Phi\hat{\Theta}$$

where $\hat{\Theta}$ is the estimated parameter vector. Then the cost function can be written

$$J = (\xi - \Phi\hat{\Theta})^T (\xi - \Phi\hat{\Theta}) \quad (3.7)$$

The least-squares solution is obtained by setting $\delta J / \delta \hat{\Theta} = 0$ which results in

$$\hat{\Theta} = (\Phi^T \Phi)^{-1} \Phi^T \xi \quad (3.8)$$

The least-squares solution is derived through deterministic arguments and can be used when there is no associated probability density function of Θ and ξ .

3.3.2 Recursive Least-Squares Method

The method introduced in Section 3.3.1 is commonly referred to as the batch processing least-squares method because the l data points are processed simultaneously. In case there is new data available after having determined an estimate based on the l data, it is necessary to completely reprocess the old data. In essence, the estimate $\hat{\Theta}$ based on Φ_l is discarded and the solution is recomputed. This problem is often found in real time system identification and on-line system identification. The recursive, also so called sequential least-squares method, considers the determination of the least-squares estimate from an estimate based on Φ_l and the new data Φ_{l+1} . The derivation of the recursive least squares method can be found in Sorenson⁴¹ (1980), and only the results will be given here.

$$\hat{\Theta}_k = \hat{\Theta}_{k-1} + K_k [\xi_k - \Phi_k \hat{\Theta}_{k-1}] \quad (3.9)$$

where the filter gain K_k is given as

$$K_k = P_k \Phi_k^T R_k^{-1} \quad (3.9)$$

and R_k is the covariance matrix of the observation and P_k is the error covariance matrix.

3.3.3 Maximum Likelihood Method

Assuming the outcome ξ of an experiment is dependent on an unknown parameter sequence Θ , then the maximum likelihood estimate of the parameters Θ are the values for which the observation ξ are most likely to occur. That is, one has to maximize the so called likelihood function, which is composed of the conditional probability density function of the observation ξ given Θ :

$$f_{ml}(\xi|\Theta) = \frac{1}{(2\pi)^{\frac{p}{2}} |R|^{\frac{1}{2}}} \exp \left[-\frac{1}{2} (\xi - \Phi \Theta)^T R^{-1} (\xi - \Phi \Theta) \right] \quad (3.10)$$

where R is the covariance matrix of a zero-mean, gaussian distributed observation, and $f_{ml}(\xi|\Theta)$ is the maximum likelihood function. Since maximizing this likelihood function results in maximizing the exponent in the bracket of Equation (3.10), this problem can be treated as minimizing a weighted sum of least squares. The result is obtained in the same way as given in Section 3.3.1:

$$\hat{\Theta} = (\Phi^T R^{-1} \Phi)^{-1} \Phi^T R^{-1} \xi \quad (3.11)$$

The maximum likelihood method can handle one of the most general identification problems, where one has to extract parameters for any type of system from data containing both measurement and process noise. The result is analogous to the solution of the weighted least-squares solution, though one can use the covariance matrix of the observation as a selection of the weighting matrix.

3.3.4 Comparison and Applicability of Parameter Estimators

It is worthwhile to mention the four statistical properties used to characterize the parameter estimation methods. Assume that $\hat{\Theta}$ is the estimation of Θ based on l observations. $\hat{\Theta}$ is *unbiased* if

$$\lim_{l \rightarrow \infty} E[\hat{\Theta}_l] = \Theta \quad (3.12)$$

If

$$\lim_{l \rightarrow \infty} P[(\hat{\Theta}_l - \Theta) = 0] = 1 \quad (3.13)$$

the estimate $\hat{\Theta}$ is considered as *consistent*. The *efficiency* of an estimation $\hat{\Theta}_l^{(1)}$ compared to $\hat{\Theta}_l^{(2)}$ is defined as the following ratio:

$$\eta = \frac{E[(\Theta - \hat{\Theta}_l^{(1)})^2]}{E[(\Theta - \hat{\Theta}_l^{(2)})^2]} \quad (3.14)$$

When $\eta < 1$, the estimation $\hat{\Theta}_l^{(1)}$ is more efficient than $\hat{\Theta}_l^{(2)}$. The estimated parameter vector $\hat{\Theta}$ is *sufficient*, if the conditional expectation

$$E[\hat{\Theta}_l | (y_1, y_2, \dots, y_l)] \quad (3.15)$$

of the parameter vector $\hat{\Theta}$ is independent of the parameter vector Θ . The sequence y_k represents a series of observations. The estimation is *sufficient*, if no other estimation can contribute any more information about the parameter vector Θ .

The batch processing least-squares estimation method is a very general, robust estimator. The estimate $\hat{\Theta}$ is unbiased, it will be shown in Chapter V, that it is also a *consistent* estimator. This estimator is well suited for off-line system identification, in contrary to the sequential or recursive least-squares estimation method, which can be used for on-line system identification. The recursive least-square estimator can be compared to the Kalman filter, and a similar problematic is found of finding the initial weighting matrix. Hence, the maximum likelihood estimator is also a *consistent* estimator and is asymptotically unbiased. Though, in the following system identification methods, we will make ample use of the batch least-squares method, and in some instances will use the recursive least-squares estimation method.

3.4 Direct System Identification

There exists several open-loop system identification methods which are quite practical. For example the method developed by Chen et al.⁶ is capable of identifying a state space model for an open-loop system from a finite difference model. The ARX model is derived through Kalman filter theory. Juang et al.⁷ developed a system identification method which also uses open-loop system input/output data, but employs a state observer, such that the ARX model needs a much lower order to represent the same system accurately, and the derivations are based on a deterministic approach. Chen et al.⁹ and Juang et al.¹⁰ used projection filters to develop the identification algorithm for stochastic systems. The relationship between the state-space model and the ARX model is derived based upon optimal estimation theory. Huang et al.¹² uses the z-transformation to derive the relationship between the state-space model and the ARX model for closed loop stochastic systems using the direct system identification method.

In the following an open-loop system identification method (OKID) is introduced, which will be used in the following chapters periodically.

3.4.1 Calculation of Observer and System Markov Parameters

Considering a stochastic, discrete time, linear autonomous system given in state-space form:

$$x_{k+1} = Ax_k + Bu_k + w_k \quad (3.16)$$

$$y_k = Cx_k + Du_k + v_k \quad (3.17)$$

where $x \in R^{n \times 1}$, $u \in R^{s \times 1}$, $y \in R^{m \times 1}$ are state, input and output vectors, respectively; w_k is the process noise, v_k is the measurement noise; $[A, B, C, D]$ are the state-space parameters. Sequences w_k and v_k are assumed to be Gaussian, white, zero-mean, and stationary with covariance matrices Q and R respectively.

Introducing a typical Kalman filter, one can write the following system equations:

$$\hat{x}_{k+1} = A\hat{x}_k + Bu_k + K\epsilon_k \quad (3.18)$$

where \hat{x}_k is the estimated state, K is the steady state Kalman filter gain, and ϵ_k is the innovation, or the so called the residual. The estimated measurement is then obtained by comparing the Equation (3.18) for \hat{x}_k with Equation (3.17)

$$\hat{y}_k = C\hat{x}_k + Du_k \quad (3.19)$$

noting that $\epsilon_k = y_k - \hat{y}_k$. Than one can easily obtain the following equation

$$\hat{x}_{k+1} = [A - KC]\hat{x}_k + [B - KD]u_k + Ky_k$$

or

$$x_{k+1} = \bar{A}x_k + \bar{B}\vartheta_k \quad (3.20)$$

where $\bar{A} = A - KC$, $\bar{B} = [B - KD \ K]$, and the information matrix $\vartheta_k = \begin{bmatrix} u_k \\ y_k \end{bmatrix}$.

Defining

$$\bar{y} = [y_q \ y_{q+1} \ \dots \ y_{l-1}] \quad (3.21)$$

$$\bar{V} = \begin{bmatrix} u_q & u_{q+1} & \dots & u_{l-1} \\ \vartheta_{q-1} & \vartheta_q & \dots & \vartheta_{l-2} \\ \dots & \dots & \dots & \dots \\ \vartheta_0 & \vartheta_1 & \dots & \vartheta_{l-q-1} \end{bmatrix}$$

and

$$\bar{Y} = \begin{bmatrix} D & C\bar{B} & C\bar{A}\bar{B} & \dots & C\bar{A}^{q-1}\bar{B} \end{bmatrix} \quad (3.21)$$

Then one can write

$$\bar{y} = \bar{Y}\bar{V} + \varepsilon + C\bar{A}^q \hat{x} \quad (3.22)$$

where $\hat{x} = [\hat{x}_0 \ \hat{x}_1 \ \hat{x}_2 \ \dots \ \hat{x}_{l-q-2}]$ and $\varepsilon = [\varepsilon_q \ \varepsilon_{q+1} \ \varepsilon_{q+2} \ \dots \ \varepsilon_{l-1}]$.

and l is the data length. If q is large enough, the term $C\bar{A}^q$ becomes zero and one can write Equation (a)

$$\bar{y} = \bar{Y}\bar{V} + \varepsilon \quad (3.23)$$

Employing the least-squares method, one can compute the sequence \bar{Y} , which are the observer Markov parameters:

$$\bar{Y} = \bar{y}\bar{V}^T [\bar{V}\bar{V}^T]^{-1} \quad (3.24)$$

The obtained observer Markov parameters are partitioned as follows:

$$\bar{Y} = [\bar{Y}_0 \ \bar{Y}_1 \ \bar{Y}_2 \ \dots \ \bar{Y}_q] \quad (3.25)$$

than

$$\bar{Y}_0 = D \quad (3.26 \text{ a})$$

$$\bar{Y}_k = C\bar{A}^{k-1}\bar{B} = [\bar{Y}_k^{(1)} \ \bar{Y}_k^{(2)}] \quad (3.26 \text{ b})$$

To recover the system Markov parameter, one can compute

$$Y_0 = \bar{Y}_0 = D \quad (3.27)$$

$$Y_k = \bar{Y}_k^{(1)} - \sum_{i=1}^k \bar{Y}_i^{(2)} Y_{k-i} \quad (3.28)$$

Once the system Markov parameter are obtained, one can determine the observer gain

Markov parameters as follows:

$$Y_1^O = \bar{Y}_1^{(2)} = CK \quad (3.29)$$

$$Y_k^O = \bar{Y}_k^{(2)} - \sum_{i=1}^{k-1} \bar{Y}_i^{(2)} Y_{k-i}^O \quad (3.30)$$

The system is uniquely determined by its Markov parameter.

3.4.2 Eigensystem Realization

In order to recover the system matrices, an eigensystem realization method is used, as is explained in the following.

As a first step, a block Hankel matrix $H(0)$ is constructed.

$$H(0) = \begin{bmatrix} Y_1 & Y_2 & \dots & Y_\beta \\ Y_2 & Y_3 & \dots & Y_{\beta+1} \\ \dots & \dots & \dots & \dots \\ Y_\alpha & Y_{\alpha+1} & \dots & Y_{\alpha+\beta-1} \end{bmatrix} \quad (3.31)$$

Using the singular value decomposition, the block Hankel matrix $H(0)$ is factorized as follows:

$$H(0) = R\Sigma S^T \quad (3.32)$$

where $R \in R^{m \times m}$ and $S \in R^{n \times n}$ are two orthogonal matrices and $R^T R = I_m$ and

$S^T S = I_n$. $\Sigma = \begin{bmatrix} s & 0 \\ 0 & 0 \end{bmatrix}$ and $s = \text{diag}[\sigma_1, \sigma_2, \dots, \sigma_n]$. σ_i are the singular values and are

in the following order:

$$\sigma_1 \geq \sigma_2 \geq \dots \geq \sigma_r > 0 \quad (3.33)$$

where $r = \text{rank}\{H(0)\}$. The order of the identified system is then determined by examining the magnitudes of the singular values. The singular values with relatively high magnitude are counted, while the singular values with relatively low magnitude are assumed to be noise related. The number of relevant singular values is the order of the identified system.

A construction of a minimum order system representation can be established as follows:

$$\hat{A} = \Sigma_n^{-1/2} R_n^T H(1) S_n \Sigma_n^{-1/2} \quad (3.34)$$

$$\hat{B} = \Sigma_n^{-1/2} S_n^T E_r \quad (3.35)$$

$$\hat{C} = E_m^T R_n \Sigma_n^{1/2} \quad (3.36)$$

where $E_r^T = [I_r \ 0_r \ \dots \ 0_r]$, $E_m^T = [I_m \ 0_m \ \dots \ 0_m]$ and m are the number of outputs and r the number of inputs.

3.4.3 Step-by-Step Procedure for System Identification using OKID

The following is a brief description of a step-by-step procedure for system identification using OKID.

1. Form an information matrix and an output vector, using Equation (3.21), and estimate the coefficient matrices of the ARX model and the observer Markov parameters by invoking the least-squares method, Equation (3.24) and (3.25).
2. Recover the system Markov parameters, using Equation (3.27) and (3.28) and the observer gain Markov parameters, Equation (3.29) and (3.30).
3. Realize the open-loop system matrices from the system Markov parameters by forming a block Hankel matrix and using singular value decomposition, Equation (3.31), (3.32) and (3.34 - 3.36).

3.5 Indirect System Identification¹

As mentioned above, the indirect system identification method calculates first the closed-loop system Markov parameters and then uses the known controller dynamics to compute the open-loop Markov parameters. The following algorithm can be applied to stochastic, linear, autonomous systems which are excited by random inputs. In the first section, the relationship between the closed-loop state space and ARX models is shown. The next section deals with the problem of the estimation of the parameter of the ARX model. Once the parameters are found, it will be shown how to compute the Markov

1. The description and derivations are from Min-Hung Hsiao, "Explicit and Iterative LQG Controller Design," Ph.D. dissertation, Old Dominion University, pp. 55-70.

parameters of the closed loop system and Kalman filter as well as the Markov parameters of the open loop system and Kalman filter. A distinction will be made for closed loop identification with full-state feedback.

3.5.1 Relationship between the State-Space and ARX Models

A finite-dimensional, linear, discrete-time, autonomous system can be modeled as:

$$x_{k+1} = Ax_k + Bu_k + w_k \quad (3.16)$$

$$y_k = Cx_k + v_k \quad (3.17)$$

where $x \in R^{n \times 1}$, $u \in R^{s \times 1}$, $y \in R^{m \times 1}$ are state, input and output vectors, respectively; w_k is the process noise, v_k is the measurement noise; $[A, B, C]$ are the state-space parameter. Sequences w , and v_k are assumed to be Gaussian, white, zero-mean, and stationary with covariance matrices Q and R respectively. One can derive a steady-state filter innovation model⁴²:

$$\hat{x}_{k+1} = A\hat{x}_k + Bu_k + AK\varepsilon_k \quad (3.37)$$

$$y_k = C\hat{x}_k + \varepsilon_k \quad (3.38)$$

where \hat{x}_k is the a prior estimated state, K is the steady-state Kalman filter gain and ε_k is the residual after filtering: $\varepsilon_k = y_k - C\hat{x}_k$. The existence of K is guaranteed if the system is detectable and $(A, Q^{1/2})$ is stabilizable⁴³.

On the other hand, any kind of dynamic output feedback controller can be modeled as:

$$p_{k+1} = A_d p_k + B_d y_k \quad (3.39)$$

$$u_k = C_d p_k + D_d y_k + r_k \quad (3.40)$$

where A_d , B_d , C_d and D_d are the system matrices of the dynamic output feedback controller, p_k is the controller state and r_k the reference input to the closed-loop system. Combining (3.37) and (3.38), the augmented closed-loop system dynamics becomes:

$$\eta_{k+1} = A_c \eta_k + B_c r_k + A_c K_c \varepsilon_k \quad (3.41)$$

$$y_k = C_c \eta_k + \varepsilon_k \quad (3.42)$$

where

$$\eta_k = \begin{bmatrix} \hat{x}_k \\ p_k \end{bmatrix}, A_c = \begin{bmatrix} A + BD_dC & BC_d \\ B_dC & A_d \end{bmatrix}, B_c = \begin{bmatrix} B \\ 0 \end{bmatrix},$$

$$A_c K_c = \begin{bmatrix} AK + BD_d \\ B_d \end{bmatrix}, \text{ and } C_c = [C \ 0]. \quad (b)$$

It is noted that K_c can be considered as the Kalman filter gain for the closed-loop system and the existence of the steady-state K_c is guaranteed when the closed-loop system matrix A_c is nonsingular.

$$y_k = \sum_{i=1}^{\infty} C_c \bar{A}^{i-1} A_c K_c y_{k-i} + \sum_{i=1}^{\infty} C_c \bar{A}^{i-1} B_c r_{k-i} + \varepsilon_k \quad (3.43)$$

where $\bar{A} = A_c - A_c K_c C_c$ and is guaranteed to be asymptotically stable because the steady state Kalman filter gain K_c exists. Since \bar{A} is asymptotically stable, $\bar{A}^i = 0$ if $i > q$ for a sufficiently large number q (see reference 10). Thus (3.43) becomes

$$y_k = \sum_{i=1}^q a_i y_{k-i} + \sum_{i=1}^q b_i r_{k-i} + \varepsilon_k \quad (3.44)$$

where

$$a_i = C_c \bar{A}^{i-1} A_c K_c, \text{ and } b_i = C_c \bar{A}^{i-1} B_c \quad (c)$$

The model described by Equation (3.44) is the ARX model, which directly represents the relationship between the input and output of the closed-loop system. The coefficient matrices a_i and b_i can be estimated through least-squares methods from a random excitation input r_k and the corresponding output y_k . From equation (3.44) it can be seen that parameters of the ARX model are linearly related to the closed-loop input-output data. Therefore, solving for an ARX model involves the problem of solving a linear programming problem involving an over-determined set of equations.

3.5.2 Open and Closed-Loop System and Kalman Filter Markov Parameters

In the previous section, an ARX model, which represents a closed-loop system, is identified from the closed-loop input/output data through the least-squares method. With known controller dynamics, the estimated ARX model can be transformed to an open-loop state-space model by the following steps. First, the closed-loop system and Kalman filter Markov parameters are calculated from the estimated coefficient matrices of the ARX model. Second, the open-loop system and Kalman filter Markov parameters are derived from the closed-loop system Markov parameters, the closed-loop Kalman filter Markov parameters, and the known controller Markov parameters. Third, the open-loop state-space model is realized by using singular-value decomposition for a Hankel matrix formed by the open-loop system Markov parameters. Finally, an open-loop Kalman filter gain is calculated from the realized state-space model and the open-loop Kalman filter Markov parameters through least-squares.

The z-transform of the open-loop state-space model (3.37) yields

$$\hat{x}(z) = (z - A)^{-1} (Bu(z) + AK\varepsilon(z)) \quad (3.45)$$

Substituting (3.45) to the z-transform of (3.17), one has

$$y(z) = C(z - A)^{-1} (Bu(z) + AK\varepsilon(z)) + \varepsilon(z) \quad (3.46)$$

$$= \sum_{k=1}^{\infty} Y(k)z^{-k}u(z) + \sum_{k=0}^{\infty} N(k)z^{-k}\varepsilon(z) \quad (3.47)$$

where $Y(k) = CA^{k-1}B$ is the open-loop system Markov parameter, $N(k) = CA^{k-1}AK$ open-loop Kalman filter Markov parameter, and $N(0)=I$ which is an identity matrix. Similarly, for the dynamic output feedback controller (3.39) and (3.40) and the closed-loop state-space model (3.41) and (3.42), one can derive

$$u(z) = \sum_{k=0}^{\infty} Y_d(k)z^{-k}y(z) + r(z) \quad (3.48)$$

$$y(z) = \sum_{k=1}^{\infty} Y_c(k)z^{-k}r(z) + \sum_{k=0}^{\infty} N_c(k)z^{-k}\varepsilon(z) \quad (3.49)$$

where $Y_d(k) = C_c A_d^{k-1} B_d$ is the controller Markov parameter, $Y_c(k) = C_c A_c^{k-1} B_c$ the closed loop system Markov parameter, and $N_c(k) = C_c A_c^{k-1} A_c K_c$ the closed-loop Kalman filter Markov parameters. It is also noted that $Y_c(0) = D_d$ and $N_c(0) = I$.

The z-transformation of the ARX model (3.44) yields

$$\left(I - \sum_{i=1}^q a_i z^{-i} \right) y(z) = \sum_{i=1}^q b_i z^{-i} r(z) + \varepsilon(z) \quad (3.50)$$

Applying long division to (3.50), one has

$$\begin{aligned} y(z) = & [b_1 z^{-1} + (b_2 + a_1 b_1) z^{-2} + (b_3 + a_1(b_2 + a_1 b_1) + a_2 b_1) z^{-3} + \dots] r(z) \\ & + [I + a_1 z^{-1} + (a_1 a_1 + a_2) z^{-2} + (a_1(a_1 a_1 + a_2) + a_2 a_1 + a_3) z^{-3} + \dots] \varepsilon(z) \end{aligned} \quad (3.51)$$

After comparing with (3.49), the closed-loop system and Kalman filter Markov parameters can be recursively calculated from the estimated coefficient matrices of the ARX model.

$$Y_c(k) = b_k + \sum_{i=1}^k a_i Y_c(k-i) \quad (3.52)$$

$$N_c(k) = \sum_{i=1}^k a_i N_c(k-i) \quad (3.53)$$

It is noted that $Y_c(0)=0$, $N_c(0)=I$, and $a_i=b_i=0$, when $i>q$. One may obtain (3.52) and (3.53) from (c) and the definition of the Markov parameters^{16, 17}. However, the derivation is much more complex.

Next, the open-loop system and Kalman filter Markov parameters can be derived from the closed-loop system Markov parameters, the closed-loop Kalman filter Markov parameters, and the known controller Markov parameters. Substituting (3.48) into (3.47) yields

$$y(z) = \left(\sum_{k=1}^{\infty} Y(k) z^{-k} \right) \left(\sum_{k=0}^{\infty} Y_d(k) z^{-k} y(z) \right) + \sum_{k=1}^{\infty} Y(k) z^{-k} r(z) + \sum_{k=0}^{\infty} N(k) z^{-k} \varepsilon(z)$$

$$= \sum_{k=1}^{\infty} \alpha_k z^{-k} y(z) + \sum_{k=1}^{\infty} Y(k) z^{-k} r(z) + \sum_{k=1}^{\infty} N(k) z^{-k} \varepsilon(z) \quad (3.54)$$

where $\alpha_k = \sum_{i=1}^{\infty} Y(i) Y_d(k-i)$. Rearranging (3.54), one has

$$\left(I - \sum_{k=1}^{\infty} \alpha_k z^{-k} \right) y(z) = \sum_{k=1}^{\infty} Y(k) z^{-k} r(z) + \sum_{k=0}^{\infty} N(k) z^{-k} \varepsilon(z) \quad (3.55)$$

Similarly, one can apply long division to (3.55), and then compare it with (3.49), to describe the close-loop system Markov parameters recursively in terms of the open-loop system and the controller Markov parameters.

$$Y_c(j) = Y(j) + \sum_{k=1}^{\infty} \alpha_k Y_c(j-k) = Y(j) + \sum_{k=1}^j \sum_{i=1}^k Y(i) Y_d(k-i) Y_c(j-k) \quad (3.56)$$

And the closed-loop Kalman filter Markov parameters can be recursively expressed in terms of the open-loop system Markov parameters, the open-loop Kalman filter Markov parameters, and the controller Markov parameters.

$$N_c(j) = N(j) + \sum_{k=1}^j \alpha_k N_c(j-k) = N(j) + \sum_{k=1}^j \sum_{i=1}^k Y(i) Y_d(k-i) N_c(j-k) \quad (3.57)$$

Rearranging (3.56) and (3.57), one has

$$Y(j) = Y_c(j) - \sum_{k=1}^j \sum_{i=1}^k Y(i) Y_d(k-i) Y_c(j-k) \quad (3.58)$$

$$N(j) = N_c(j) - \sum_{k=1}^j \sum_{i=1}^k Y(i) Y_d(k-i) N_c(j-k) \quad (3.59)$$

Equations (3.58) and (3.59) show that one can recursively calculate the open-loop system and Kalman filter Markov parameters from the closed-loop system Markov parameters (from (3.52), the closed-loop Kalman filter Markov parameters (from (3.53)), and the known controller Markov parameters $Y_d(k) = C_d A_d^{k-1} B_d$. It is noted that $Y_c(0) = 0$

and $N_c(0) = I$. One can easily verify (3.58) and (3.59) from (b), and also from the definition of the Markov parameters.

3.5.3 Step-by-Step Procedure for System Identification with Output Feedback

The above outlined method for identifying an open-loop state-space model from closed-loop input/output data with a known dynamic output feedback controller is in the following summarized by a step-by-step procedure

1. Estimate the coefficient matrices of the ARX model from closed-loop input/output data by using a least-squares method.
2. Compute the open-loop system and Kalman filter Markov parameters from the estimated coefficient matrices of the ARX model by using Equation (3.52) and (3.53).
3. Determine the open-loop system and Kalman filter Markov parameters from the closed-loop system Markov parameters, the closed-loop Kalman filter Markov parameters, and the controller Markov parameters calculated from the known controller dynamics, by using Equation (3.58) and (3.59), respectively.
4. Realize the open-loop system matrices from the open-loop system Markov parameters by using Equation (3.31) and (3.34-3.36).

3.5.4 Closed-Loop Identification with Full-State Feedback

This section deals with a special case of the aforementioned closed-loop identification method. If a constant-gain full-state feedback controller is used, the open-loop system can be identified by following a simpler procedure^{12,44}. An open-loop system with a full-state sensor and a constant gain full-state feedback controller can be modeled as:

$$x_{k+1} = Ax_k + Bu_k + w_k \quad (3.16)$$

$$y_k = x_k + v_k \quad (3.60)$$

$$u_k = -Fy_k + r_k \quad (3.61)$$

where F is the known constant feedback gain and r_k is the reference input to the closed-loop system. After applying filter innovation model⁴¹ to the open-loop system and eliminating control input u_k , the closed-loop system becomes

$$\hat{x}_{k+1} = (A - BF)\hat{x}_k + Br_k + (AK - BF)\epsilon_k \quad (3.62)$$

$$y_k = \hat{x}_k + \epsilon_k \quad (3.63)$$

Comparing (3.62) and (3.63) with (3.41) and (3.42), one can have $\eta_k = \hat{x}_k$, $A_c = A - BF$, $B_c = B$, $A_c K_c = AK - BF$, and $C_c = I$. Then one can identify the closed-loop system matrices and Kalman filter gain by the same way as the proceeding section. If the identified closed-loop system matrices and Kalman filter gain are described by a quadruplet, $\hat{A}_c, \hat{B}_c, \hat{C}_c, \hat{A}_c \hat{K}_c$, one needs to transform it to the same coordinate used in (3.62) and (3.63), so that the controller dynamics can be removed from the closed-loop system. Since full-state feedback is used, the identified output matrix \hat{C}_c is a square matrix, and is generally invariable. Then one may use \hat{C}_c^{-1} as the transformation matrix to transform the identified quadruplet to be $[\hat{C}_c \hat{A}_c \hat{C}_c^{-1}, \hat{C}_c \hat{B}_c, I, \hat{C}_c \hat{A}_c \hat{K}_c]$ where I is an identity matrix. Comparing the transformed quadruplet with (3.62) and (3.63), one can easily obtain

$$A - BF = \hat{C}_c \hat{A}_c \hat{C}_c^{-1}, B = \hat{C}_c \hat{B}_c, AK - BF = \hat{C}_c \hat{A}_c \hat{K}_c$$

The identified open-loop system matrices and Kalman filter gain become

$$A = \hat{C}_c \hat{A}_c \hat{C}_c^{-1} + \hat{C}_c \hat{B}_c F, B = \hat{C}_c \hat{B}_c, C = I, K = A^{-1}(\hat{C}_c \hat{A}_c \hat{K}_c + BF)$$

If sensors are available to provide all the state information, one can choose a constant gain controller, such that the closed-loop system has the same dimension as the open-loop system.

3.6 Coordinate Transformation

For any dynamical systems, although its system Markov parameter is unique, the realized state-space model is not unique. If one needs to compare the identified state-space model with the analytical model, both models have to be in the same coordinates. In this section, a unique transformation matrix is presented to transform any realized state-space model to a form usually used for a structure dynamic system so that any identified system parameter can be compared with the corresponding analytical one. This unique transformation matrix exists only when at least one half of the states can be measured directly. If

this condition is not satisfied, other transformation matrices may exist but they are usually not unique.

Consider a structural dynamic system

$$M\ddot{p} + D\dot{p} + Kp = Gu \quad (3.64)$$

where p is displacement, u control force, G control influence matrix and M , D and K are mass, damping and stiffness matrices, respectively. Then the state-space equation and output equation are,

$$\dot{x} = A_m x + B_m u \text{ and } y = C_m x, \quad (3.65)$$

where $x = \begin{bmatrix} p \\ \dot{p} \end{bmatrix}$, $A_m = \begin{bmatrix} 0 & I \\ -M^{-1}K & -M^{-1}D \end{bmatrix}$, $B_m = \begin{bmatrix} 0 \\ M^{-1}G \end{bmatrix}$ and C_m is the output matrix.

If half of the states can be measured directly, then $C_m = \begin{bmatrix} I & 0 \end{bmatrix}$. Now, one may first convert the realized discrete-time system $[A, B, C]$ to a continuous-time system $[A_c, B_c, D]$. If A is diagonalized by matrix Q , then

$$Q^{-1}AQ = \Lambda$$

$$A_c = Q \frac{\ln(\Lambda)}{T} Q^{-1} \quad (3.66)$$

$$B_c = (A - I)^{-1} A_c B \quad (3.67)$$

where T is the sampling time. It is assumed that the matrix $\begin{bmatrix} C \\ CA_c \end{bmatrix}$ is full rank. Let the

transformation matrix P be

$$P = \begin{bmatrix} P_1 & P_2 \end{bmatrix} = \begin{bmatrix} C \\ CA_c \end{bmatrix}^{-1} \quad (3.68)$$

then

$$P^{-1}P = \begin{bmatrix} C \\ CA_c \end{bmatrix} \begin{bmatrix} P_1 & P_2 \end{bmatrix} = \begin{bmatrix} CP_1 & CP_2 \\ CA_c P_1 & CA_c P_2 \end{bmatrix} = \begin{bmatrix} I & 0 \\ 0 & I \end{bmatrix}$$

$$P^{-1}A_cP = \begin{bmatrix} C \\ CA_c \end{bmatrix} A_c \begin{bmatrix} P_1 & P_2 \end{bmatrix} = \begin{bmatrix} CA_cP_1 & CA_cP_2 \\ CA_c^2P_1 & CA_c^2P_2 \end{bmatrix} = \begin{bmatrix} 0 & I \\ X & X \end{bmatrix}$$

$$CP = \begin{bmatrix} CP_1 & CP_2 \end{bmatrix} = \begin{bmatrix} I & 0 \end{bmatrix} \quad (3.69)$$

Note that $CP = C_m$. As a result, the identified continuous-time model $[A_c, B_c, C]$ can be transformed to be $[P^{-1}A_cP, P^{-1}B_c, CP]$ which is in the form of Equation (3.65). Then both the identified and analytical models are in the same coordinate and can be compared.

CHAPTER IV

ACCURACY MEASURES OF SYSTEM IDENTIFICATION PROCESSES

4.1 Introduction

In the first part, the ARX model for a finite-dimensional system is developed for a system with or without having a state controller. It is shown that both ARX models are of the same type, and possess the same accuracy problematic. Although for the controlled system the accuracy aspects are addressed with the help of the augmented system matrix, the system without controller can be compared to the latter one. In the third part, it is shown that the inaccuracies produced during the system identification process, starting from the ARX model through the identified open-loop Markov parameters, are of less significance, even with moderate noise levels, than the error introduced by the ARX model, the parameter estimation error of the ARX model, which is shown in part four. In part five, the influence of the process noise to the system identification accuracy is investigated.

4.2 ARX Model Representation

The ARX model is one of the most simple input-output descriptions and is basically a linear difference equation. In some literature it is also called an equation error model. As outlined in Chapter III, it represents the parameterization of a linear time invariant stochastic system. AR refers to the autoregressive part and X to the extra input, which is the exogenous variable in the field of econometrics. In this work, the ARX model represents also a finite impulse response.

System identification using ARX models have been studied extensively in the literature. Gunnarsson⁴⁵ (1991) investigated the aspects of accuracy of recursively identified ARX models in the frequency domain. Most recent literature deals with time varying

systems, such as Millner⁴⁶ (1987), Karaboyas et al.^{47,48} (1990) and (1991), Mosca et al.⁴⁹ (1989) and especially McGraw et al.⁵⁰ (1993) give conditions to use ARX models instead of ARMAX models.

In the following, the derivation of an ARX model is given. A finite-dimensional system can be modeled by the following linear, autonomous, stochastic model in discrete-time:

$$x_{k+1} = Ax_k + Bu_k + w_k \quad (4.1)$$

$$y_k = Cx_k + v_k \quad (4.2)$$

The noise sequences w_k and v_k are assumed to be white, gaussian with zero mean and represent the process noise and the measurement noise, having the covariance matrices Q and R , respectively. The vectors $x \in R^{n \times 1}$, $u \in R^{ni \times 1}$, $y \in R^{no \times 1}$ are state, input and output vectors, respectively. Utilizing the steady state filter innovation model,

$$\hat{x}_{k+1} = A\hat{x}_k + Bu_k + AK\varepsilon_k \quad (4.3)$$

$$y_k = C\hat{x}_k + \varepsilon_k \quad (4.4)$$

Where the term $\varepsilon_k = y_k - C\hat{x}_k$ contains the new information, since it cannot be obtained from the previous data. Therefore it is called innovation. Using (4.4) into (4.3):

$$\begin{aligned} \hat{x}_{k+1} &= A\hat{x}_k + Bu_k - AKC\hat{x}_k + AKy_k \\ \hat{x}_{k+1} &= \bar{A}\hat{x}_k + Bu_k + AKy_k \end{aligned} \quad (4.5)$$

where $\bar{A} = A(I_n - KC)$

The steady state Kalman filter gain K is guaranteed if the system is detectable and $(A, Q^{1/2})$ is stabilizable⁴³.

Rewriting Equation (4.4) in input/output description:

$$\begin{aligned} y_k &= C\hat{x}_k + \varepsilon_k \\ \hat{x}_k &= \bar{A}\hat{x}_{k-1} + Bu_{k-1} + AKy_{k-1} \end{aligned}$$

$$\begin{aligned}
y_k &= C\bar{A}\hat{x}_{k-1} + CBu_{k-1} + CAKy_{k-1} + \varepsilon_k \\
&\vdots \\
y_k &= CAKy_{k-1} + C\bar{A}AKy_{k-2} + \dots + C\bar{A}^{q-1} + \\
&\quad + CBu_{k-1} + C\bar{A}Bu_{k-2} + \dots + C\bar{A}^{q-1}ABu_{k-q} + \\
&\quad + C\bar{A}^q\hat{x}_{k-q} + \varepsilon_k
\end{aligned}$$

which can be rewritten as follows

$$y_k = \sum_{i=1}^q C\bar{A}^{i-1}AKy_{k-i} + \sum_{i=1}^q C\bar{A}^{i-1}Bu_{k-i} + C\bar{A}^q\hat{x}_{k-q} + \varepsilon_k \quad (4.6)$$

If $A(I_n - KC)$ is asymptotically stable, and the model order q large enough, than $\bar{A}^q \equiv 0$ and the finite difference model can be rewritten as:

$$y_k = \sum_{i=1}^q C\bar{A}^{i-1}AKy_{k-i} + \sum_{i=1}^q C\bar{A}^{i-1}Bu_{k-i} + \varepsilon_k \quad (4.7-a)$$

Defining the matrix coefficient a_i and b_i :

$$a_i \equiv C\bar{A}^{i-1}AK \text{ and } b_i \equiv C\bar{A}^{i-1}B$$

Then the ARX model can be rewritten as follows:

$$y_k = \sum_{i=1}^q a_i y_{k-i} + \sum_{i=1}^q b_i u_{k-i} + \varepsilon_k \quad (4.7-b)$$

If the system is being controlled by some feedback controller, for example a dynamic output feedback controller of the form:

$$p_k = A_d p_k + B_d y_k \quad (4.8)$$

$$u_k = C_d p_k + D_d y_k + r_k \quad (4.9)$$

where p_k is the controller state and r_k the reference input of the closed loop system. Again using the steady state filter innovation model (4.3) and (4.4), the augmented closed loop system dynamics can be written as follows:

$$\begin{aligned}
\hat{x}_{k+1} &= A\hat{x}_k + B\{C_d p_k + D_d y_k + r_k\} + AK\epsilon_k \\
&= A\hat{x}_k + BC_d p_k + BD_d y_k + Br_k + AK\epsilon_k \\
p_{k+1} &= A_d p_k + B_d C\hat{x}_k + B_d \epsilon_k
\end{aligned}$$

In matrix form:

$$\begin{aligned}
\begin{bmatrix} \hat{x} \\ p \end{bmatrix}_{k+1} &= \begin{bmatrix} A + BD_d C & BC_d \\ B_d C & A_d \end{bmatrix} \begin{bmatrix} \hat{x} \\ p \end{bmatrix}_k + \begin{bmatrix} B \\ 0 \end{bmatrix} r_k + \begin{bmatrix} AK + BD_d \\ B_d \end{bmatrix} \epsilon_k \\
y_k &= \begin{bmatrix} C & 0 \end{bmatrix} \begin{bmatrix} \hat{x} \\ p \end{bmatrix}_k + \epsilon_k
\end{aligned}$$

Using the following notation:

$$\eta = \begin{bmatrix} \hat{x} \\ p \end{bmatrix}; A_c = \begin{bmatrix} A + BD_d C & BC_d \\ B_d C & A_d \end{bmatrix}; B_c = \begin{bmatrix} B \\ 0 \end{bmatrix}; A_c K_c = \begin{bmatrix} AK + BD_d \\ B_d \end{bmatrix}$$

$$\text{and } C_c = \begin{bmatrix} C & 0 \end{bmatrix}$$

than the augmented system can be stated as follows:

$$\eta_{k+1} = A_c \eta_k + B_c r_k + A_c K_c \epsilon_k \quad (4.10)$$

$$y_k = C_c \eta_k + \epsilon_k \quad (4.11)$$

K_c is the Kalman filter gain for the closed loop system and the existence of the steady state K_c is guaranteed when the closed loop system matrix A_c is nonsingular. Substituting Equation (4.11) into (4.10), one can write

$$\begin{aligned}
\eta_{k+1} &= A_c \eta_k + B_c r_k + A_c K_c y_k - A_c K_c C_c \eta_k \\
&= (A_c - A_c K_c C_c) \eta_k + B_c r_k + A_c K_c y_k
\end{aligned}$$

Now one can use the following notation:

$$\bar{A}_c = A_c - A_c K_c C_c$$

$$\text{then} \quad \eta_{k+1} = \bar{A}_c \eta_k + B_c r_k + A_c K_c y_k \quad (4.12)$$

Using the same approach as above, Equation (4.12) can be rewritten in terms of input/output description.

$$\begin{aligned}
y_k &= C_c \eta_k + \varepsilon_k \\
\eta_k &= \bar{A}_c \eta_{k-1} + B_c r_{k-1} + A_c K_c y_{k-1} \\
y_k &= C_c \bar{A}_c \eta_{k-1} + C_c B_c r_{k-1} + C_c A_c K_c y_{k-1} + \varepsilon_k \\
y_k &= C_c \bar{A}_c^2 \eta_{k-2} + C_c \bar{A}_c B_c r_{k-2} + C_c \bar{A}_c A_c K_c y_{k-2} \\
&\quad + C_c B_c r_{k-1} + C_c A_c K_c y_{k-1} + \varepsilon_k \\
&\vdots \\
y_k &= C_c A_c K_c y_{k-1} + C_c \bar{A}_c K_c y_{k-2} + C_c \bar{A}_c^2 K_c y_{k-2} + \dots + \\
&\quad + C_c B_c r_{k-1} + C_c \bar{A}_c B_c r_{k-2} + C_c \bar{A}_c^2 B_c r_{k-3} + \dots + \\
&\quad + C_c \bar{A}_c^q \eta_{k-q} + \varepsilon_k
\end{aligned}$$

which can be reformulated as follows:

$$y_k = \sum_{i=1}^q C_c \bar{A}_c^{i-1} A_c K_c y_{k-i} + \sum_{i=1}^q C_c \bar{A}_c^{i-1} B_c r_{k-i} + C_c \bar{A}_c^q \eta_{k-q} + \varepsilon_k \quad (4.13)$$

As in the previous part, one can conclude that if $(A_c - A_c K_c C_c)$ is asymptotically stable, and the model order q large enough, than $\bar{A}_c^q \equiv 0$ and the ARX - model can be given as

$$y_k = \sum_{i=1}^q C_c \bar{A}_c^{i-1} A_c K_c y_{k-i} + \sum_{i=1}^q C_c \bar{A}_c^{i-1} B_c r_{k-i} + \varepsilon_k \quad (4.14)$$

Equation (4.14) is of the same form as Equation (4.7-a). For both of the developed ARX models, the same criterion is applied, namely that $\bar{A}^q \equiv 0$ and $\bar{A}_c^q \equiv 0$, respectively. This is only true if \bar{A} and \bar{A}_c , in the case where the system is being controlled, is stable. Since the steady-state Kalman filter gain exists, \bar{A} and \bar{A}_c are asymptotically stable. Asymptotically stable condition does not imply that q , the ARX model order, has to be

unpractical large. One way to guarantee that the truncation does not withhold too much information about the system is, if \bar{A} or \bar{A}_c are stable enough so that with relatively small q , $\bar{A}^q \equiv 0$ and $\bar{A}_c^q \equiv 0$.

The identification process used in this work is solely based on the ARX model representation of the true system. The system can only be identified as good as it is represented. Reviewing Equation (4.6)

$$y_k = \sum_{i=1}^q a_i y_{k-i} + \sum_{i=1}^q b_i u_{k-i} + C \bar{A}^q \hat{x}_{k-q} + \varepsilon_k \quad (4.6)$$

one can immediately single out two resources of errors, namely the term $C \bar{A}^q \hat{x}_{k-q}$ and the innovation. An additional error is introduced by using the least-squares method, therefore the parameter estimation error has to be investigated too.

4.3 Error Development during the System Identification Process

For this section, the identification process and its error detection for the Markov parameters can be represented in the following block diagram:

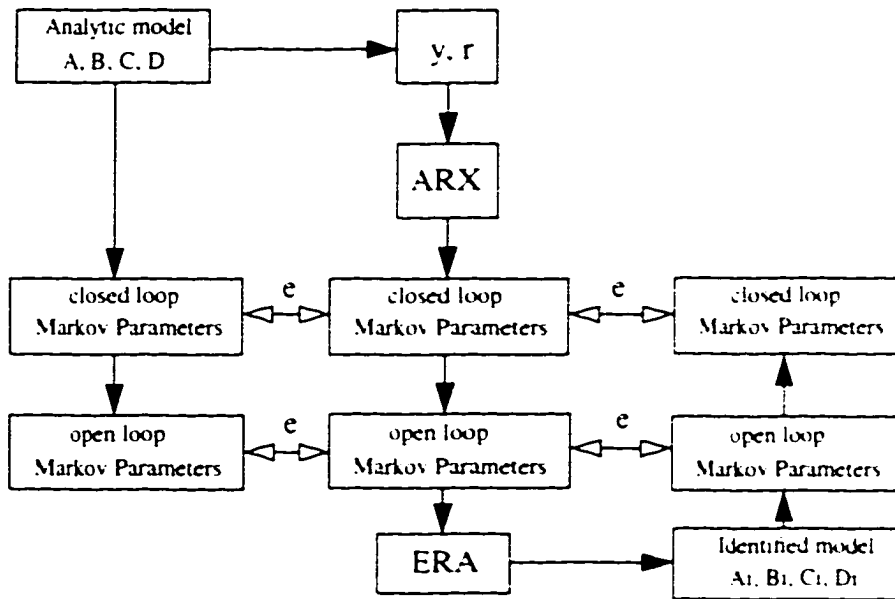


Figure 4.1 Identification schematic.

Given the analytical system, $(A \ B \ C \ D)$ and feedback dynamics, one can produce y and r , from which, using an ARX model, closed-loop and then open-loop Markov parameters can be computed. Following the procedure of system identification, one might calculate an identified system model, using eigensystem realization (ERA). From the analytical model and the identified model one can calculate directly the open-loop Markov parameters, so that one gets three sets of open-loop Markov parameters and three sets of closed-loop Markov parameters. Comparing the Markov parameters obtained from the analytical model with the identified Markov parameters, one can quantify the total error of the system identification process. Comparing the Markov parameters calculated from the ARX model, with the Markov parameters from the identified system, one will get the error composed by the noise influence and the system identification steps following the computation of the ARX model.

In the following, several comparisons between identified and calculated Markov parameters are presented. The system used for the simulations is the LAMSTAF 6 d.o.f. system for implementing the indirect and indirect closed-loop system identification methods. Both models were introduced in Chapter II, while the identification methods were given in Chapter III.

4.3.1 Closed-Loop Markov Parameters

Three sets of closed-loop Markov parameters can be computed, using the diagram given in Figure 4.2

To assure that an efficient identification is utilized, the ARX model order and the data length has to be optimized first. The optimal model order was determined by using a variable ARX model order and noise variance. The error deviation of the first 30 Markov parameter was computed for every data pair and than plotted into a contour plot. The error deviation of the Markov parameters is defined by

$$e = \frac{\|CA'B - \hat{C}\hat{A}'\hat{B}\|_F}{\|CA'B\|_F} \quad (4.15)$$

where the F-Norm is defined as $\sqrt{\sum (diag(X^T \times X))}$ and X is a matrix.

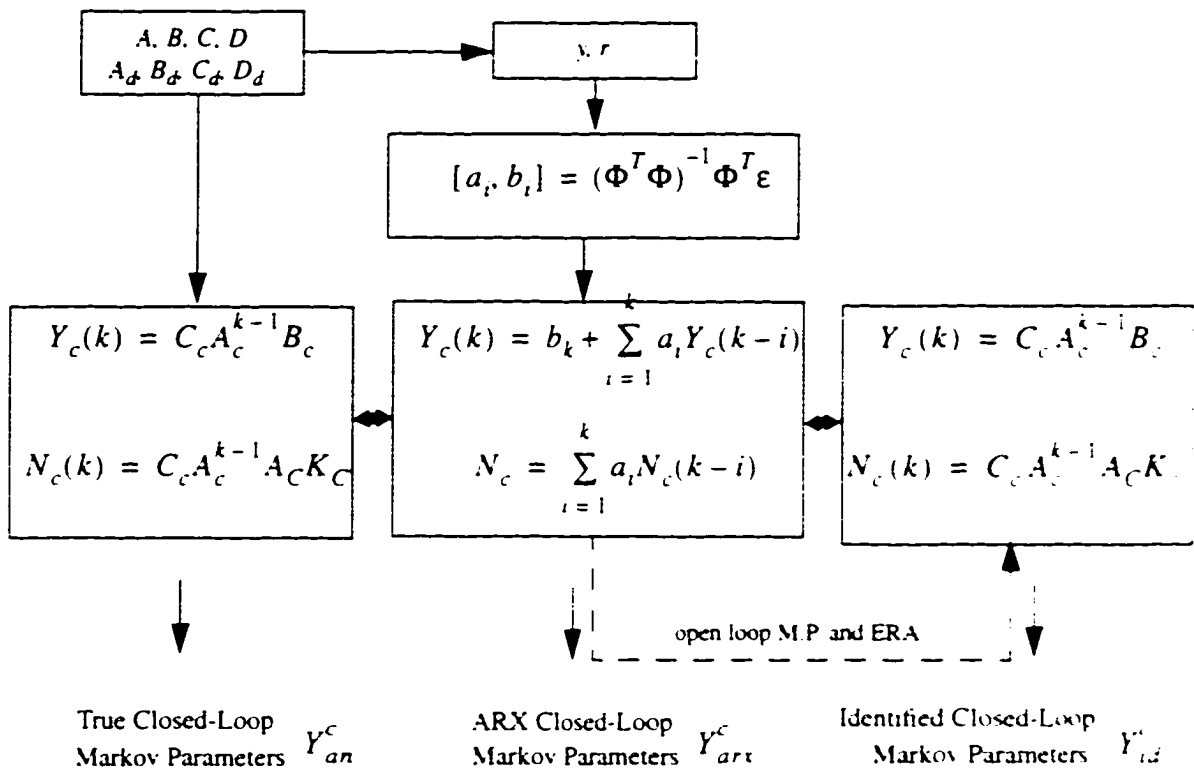


Figure 4.2 Closed-loop Markov Parameters.

Figure 4.3 depicts the contour plot for a very moderate noise range, of 0%-0.81% measurement and process noise (variance), using 5000 data points. Figure 4.4 gives the contour plot for a much larger noise level range: 0% - 3.61%. Simulations using an ARX model order of 14 indicate to provide good results for moderate to high noise levels. The determination of the data length was done in an analog fashion, while the ARX model order was kept at 14, the noise level and the number of data points were varied. Figure 4.5 depicts the contour plot for a noise range of 0% - 1% (variance) and 1000 - 5000 data points. Figure 4.6 includes a data range of 1000 - 9000 data points and a noise level range of 0% - 12.2% (variance). For the simulation of the Large Angle Magnetic Suspension Test Facility, the data length was set to be 5000.

To compare the closed-loop Markov parameters Y^c , six different noise levels were used. Table 4.1 includes the simulation results.

Table 4.1: Error Percentage of the Closed-Loop System Markov Parameters

Noise	$Y_{an}^c - Y_{id}^c$ [%]	$Y_{an}^c - Y_{arx}^c$ [%]	$Y_{arx}^c - Y_{id}^c$ [%]
0.01%	0.7156	0.7631	0.4125
1.0%	6.7190	7.5804	3.3978
5.0%	12.507	13.629	6.8302
10.0%	17.756	19.275	9.4349
15.0%	24.655	26.647	11.847
20.0%	27.262	30.700	13.033

The error between the analytical and identified, and the analytical and the closed-loop Markov parameter derived from the estimated ARX model parameters, are almost the same. The error is significantly lower between the 'ARX-model' Markov parameters and the identified closed-loop Markov parameters. Figure 4.7 shows the three sets of the (1,1) element closed-loop Markov parameters for the case of 5% measurement and process noise (variance).

4.3.2 Open-Loop Markov Parameters

To calculate the open-loop Markov parameters, one can use the following formulas for the indirect identification method:

$$Y(j) = Y_c(j) - \sum_{k=1}^j \sum_{i=1}^k Y(i) Y_d(k-i) Y_c(j-k) \quad (4.16)$$

$$N(j) = N_c(j) - \sum_{k=1}^j \sum_{i=1}^k Y(i) Y_d(k-i) N_c(j-k) \quad (4.17)$$

And for the direct method:

$$\bar{Y}_k = \begin{bmatrix} \bar{Y}_k^{(1)} & -\bar{Y}_k^{(2)} \end{bmatrix}, \text{ where } \bar{Y}_0 = D \text{ (see Equation 3.25)}$$

$$Y_k = \bar{Y}_k^{(1)} - \sum_{i=1}^k \bar{Y}_k^{(2)} Y_{k-i} \quad (4.18)$$

Comparing the analytical, 'true', Markov parameters with the one derived using the input output data and the identified system, one can compose Table 4.2.

Table 4.2: Error Percentage of the Open-Loop System Markov Parameters

Noise	$Y_{an}-Y_{arx}$ indirect	$Y_{an}-Y_{id}$ indirect	$Y_{arx}-Y_{id}$ indirect	$Y_{an}-Y_{arx}$ direct	$Y_{an}-Y_{id}$ direct	$Y_{arx}-Y_{id}$ direct
0.01%	0.4074	0.4085	0.0303	0.4010	0.4099	0.0239
1.0%	3.0263	3.0134	0.2441	2.1480	2.1151	0.2278
5.0%	5.1982	5.4720	0.5036	5.3774	5.2951	0.4723
10.0%	7.2277	7.1515	0.7069	7.4325	7.3660	0.6623
15.0%	10.913	11.275	0.8563	7.5199	7.3165	0.8536
20.0%	24.169	25.790	0.8967	19.965	21.108	0.9140

Table 4.2 indicates the same trend found in Table 4.1, the major contribution of the error in the system identification process is introduced by the approximated system description of the ARX model. The error developed during the process of computing the identified system matrices from the identified open-loop Markov parameters is negligible, even with high measurement and process noise levels. Figure 4.8 depicts the three open-loop Markov parameters, (1,1) element, for the system with 5% measurement and process noise (variance).

4.4 Accuracy of the ARX Parameterization

Probably the most efficient way to determine if the ARX model representation is good enough, is to use the identified model, and generate a new set of data, which then can be compared to the set of data obtained using the analytical model, or in practice the physical system. Since we are at this point not interested in the accuracy of the simulation results, but in quantifying the accuracy of the ARX parameterization, we do not need to generate new data sets. Obviously, a simple way to determine if the ARX model describes the system well enough is to plot the output of the system and compare it with the analytical data.

In this section, the ARX parameterization is investigated using correlation analysis. Also an attempt is made to quantify the information contents truncated by the ARX model representation of the actual system.

4.4.1 Output Description

The correlation of two processes indicates the linear relationship between those two processes. The correlation coefficient r is bounded to be in the interval $-1 \leq r \leq 1$. One can utilizing r to measure the usefulness of the regression of two different output description. In fact, the square of r times 100 is the percentage of the data which can be explained by the linear relationship. Table 4.3 gives the different correlation coefficient for the simulation results of the LAMSTF 6 d.o.f. system, using three noise levels.

Table 4.3: Correlation Coefficient for the Outputs

Noise Variance	r $[y_{an}-y_{arx-id}]$	r $[y_{an}-y_{arx}]$	r $[y_{an}-y_{rr}]$	r $[y_{arx}-y_{arx-id}]$
0.001%	0.9928	0.9983	1.0	0.9901
1.0%	0.9820	0.9908	0.9951	0.9869
5.0%	0.9662	0.9733	0.9889	0.9700

In the table, y_{an} is the output generated from the analytical model including noise, y_{arx-id} is the output computed from the identified, or estimated, ARX model parameters, y_{arx} is the output given by the ARX model constructed from the simulated data and the analytical ARX model parameters, y_{rr} is the analytical output of the system, having no noise influence included. From Table 4.3, one can see that y_{arx} is slightly less accurate than the output representation of y_{an} . The correlation between y_{an} and y_{rr} shows the influence of the process and measurement noise. With no noise, we have a perfect match between y_{an} and y_{rr} while with increasing noise level, the relationship drops too. The correlation between y_{an} and y_{rr} represents an upper bound for the accuracy of the other output descriptions.

If it is possible to plot an output representation as a function of the frequency, the characteristic of the output representation can be investigated in some different fashion.

Using the power density spectrum estimation of a random vector, one can describe the frequency content of the signal, represented by the vector. Since we deal with a finite length of data, we have to estimate the power spectral density. For the simulation, Welch's method¹ to estimate the power spectral densities was employed. The correlation coefficient can take on any value between 0 and 1, where one means that the linear description is perfect and zero means there is no linear correlation existing. If one interested in the frequency at which the linear correlations either at best, or not existing, one can plot the coherence function estimate. Given the power spectral densities estimations of two random vectors, the coherence function is given as:

$$C_{xy}(w) = \frac{|P_{xy}(w)|^2}{P_{xx}(w)P_{yy}(w)} \quad (4.19)$$

This quotient is a real number between 0 and 1, which measures the correlation between x and y at the frequency w .

Figure 4.9 depicts the coherence function estimate for different output descriptions of the LAMSTF system, using a noise level of 5% (variance). As one can see the low frequencies of the output is well represented, while for higher frequencies the correlation coefficient drops. This is to be credited partially to the limited sampling time of the data acquisition, where a sampling frequency of 1000 Hz is used for this simulation. The coherence function estimate of the two ARX model representation, the analytical one, y_{arx} , and the model based on the input output data, y_{arx_id} , indicates that the ARX model representation is mainly responsible for the identification error. Since the system has seven outputs, a richer conclusion is not possible, other than a confirmation of the results gathered in the previous section.

4.4.2 Quantification of the Truncation Error of the ARX Model

Another concern related to the accuracy aspects are the neglected terms in Equation (4.6). The quantities $C\bar{A}^q\hat{x}_{k-q}$ and ϵ_k are being neglected for the system representation using an ARX model. The goal in this section is to quantify the information

1. Welch, Peter D. "The Use of Fast Fourier Transform for the Estimation of Power Spectra. A Method Based on Time Averaging over Short, Modified Periodograms." *IEEE Trans. Audio Electroacoust.* Vol AU-15, 1967: pp. 70-73.

contents associated with the truncated terms. For this purpose, the same methodology is applied as in the previous subsection.

Figure 4.10 depicts the two neglected terms for the first output of the LAMSTF 6 d.o.f. system over the whole data length, and Figure 4.11 shows the neglected terms for the first output over the last 100 data points. Figure 4.12 graphs the coherence function estimate for $C\bar{A}^{-q}\hat{x}_{k-q}$ and y_{an} , while Figure 4.13 depicts the coherence function estimate for ε_k and y_{an} . From the graphs, one can recognize that the first term, $C\bar{A}^{-q}\hat{x}_{k-q}$ has a linearly related information content in the low frequency area, while the innovation does contain information relevant to y_{an} in the higher frequencies. Since all the closed-loop poles of the system, and most of the open-loop poles of the system are in the low frequency area, the neglected term $C\bar{A}^{-q}\hat{x}_{k-q}$ clearly bears important information about the system to be identified.

4.5 Influence of the Process Noise to the System Identification

Describing a stochastic, finite dimensional, linear, discrete-time, autonomous system, one can use Equation (4.1)

$$x_{k+1} = Ax_k + Bu_k + w_k \quad (4.1)$$

$$y_k = Cx_k + v_k \quad (4.2)$$

To ensure stability, and assuming all the states are measurable, a general dynamic output feedback controller is used

$$p_k = A_d p_k + B_d y_k \quad (4.8)$$

$$u_k = C_d p_k + D_d y_k + r_k \quad (4.9)$$

then the augmented system can be written as follows:

$$\begin{aligned} x_{k+1} &= Ax_k + B(C_d p_k + D_d y_k + r_k) + w_k \\ &= (A + BD_d C)x_k + BC_d p_k + Br_k + BD_d v_k + w_k \end{aligned} \quad (4.20)$$

$$p_{k+1} = A_d p_k + B_d Cx_k + B_d v_k \quad (4.21)$$

writing these equations in compact form:

$$\begin{bmatrix} x \\ p \end{bmatrix}_{k+1} = \begin{bmatrix} A + BD_d C & BC_d \\ B_d C & A_d \end{bmatrix} \begin{bmatrix} x \\ p \end{bmatrix}_k + \begin{bmatrix} B \\ 0 \end{bmatrix} r_k + \begin{bmatrix} BD_d \\ B_d \end{bmatrix} v_k + \begin{bmatrix} I_n \\ 0 \end{bmatrix} w_k$$

$$y_k = \begin{bmatrix} C & 0_n \end{bmatrix} \begin{bmatrix} x \\ p \end{bmatrix}_k + v_k$$

defining new variables:

$$\Psi \equiv \begin{bmatrix} x \\ p \end{bmatrix}; \quad A_c \equiv \begin{bmatrix} A + BD_d C & BC_d \\ B_d C & A_d \end{bmatrix}; \quad B_c \equiv \begin{bmatrix} B \\ 0 \end{bmatrix}; \quad \tau_v \equiv \begin{bmatrix} BD_d \\ B_d \end{bmatrix}; \quad C_c \equiv \begin{bmatrix} C & 0 \end{bmatrix} \quad (4.22)$$

where A_c , B_c and C_c have the same definitions as defined earlier. The augmented system can be stated as follows:

$$\Psi_{k+1} = A_c \Psi_k + B_c r_k + \tau_v v_k + \tau_w w_k \quad (4.23)$$

$$y_k = C_c \Psi_k + v_k \quad (4.24)$$

Substituting (4.24) into (4.23):

$$\Psi_{k+1} = (A_c - \tau_v C_c) \Psi_k + B_c r_k + \tau_v v_k + \tau_w w_k$$

defining $\Lambda = A_c - \tau_v C_c$

$$\Psi_{k+1} = \Lambda \Psi_k + B_c r_k + \tau_v v_k + \tau_w w_k \quad (4.25)$$

Rewriting (4.24) in terms of input/output descriptions; using (4.25) yields:

$$y_k = C_c \Psi_k + v_k$$

$$\Psi_k = \Lambda \Psi_{k-1} + B_c r_{k-1} + \tau_v v_{k-1} + \tau_w w_{k-1}$$

$$y_k = C_c \Lambda \Psi_{k-1} + C_c B_c r_{k-1} + C_c \tau_v v_{k-1} + C_c \tau_w w_{k-1} + v_k$$

$$\Psi_{k-1} = \Lambda \Psi_{k-2} + B_c r_{k-2} + \tau_v v_{k-2} + \tau_w w_{k-2}$$

$$\begin{aligned} y_k = & C_c \Lambda^2 \Psi_{k-2} + C_c \Lambda B_c r_{k-2} + C_c \Lambda \tau_v v_{k-2} + C_c \Lambda \tau_w w_{k-2} + \\ & + C_c B_c r_{k-1} + C_c \tau_v v_{k-1} + C_c \tau_w w_{k-1} + v_k \end{aligned}$$

$$\begin{aligned} y_k = & C_c \Lambda^3 \Psi_{k-3} + C_c \Lambda^2 B_c r_{k-3} + C_c \Lambda^2 \tau_v v_{k-3} + C_c \Lambda^2 \tau_w w_{k-3} + \\ & + C_c \Lambda B_c r_{k-2} + C_c \Lambda \tau_v v_{k-2} + C_c \Lambda \tau_w w_{k-2} + \end{aligned}$$

$$+ C_c B_c r_{k-1} + C_c \tau_v y_{k-1} + C_c \tau_w w_{k-1} + v_k$$

$$y_k = \sum_{i=1}^q C_c \Lambda^{i-1} B_c r_{k-i} + \sum_{i=1}^q C_c \Lambda^{i-1} \tau_v y_{k-i} + \sum_{i=1}^q C_c \Lambda^{i-1} \tau_w w_{k-i} + v_k + C_c \Lambda^q \Psi_{k-q} \quad (4.26)$$

Equation (4.26) represents the parameterization of the true system, where the regressor vector is composed of the input, output and the process noise. Investigating the term $C_c \Lambda^q$, as is shown when q is large enough, $\Lambda^q \cong 0$ and the parameterization can be given:

$$y_k = \sum_{i=1}^q C_c \Lambda^{i-1} B_c r_{k-i} + \sum_{i=1}^q C_c \Lambda^{i-1} \tau_v y_{k-i} + \sum_{i=1}^q C_c \Lambda^{i-1} \tau_w w_{k-i} + v_k \quad (4.27)$$

The term $\sum_{i=1}^q C_c \Lambda^{i-1} \tau_w w_{k-i}$ represents the process noise influence on the ARX parameterization. Expanding this term yields:

$$\begin{bmatrix} C & 0 \end{bmatrix} \begin{bmatrix} A & BC_d \\ 0 & A_d \end{bmatrix}^{i-1} \begin{bmatrix} I_n \\ 0 \end{bmatrix} w_{k-i} \quad (4.28)$$

Using $i=1,2,\dots,q$, the process noise influence is

$$CAw_{k-1} + CA^2w_{k-2} + \dots + CA^qw_{k-q} \quad (4.29)$$

which leads to the following conclusion that the controller does have no influence on limiting the influence of the process noise for the ARX model representation.

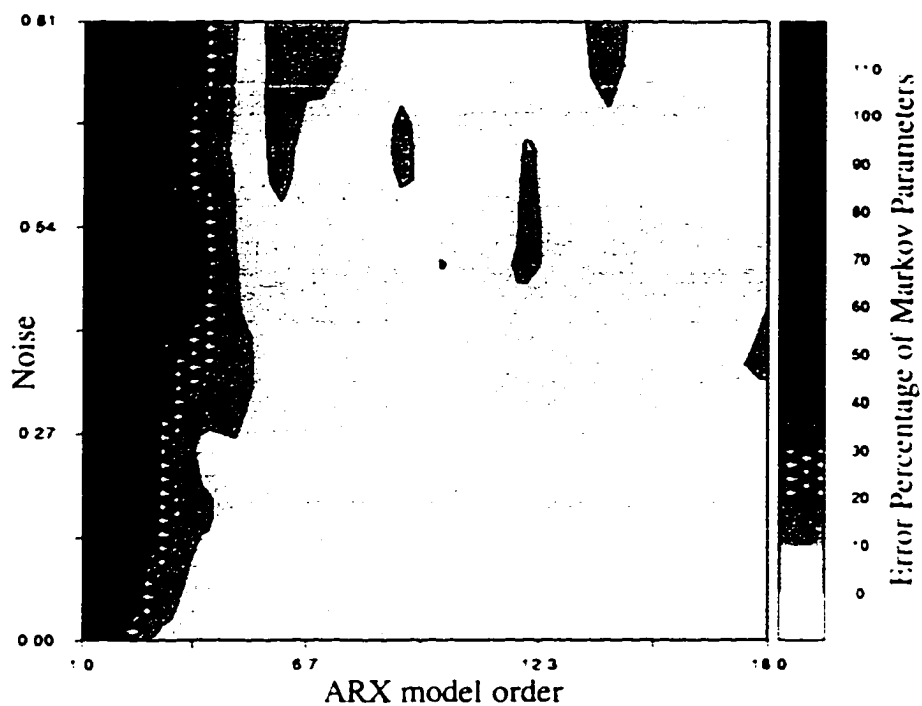


Figure 4.3 Contour plot of the percentage of error deviation of the system Markov Parameters for a variable ARX model order and noise level, using 5000 data points.

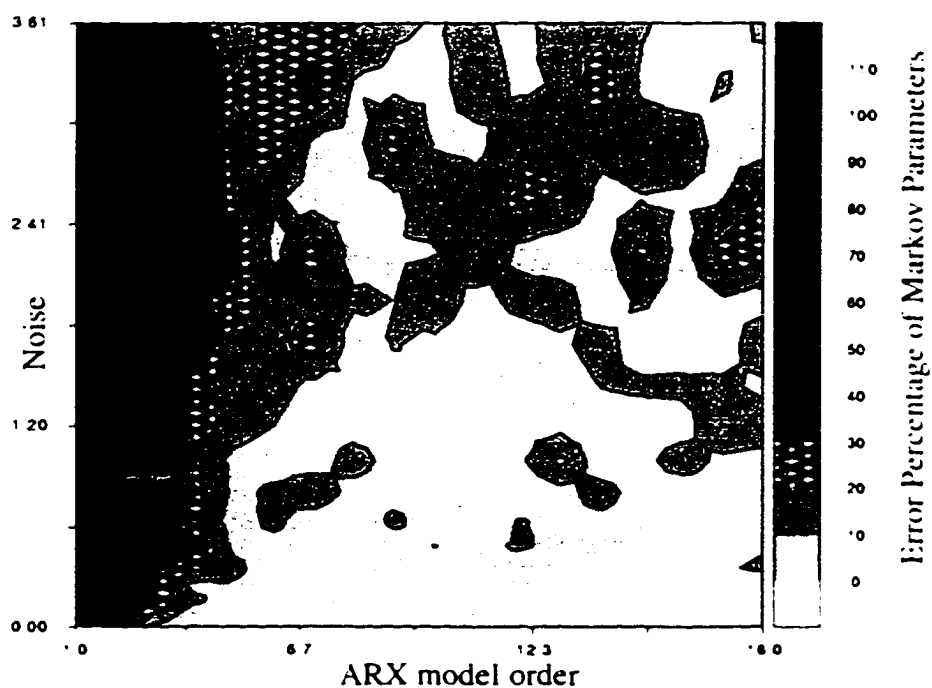


Figure 4.4 Contour plot of the percentage of error deviation of the system Markov Parameters for a variable ARX model order and noise level, using 5000 data points.

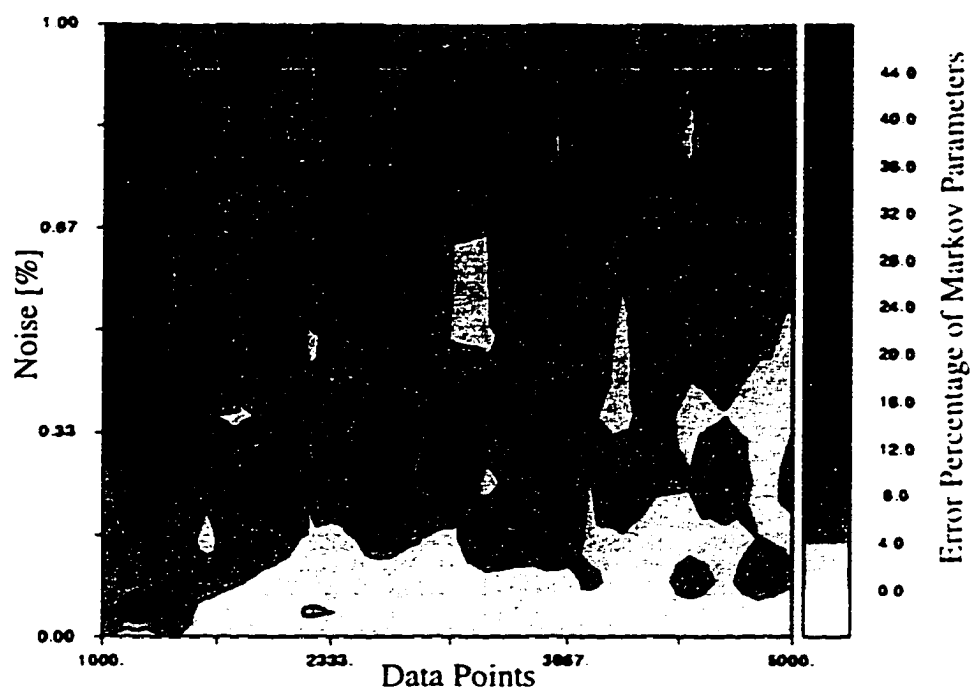


Figure 4.5 Contour plot of the error percentage of the system Markov parameters for a variable data length and noise level, using an ARX model order of 14.

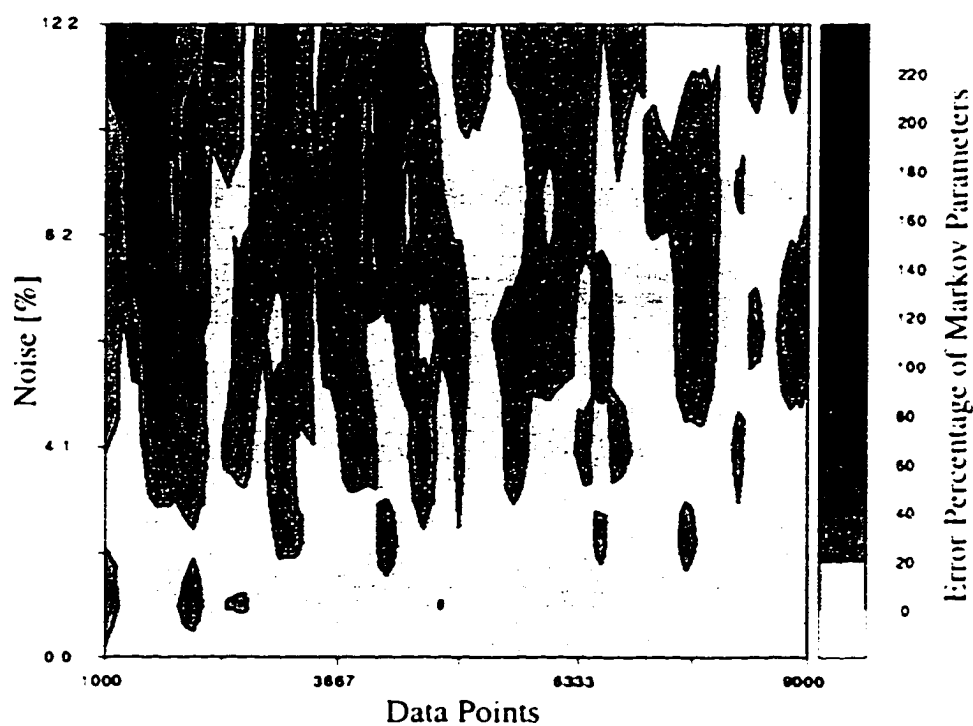


Figure 4.6 Contour plot of the error percentage of the system Markov parameters for a variable data length and noise level, using an ARX model order of 14.

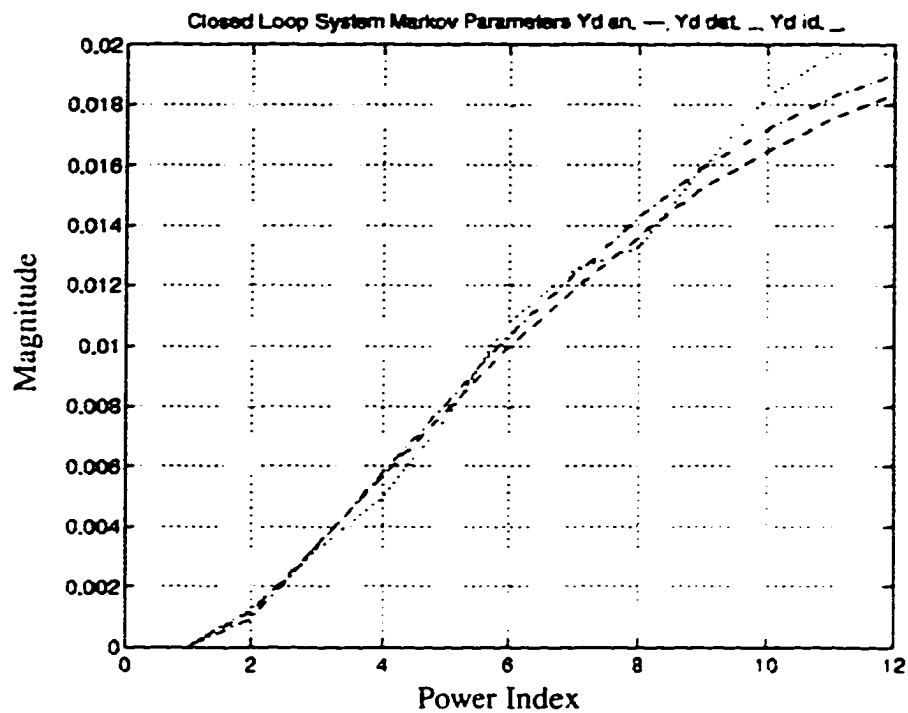


Figure 4.7 Closed-loop system Markov parameters, (1,1) element, using the LAMSTF 6 d.o.f. system and 5% measurement and process noise (variance).

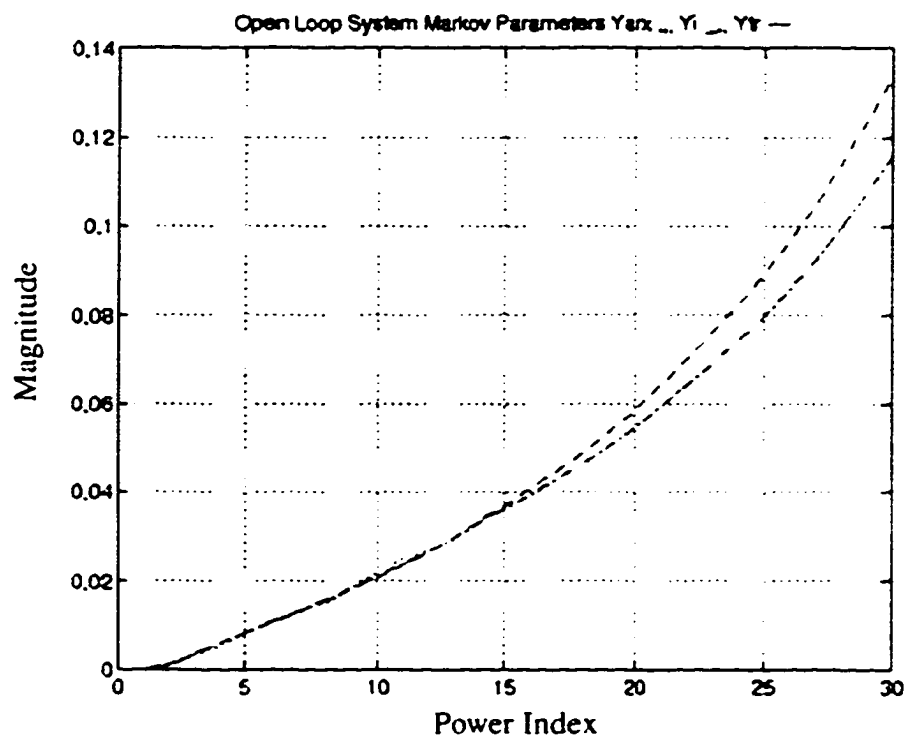


Figure 4.8 Open-loop system Markov parameters, (1,1) element, using the LAMSTF 6 d.o.f. system and 5% measurement and process noise (variance).

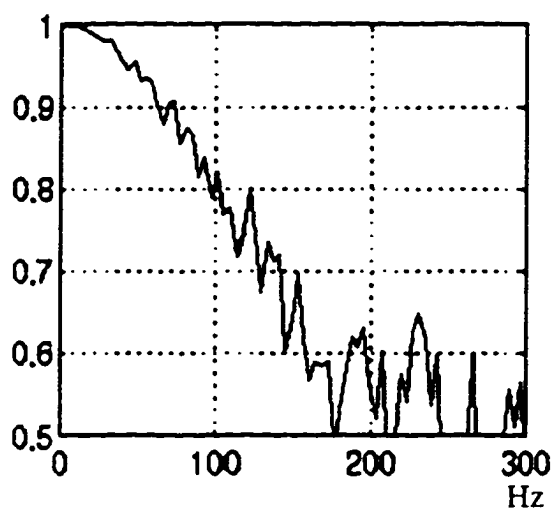
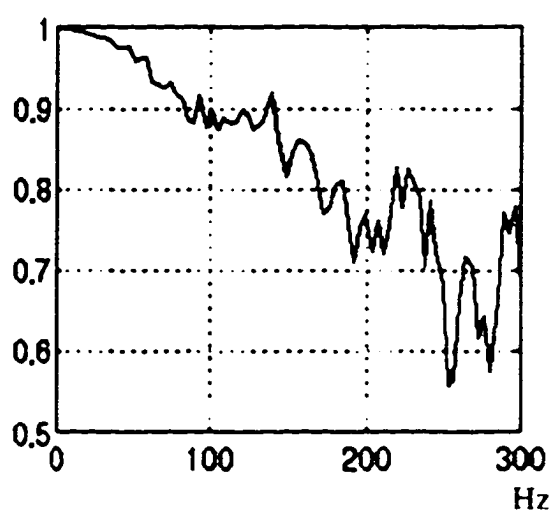
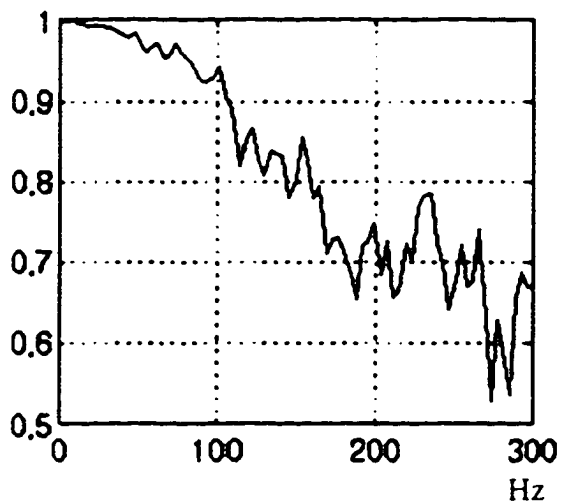
Coherence Function Est. for y_{an} and y_{arx} Coherence Function Est. for y_{an} and y_{arx_id} Coherence Function Est. for y_{arx} and y_{arx_id} 

Figure 4.9 Coherence Function Estimate for y_{arx} , y_{arx_id} , y_{an} , using the LAMSTF 6 d.o.f. system and 5% measurement and process noise (variance).

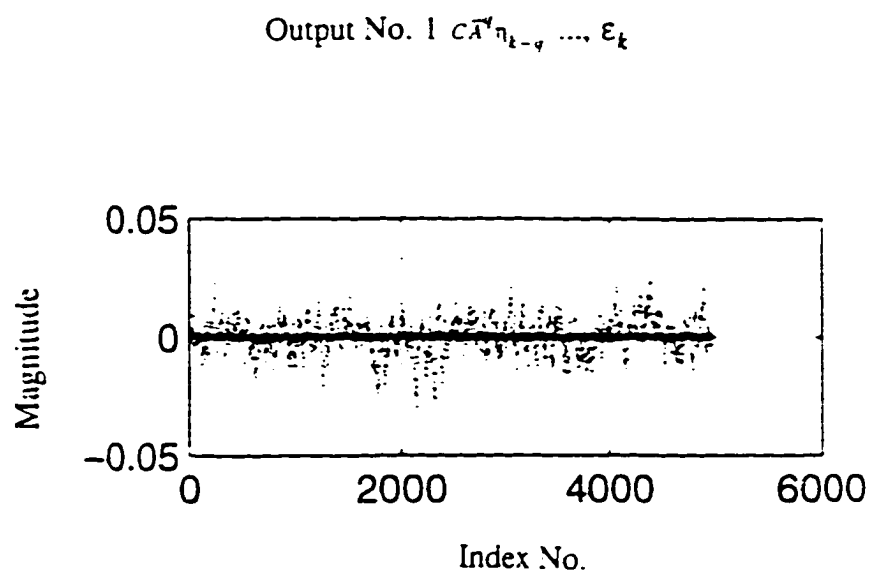


Figure 4.10 $C\bar{A}^q \eta_{k-q}$ and ϵ_k for the first output of the LAMSTF 6 d.o.f. system.

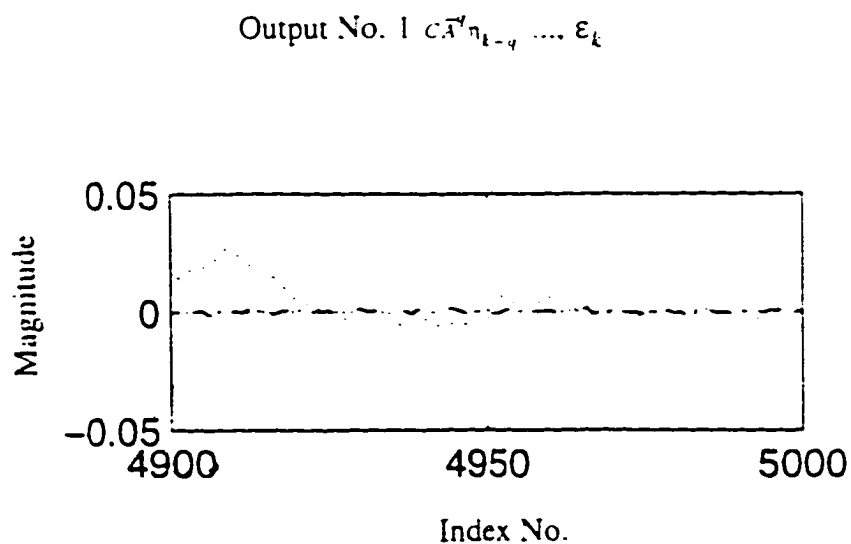


Figure 4.11 $C\bar{A}^q \eta_{k-q}$ and ϵ_k for the first output using 100 data points.

Coherence Function Estimate of y_{an} and $C\bar{A}^q\eta_{k-q}$

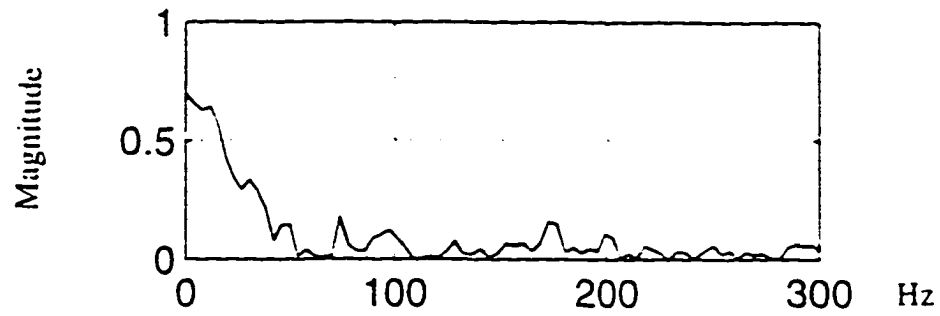


Figure 4.12 Coherence Function Estimate for y_{an} , $C\bar{A}^q\eta_{k-q}$ and ϵ_k for 5% noise.

Coherence Function Estimate of y_{an} and ϵ_k

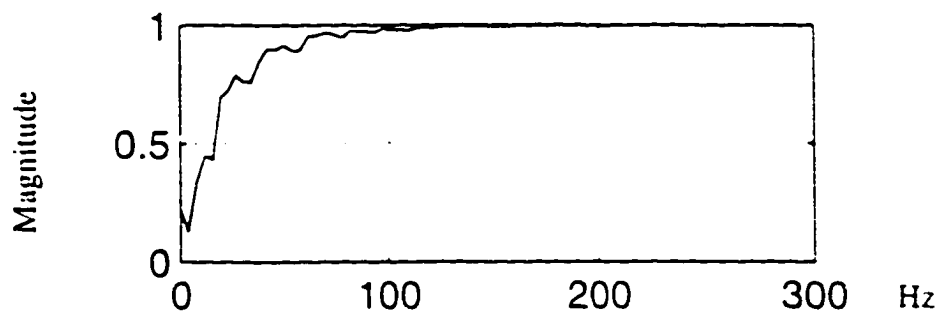


Figure 4.13 Coherence Function Estimate for y_{an} and ϵ_k for 5% noise (variance).

CHAPTER V

A NOTE ON IDENTIFIABILITY

5.1 Introduction

Identifiability is characterized by the ability to deduce all necessary information from a data set of observations of an object, so that the object can be uniquely determined. One can distinguish between three different identifiability terms, depending on what the objective is. Parameter identifiability is the discipline where model parameters are deduced from observations. It gives information about the internal model parameters from data concerning the external system behavior. System identifiability describes the ability to identify a system from data generated by the system itself. Structural identifiability defines the capability of obtaining knowledge of the internal structure of a system from input/output data.

Ljung et al.¹⁸ (1974) and Gustavsson et al.³ (1977) divided the identifiability problem in a systematic manner: the identification experiment is depending on the system S , the model M and its parameterization, where the parameter vector is denoted as Θ , the experimental condition X and the identification method J . The systems considered are linear, multivariable, stochastic, for example the system can be given in the following form:

$$y(z) = G_S(q^{-1})u(t) + H_S(q^{-1})e(t) \quad (5.1)$$

where $y(t)$ is the output vector, $u(t)$ corresponds to the input, and $e(t)$ is a sequence of independent, random vectors with zero mean and the backward shift operator is denoted as q^{-1} . To derive a model, the system is parameterized by a vector Θ . If this parameter is varied over a feasible region of values, the model becomes a model structure. Experimental conditions contain informations on the design of the input. Following Ljung's¹ definitions, one can state the following set:

$$D_T(S, M) = \{ \Theta | G_{M(\Theta)}(z) = G_S(z) \text{ and } H_{M(\Theta)}(z) = H_S(z) \} \quad (5.2)$$

This set consists of the parameter value Θ that yield models $M(\Theta)$ with the same transfer function and the same noise characteristics as the system S . Then the following definitions are given:

Definition 5.1:

The system S is said to be system identifiable under M , J , and X , $SI(M, J, X)$, if

$$\Theta(l; S, M, J, X) \rightarrow D_T(S, M) \quad (5.3)$$

with probability one as $l \rightarrow \infty$.

Definition 5.2:

The system S is said to be strongly system identifiable under J and X , $SSI(J, X)$, if it is $SI(M, J, X)$ for all M such that $D_T(S, M)$ is nonempty.

Definition 5.3:

The system S is said to be parameter identifiable under M , J , and X , $PI(M, J, X)$, if it is $SI(M, J, X)$ and $D_T(S, M)$ consists of only one element.

In the following, a short overview of system identifiability is given, followed by a survey of the parameter identifiability problem. In the later part, parameter identifiability is attempted to be applied to identification methods, using an ARX model description (parameterization) of linear autonomous stochastic systems.

5.2 System Identifiability

System identifiability concerns, as mentioned above, the capability of inferring information from generated data from the system, about the system. Systems can be treated as abstract objects and its parameterization is of no concern at this point. The outcome depends on the information content of the data and on the identification procedure for modeling the observed data. Most studies were done for linear autonomous systems, which are controllable and observable. Deterministic system identifiability from arbitrary exact data was studied by, among others, Grewald and Glover et al.⁵¹ (1976), Sontag et al.^{52,53} (1979) and (1980), Kalman⁵⁴ (1983), Chen⁵⁵ (1987) and Heij⁵⁶ (1993). Heij⁵⁷ (1992) investigated the question of identifiability of finite dimensional linear time invariant deterministic systems on the basis of observed data. The minimum number of

observations is expressed in terms of the rank of autoregressive representations. System identifiability for deterministic and stochastic systems were treated by Staley et al.⁵⁸ (1970), where the system is represented by linear scalar difference equations and identifiability is given in terms of observability.

The subject of structural identifiability and system identifiability are sometimes treated in the same way. The term structural Identifiability was introduced by Bellman et al.⁵⁹ (1970), where the possibility of finding a unique minimum of a given cost function for a specific structure is investigated. The structure contains the information of the couplings between the states and the inputs and outputs. Bellman concludes that for linear systems, all structures are identifiable whose parameters are uniquely given by the impulse response.

5.3 Parameter Identifiability

Parameter identifiability is an extensively studied field in the controls and mathematical community. Tse et al.⁶⁰ (1972) defines identifiability of model parameters in terms of consistency in the probability of the parameter estimate. He also establishes necessary and sufficient tests for parameters to be identifiable. It is shown that if the minimal dimension of the system is known, then controllability, observability, and stability imply identifiability, except for the initial condition. Glover et al.⁶¹ (1974) investigates the problem of parameterization, having one of the objective of addressing the identifiability problem. He shows the importance of canonical representation for controllable linear system. The conditions for identifiability from the spectral density for systems driven by white noise is derived. Also conditions for local and global identifiability, based on the system transfer function, are given. Ljung et al.¹⁸ (1974) studies the identifiability problem conceptual for closed loop systems. Soederstroem et al.⁶² (1975) investigates the identifiability problem for data obtained from closed loop experiments of noise free systems restricted to single-input output. Correa et al.^{63,64} (1984), uses instead of canonical forms, pseudo canonical forms, to establish the relationship between state-space form, and matrix fraction descriptions (MFDs) and finite difference equations. It is also shown how to remove the dependencies of the parameters in the MFDs, by ordering the output variables. In the second part of Correa's work, the estimation of parameters from pseudo-canonical, input-output

models is treated. Gevers et al.⁶⁵ (1984) takes another approach, instead of using canonical forms, he makes use of so called overlapping forms to represent multivariable systems. Also uniquely identifiable parametrization are given, using overlapping forms, for state-space and ARMA models from a Hankel matrix composed of Markov parameters. Swami et al.⁶⁶ (1992) looks at estimation of AR order and identifiability of parameters, where single-input output ARMA models are considered, in addition to colored additive measurement noise. Van Den Hof et al.⁶⁷ (1992) raises concerns about identifiability for systems operating in closed-loop with delays in the plant and/or the controller. Conditions are developed such that the LS method is able to consistently estimate the open-loop plant. Ljung et al.⁶⁸ (1994) defines global identifiability for model parameters, which is the decision if all the free parameters of a model structure can be uniquely recovered from data. He shows how to reduce the question for global structural identifiability to the question of whether the given model structure can be rearranged as a linear regression. Also the problem of persistent excitation for the input is treated.

5.3.1 Canonical Forms and Identifiability

If the system (A, B, C, D) is parameterized by the unknown parameter Θ , it is desired to achieve the following two properties: *Property 1*: The parameterization should be identifiable in some sense. *Property 2*: All systems in an appropriate class can be represented by the parameterization.

Canonical forms are one approach to this parameterization problem, especially for deterministic systems. A requirement is the minimality, or at least a strong limitation, of the number of the significant parameters of the model and this means the choice of a suitable canonical, or quasi-canonical form. Several authors investigated the approach using canonical forms, such as Fisher⁶⁹ (1966), Mayne⁷⁰ (1972), Denham⁷¹ (1974), Hsiao⁷² (1983), Gevers & Werts^{65,73} (1984, 1987) and Hannan and Deistler⁷⁴ (1988).

5.3.2 Process Identification of Linear Time Invariant Deterministic Systems, with Single Output: the Role of the Initial Condition

Consider a unforced system given by Equation (5.4) and (5.5).

$$x_{k+1} = Ax_k \quad (5.4)$$

$$y_k = Cx_k \quad (5.5)$$

The identified system is of the same form and is given by

$$\hat{x}_{k+1} = \Lambda \hat{x}_k \quad (5.6)$$

$$y_k = \Gamma \hat{x}_k \quad (5.7)$$

The following necessary and sufficient conditions for the identifiability aspect can be given, using Lee⁷⁵ (1964):

Definition 5.4:

A system of Equation (5.4) is said to be *n-identifiable* if it is possible to determine the system matrix A by measurement of all the x variables.

Definition 5.5:

A system given by Equations (5.4) and (5.5) is said to be *l-identifiable* if it is possible to determine Λ and Γ such that Equations (5.6) and (5.7) are equivalent to Equations (5.4) and (5.5) in the sense mentioned by measurement of y_k only.

The *n-identifiability* condition can be shown as follows:

$$\begin{aligned} x_1 &= Ax_0 \\ x_2 &= Ax_1 = A^2 x_0 \\ &\vdots \\ x_k &= Ax_{k-1} = A^{k-1} x_0 \end{aligned}$$

Then a matrix can be built after n measurements, if all the variables can be observed:

$$\begin{bmatrix} x_1 | x_2 | \dots | x_k \end{bmatrix} = \begin{bmatrix} Ax_0 | Ax_1 | Ax_2 | \dots | Ax_{k-1} \end{bmatrix} = A \begin{bmatrix} x_0 | x_1 | x_2 | \dots | x_{k-1} \end{bmatrix} \quad (5.8)$$

If A is to be determined uniquely, the matrix

$$\Psi = \begin{bmatrix} x_0 | x_1 | x_2 | \dots | x_{k-1} \end{bmatrix}$$

must be nonsingular. Therefore, one can define the *n-identifiability* condition by the matrix Ψ

$$\Psi = \begin{bmatrix} x_0 & | & x_1 & | & x_2 & | & \dots & | & x_{k-1} \end{bmatrix} = \begin{bmatrix} x_0 & | & Ax_0 & | & A^2x_0 & | & \dots & | & A^{k-1}x_0 \end{bmatrix} \quad (5.9)$$

Equation (5.4) is *n-identifiable* if Equation (5.9) is nonsingular. This means that the initial conditions for this system must excite all modes of the system. If the system is identifiable, then the initial conditions must have nontrivial projections on to all the eigenvectors of A , so as to excite all modes of the system.

It can be shown, that the necessary and sufficient condition for the solution of the *l-identifiability* problem is that the system is *n-identifiable* and that A, C is an observable pair. If (A, C) is not observable, than there is no way to determine x_k , even if A is known. Similarly if (A, x_0) is not an identifiable pair than one cannot determine A even if all of the x_k are measurable. In the following, it is shown that the combination of these two conditions is sufficient for *l-identifiability*.

Define

$$\eta_k \equiv \begin{bmatrix} y_1 \\ y_2 \\ \dots \\ y_k \end{bmatrix} \Rightarrow \eta_k = \begin{bmatrix} CA \\ CA^2 \\ \dots \\ CA^k \end{bmatrix} x_0 = PAx_0$$

where the observability matrix is given as

$$P \equiv \begin{bmatrix} C \\ CA \\ \dots \\ CA^{k-1} \end{bmatrix} \quad (5.10)$$

Similarly $\eta_{k+1} = PAx_1 = PA^2x_0$

Than one can define

$$S_{2k-1} \equiv \begin{bmatrix} \eta_k | \eta_{k+1} | \dots | \eta_{2k-1} \end{bmatrix} = \begin{bmatrix} y_1 & y_2 & \dots & y_k \\ y_2 & y_3 & \dots & y_{k+1} \\ \vdots & \vdots & & \vdots \\ y_k & y_{k+1} & \dots & y_{2k-1} \end{bmatrix}$$

$$S_{2k-1} = P \begin{bmatrix} Ax_o | A^2 x_o | A^3 x_o | \dots | A^k x_o \end{bmatrix} = PA \begin{bmatrix} x_o | Ax_o | A^2 x_o | \dots | A^{k-1} x_o \end{bmatrix}$$

$$S_{2k-1} = PA\psi \text{ and therefore } A = P^{-1} S_{2k-1} \psi^{-1}$$

This means, the condition for *l-identifiability* implies observability and *n-identifiability*. Since A is not singular, observability and identifiability are necessary and sufficient to guarantee the nonsingularity of S_{2k-1} , which also is symmetric in the single output case.

In the following, only processes are being considered, where the start of the experiment lies in the remote past, such that the initial condition does not have any effect on the identifiability.

5.3.3 Identifiability of the ARX Model Coefficients

In this study, the identification methods used, are employing a parameterization of the given state-space system which yields an ARX model. The ARX model is given by

$$y_k = \sum_{i=1}^q C \bar{A}^{i-1} A K y_{k-i} + \sum_{i=1}^q C \bar{A}^{i-1} B u_{k-i} + \varepsilon_k \quad (5.11a)$$

which can be written in a simplified fashion

$$y_k = \sum_{i=1}^q a_i y_{k-i} + \sum_{i=1}^q b_i u_{k-i} + \varepsilon_k \quad (5.11b)$$

The sequence

$$\Theta = \begin{bmatrix} a_1 & b_1 & a_1 & b_1 & \dots & a_q & b_q \end{bmatrix} \quad (5.12)$$

are the to be estimated parameters. The basis for the estimation is the information matrix

$$\Phi = \begin{bmatrix} y_q^T & r_q^T & y_{q-1}^T & r_{q-1}^T & \cdots & y_1^T & r_1^T \\ y_{q+1}^T & r_{q+1}^T & y_q^T & r_q^T & \cdots & y_2^T & r_2^T \\ y_{q+2}^T & r_{q+2}^T & y_{q+1}^T & r_{q+1}^T & \cdots & y_3^T & r_3^T \\ \cdots & \cdots & \cdots & \cdots & \cdots & \cdots & \cdots \\ \cdots & \cdots & \cdots & \cdots & \cdots & \cdots & \cdots \\ y_{l-1}^T & r_{l-1}^T & y_{l-2}^T & r_{l-2}^T & \cdots & y_{l-q}^T & r_{l-q}^T \end{bmatrix} \quad (5.13)$$

The output sequence is defined as

$$\xi = [y_{q+1} \ y_{q+2} \ \cdots \ y_l] \quad (5.14)$$

Then, one can show that

$$\xi = \Phi\Theta + \varepsilon \quad (5.15)$$

Since $(l-q) > q$, one can use a least-squares method:

Define the error equation as

$$\varepsilon = \xi - \Phi\Theta \quad (5.16)$$

and minimize it according to the cost function

$$J = \varepsilon^T \varepsilon = (\xi - \Phi\Theta)^T (\xi - \Phi\Theta) \quad (5.17)$$

we get the least-squares solution by setting

$$\begin{aligned} \frac{dJ}{d\Theta} &= 0 \\ \hat{\Theta} &= (\Phi^T \Phi)^{-1} \Phi^T \xi \end{aligned} \quad (5.18)$$

Since $\hat{\Theta}$ is random, one can examine the statistical properties of it:

$$\begin{aligned} E[\hat{\Theta}] &= E[(\Phi^T \Phi)^{-1} \Phi^T (\Phi\Theta + \varepsilon)] \\ &= E[\Theta] + E[(\Phi^T \Phi)^{-1} \Phi^T] E[\varepsilon] \end{aligned} \quad (5.19)$$

if all the information of the input/output data are filtered out, the sequence ξ is white, zero meaned and gaussian and therefore

$$E[\hat{\Theta}] = \Theta \quad (5.20)$$

and $\hat{\Theta}$ is an unbiased estimate of Θ .

The error covariance of the estimate can be calculated as

$$\begin{aligned} P_{\hat{\theta}} &= E[(\hat{\theta} - \theta)(\hat{\theta} - \theta)^T] \\ &= (\Phi^T \Phi)^{-1} \Phi^T R \Phi (\Phi^T \Phi)^{-1} \end{aligned}$$

where R is the covariance matrix of ϵ

$$R = \sigma^2 \times I$$

and one can write

$$\begin{aligned} P_{\hat{\theta}} &= \sigma^2 (\Phi^T \Phi)^{-1} \Phi^T \{ (\Phi^T \Phi)^{-1} \Phi^T \}^T \\ P_{\hat{\theta}} &= \sigma^2 (\Phi^T \Phi)^{-1} \end{aligned} \quad (5.21)$$

The quality of the estimate is now directly proportional to the variance of the innovation. Manipulating the equation for the error covariance of the estimation, one can write

$$P_{\hat{\theta}} = \sigma^2 (\Phi^T \Phi)^{-1} = \frac{\sigma^2}{l} \left(\frac{1}{l} \Phi^T \Phi \right)^{-1} \quad (5.22)$$

The inverse exists, if $\Phi^T \Phi$ is nonsingular. To meet this assumption, the input/output data in the information matrix has to be consistent. The type of input $\{u_k\}$ driving the system such that $\Phi^T \Phi$ is nonsingular, is called *persistently exciting*. Assuming the input is persistently exciting

$$\lim_{l \rightarrow \infty} \left(\frac{1}{l} \Phi^T \Phi \right)^{-1} = 0 \quad (5.23)$$

where ϕ is a constant nonsingular matrix. Then one can claim

$$\lim_{l \rightarrow \infty} P_{\hat{\theta}} = \lim_{l \rightarrow \infty} \frac{\sigma^2}{l} \left(\frac{1}{l} \Phi^T \Phi \right)^{-1} = 0 \quad (5.24)$$

which means that the covariance matrix of the estimation becomes zero at $l \rightarrow \infty$ and the estimate of the ARX model coefficients approach the true value of the ARX model coefficients, $\hat{\theta} = \theta$.

Hsia⁷⁶ (1977) defines identifiability as the ability of consistently estimate the parameters of the system. A linear system is identifiable if the system is stable (ξ is

bounded) and the input test signal is persistently exciting, so that $\Phi^T \Phi$ is nonsingular. Hence we showed that for $l \rightarrow \infty$, $\hat{\Theta} = \Theta$ and therefore $\hat{\Theta}$ is a consistent estimator of Θ and we can claim the system is identifiable. A information matrix Φ which satisfies the above mentioned properties and having the knowledge of the order of the stable, time invariant system, guaranties identifiability.

5.3.4 Experimental Condition for Identifiability

In the above section, identifiability is shown to exist, if the information matrix is composed of persistently exciting signals. It indicates the importance of selecting the correct experimental conditions for the system identification process. In this section, we attempt to gain more insight of persistently exciting signals, since selecting an input signal is directly related to the experimental conditions.

The estimation problem was stated in Section 5.3.3 as

$$\xi = \Phi \Theta$$

where ξ is given in Equation (5.14), Θ in Equation (5.13) and Φ in Equation (5.12). Defining the residual as

$$\varepsilon = y_k - \hat{y}_k = y_k - \bar{\Phi}_{k-1} \Theta \quad (5.25)$$

where

$$\Phi = \begin{bmatrix} \bar{\Phi}_q \\ \bar{\Phi}_{q+1} \\ \bar{\Phi}_{q+2} \\ \dots \\ \bar{\Phi}_{k-1} \\ \dots \\ \bar{\Phi}_{i-1} \end{bmatrix} \quad (5.26)$$

The least-squares error can be written as given in Equation (5.17):

$$\begin{aligned} J(\Theta, k) &= \sum_{i=1}^k \varepsilon_i^2 = \sum_{i=1}^k (y_i - \bar{\Phi}_{i-1} \Theta)^2 \\ &= (\xi - \Phi \Theta)^T (\xi - \Phi \Theta) \end{aligned}$$

Then the solution of the least-squares estimation is given by the following theorem:

Theorem 5.1:

$J(\Theta, k)$ is minimal for $\hat{\Theta}$ if $\Phi^T \Phi \hat{\Theta} = \Phi^T \xi$. If the matrix $\Phi^T \Phi$ is nonsingular, the minimum is unique and given by $\hat{\Theta} = (\Phi^T \Phi)^{-1} \Phi^T \xi$.

Proof:

$J(\Theta, k)$ can be expanded as follows:

$$J(\Theta, k) = \xi^T \xi - \xi^T \Phi \Theta - \Theta^T \Phi^T \xi + \Theta^T \Phi^T \Phi \Theta \quad (5.27)$$

It is easy to see that $\Phi^T \Phi$ is always semi-positive or positive definite, and therefore $J(\Theta, k)$ has a minimum. Using completion of squares:

$$\begin{aligned} J(\Theta, k) &= \xi^T \xi - \xi^T \Phi \Theta - \Theta^T \Phi^T \xi + \Theta^T \Phi^T \Phi \Theta + \\ &\quad + \xi^T \Phi (\Phi^T \Phi)^{-1} \Phi^T \xi \\ &\quad - \xi^T \Phi (\Phi^T \Phi)^{-1} \Phi^T \xi \end{aligned} \quad (5.28)$$

which can be rearranged:

$$J(\Theta, k) = \xi^T \Phi (\Phi^T \Phi)^{-1} \Phi^T \xi + (\Theta - (\Phi^T \Phi)^{-1} \Phi^T \xi)^T \Phi^T \Phi (\Theta - (\Phi^T \Phi)^{-1} \Phi^T \xi) \quad (5.29)$$

The first term in Equation (5.29) is independent of the parameter vector Θ . The second term is clearly always positive. To establish a minimum, one sets

$$\Theta = \hat{\Theta} = (\Phi^T \Phi)^{-1} \Phi^T \xi$$

q.e.d.

Note the condition that the matrix $\Phi^T \Phi$ is invertible is called an excitation condition.

The error covariance $P_{\hat{\Theta}}$ was given in Equation (5.21). From the covariance equation, it is quite clear that the desire for consistency, or in this case identifiability, in parameter estimation leads to the convergence question of $\hat{\Theta} \rightarrow \Theta$. One way to detect consistency is if $P_{\hat{\Theta}}$ is decreasing with increasing data length. To show this, one has to answer the question of how to use least-squares methods to estimate $\hat{\Theta}$ in dynamical systems. It is generally known that the Markov parameters are the impulse response of the system. Markov parameters can be obtained from experimental data, using the frequency

response function. They build the fundamental background for the system identification methods used in this work. It can be shown that for linear time invariant system, the input response describes the system uniquely. Impulse responses are infinite dimensional. Though, for stable systems, one can truncate the diminishing portion and obtain finite impulse response (FIR) or transversal filters. The ARX model is also a FIR model:

$$y_k = \sum_{i=1}^q a_i y_{k-i} + \sum_{i=1}^q b_i u_{k-i} = \bar{\Phi}_{k-1}^T \Theta$$

As mentioned above the parameter $\hat{\Theta}$ cannot be estimated unless the condition on the input signal is fulfilled. Using the above system, one can formulate the consistency problem for each input/output vector as follows: $\Phi^T \Phi =$

$$\begin{bmatrix}
 y_q & y_{q+1} & y_{q+2} & \dots & y_{q+k} & \dots & y_{l-1} \\
 r_q & r_{q+1} & r_{q+2} & \dots & r_{q+k} & \dots & r_{l-1} \\
 y_{q-1} & y_q & y_{q+1} & \dots & y_{q+k-1} & \dots & y_{l-2} \\
 r_{q-1} & r_q & r_{q+1} & \dots & r_{q+k-1} & \dots & r_{l-2} \\
 y_{q-2} & y_{q-1} & y_q & \dots & y_{q+k-2} & \dots & y_{l-3} \\
 r_{q-2} & r_{q-1} & r_q & \dots & r_{q+k-2} & \dots & r_{l-3} \\
 \dots & \dots & \dots & \dots & \dots & \dots & \dots \\
 \dots & \dots & \dots & \dots & \dots & \dots & \dots \\
 y_1 & y_2 & y_3 & \dots & y_{k+1} & \dots & y_{l-q} \\
 r_1 & r_2 & r_3 & \dots & r_{k+1} & \dots & r_{l-1}
 \end{bmatrix}
 \begin{bmatrix}
 y_q^T & r_q^T & y_{q+1}^T & r_{q+1}^T & y_{q+2}^T & r_{q+2}^T & \dots & y_{l-1}^T & r_{l-1}^T \\
 y_{q+1}^T & r_{q+1}^T & y_q^T & r_q^T & y_{q+1}^T & r_{q+1}^T & \dots & y_2^T & r_2^T \\
 y_{q+2}^T & r_{q+2}^T & y_{q+1}^T & r_{q+1}^T & y_q^T & r_q^T & \dots & y_3^T & r_3^T \\
 \dots & \dots & \dots & \dots & \dots & \dots & \dots & \dots & \dots \\
 y_{q+k}^T & r_{q+k}^T & y_{q+k-1}^T & r_{q+k-1}^T & y_{q+k-2}^T & r_{q+k-2}^T & \dots & y_{k+1}^T & r_{k+1}^T \\
 \dots & \dots & \dots & \dots & \dots & \dots & \dots & \dots & \dots \\
 y_{l-1}^T & r_{l-1}^T & y_{l-2}^T & r_{l-2}^T & y_{l-3}^T & r_{l-3}^T & \dots & y_{l-q}^T & r_{l-q}^T
 \end{bmatrix}$$

$$= \begin{bmatrix}
 \sum_{i=q}^{l-1} y_i y_i^T & \sum_{i=q}^{l-1} y_i r_i^T & \sum_{i=q}^{l-1} y_i y_{i-1}^T & \dots & \sum_{i=q}^{l-1} y_i y_{i-q+1}^T & \sum_{i=q}^{l-1} y_i r_{i-q+1}^T \\
 \sum_{i=q}^{l-1} r_i y_i^T & \sum_{i=q}^{l-1} r_i r_i^T & \sum_{i=q}^{l-1} r_i y_{i-1}^T & \dots & \sum_{i=q}^{l-1} r_i y_{i-q+1}^T & \sum_{i=q}^{l-1} r_i r_{i-q+1}^T \\
 \sum_{i=q}^{l-1} y_{i-1} y_i^T & \sum_{i=q}^{l-1} y_{i-1} r_i^T & \sum_{i=q}^{l-1} y_{i-1} r_{i-1}^T & \dots & \sum_{i=q}^{l-1} y_{i-1} y_{i-q+1}^T & \sum_{i=q}^{l-1} y_{i-1} r_{i-q+1}^T \\
 \dots & \dots & \dots & \dots & \dots & \dots \\
 \sum_{i=q}^{l-1} r_{i-q+1} y_i^T & \sum_{i=q}^{l-1} r_{i-q+1} r_i^T & \dots & \dots & \sum_{i=q}^{l-1} r_{i-q+1} y_{i-q+1}^T & \sum_{i=q}^{l-1} r_{i-q+1} r_{i-q+1}^T
 \end{bmatrix}$$

(5.30)

The minimum, as given in Theorem 1, is unique if Equation (5.30) has full rank, which is equal to the excitation condition. One can define an empirical covariance as follows:

$$P_{\Phi} = \lim_{l \rightarrow \infty} \frac{1}{l-1-q} \left\{ \sum_{i=q}^{l-1} \begin{bmatrix} y_i y_i^T & y_i r_i^T & \dots & y_i r_{i-q+1}^T \\ r_i y_i^T & r_i r_i^T & \dots & r_i r_{i-q+1}^T \\ \dots & \dots & \dots & \dots \\ r_{i-q+1} y_i^T & r_{i-q+1} r_i^T & \dots & r_{i-q+1} r_{i-q+1}^T \end{bmatrix} \right\} \quad (5.31)$$

which means that for long data sets, the uniqueness of estimation, thus the identifiability of the model parameters Θ , is given by P_{Φ} being positive definite, and therefore the regressor set $\{y, r\}$ is persistently exciting of the order $2 \times (q+1)$.

A simple example can be given as follows. The ARX model is given in Equation (5.11b)

$$y_k = \sum_{i=1}^q a_i y_{k-i} + \sum_{i=1}^q b_i u_{k-i} \quad (5.11b)$$

If the input u to this system is at all times zero, the parameter b can not be identified. If u does not excite all the modes of the system, the parameter a is also not identifiable. This simple example emphasizes the importance of the experimental condition, in particular the role of persistently exciting signals. We can now state the following theorem:

Theorem 5.2:

A signal u is persistently exciting of order q if and only if

$$\lim_{l \rightarrow \infty} \frac{1}{l} \left\{ \sum_{k=1}^l \left(\sum_{i=1}^q b_i u_{k-i} \right) \right\}^2 > 0 \quad (5.32)$$

Proof:

Expanding the term in Equation (5.32) leads to

$$\lim_{l \rightarrow \infty} \frac{1}{l} \left\{ \sum_{k=1}^l (b_1 u_{k-1} + b_2 u_{k-2} + \dots + b_q u_{k-q}) \right\} \left\{ \sum_{k=1}^l (b_1 u_{k-1} + b_2 u_{k-2} + \dots + b_q u_{k-q}) \right\}$$

$$= \lim_{l \rightarrow \infty} \frac{1}{l} [b] \begin{bmatrix} \sum_{i=1}^l u_i u_i & \sum_{i=1}^l u_i u_{i-1} & \sum_{i=1}^l u_i u_{i-2} & \dots & \sum_{i=1}^l u_i u_{i-q} \\ \sum_{i=1}^l u_{i-1} u_i & \sum_{i=1}^l u_{i-1} u_{i-1} & \sum_{i=1}^l u_{i-1} u_{i-2} & \dots & \sum_{i=1}^l u_{i-1} u_{i-q} \\ \dots & \dots & \dots & \dots & \dots \\ \sum_{i=1}^l u_{i-q} u_i & \sum_{i=1}^l u_{i-q} u_{i-1} & \sum_{i=1}^l u_{i-q} u_{i-2} & \dots & \sum_{i=1}^l u_{i-q} u_{i-q} \end{bmatrix} [b]^T$$

If we define the covariance of this signal u as

$$P_u(k) = \lim_{l \rightarrow \infty} \frac{1}{l} \sum_{i=1}^l u_i u_{i-k} \quad (5.33)$$

Then

$$\lim_{l \rightarrow \infty} \frac{1}{l} \left\{ \sum_{k=1}^l (b_1 u_{k-1} + b_2 u_{k-2} + \dots + b_q u_{k-q}) \right\}^2 =$$

$$= \begin{bmatrix} b_1 \\ b_2 \\ \dots \\ b_q \end{bmatrix} \begin{bmatrix} P_u(0) & P_u(1) & \dots & P_u(q-1) \\ P_u(1) & P_u(0) & \dots & P_u(q-2) \\ \dots & \dots & \dots & \dots \\ P_u(q-1) & P_u(q-2) & \dots & P_u(0) \end{bmatrix} \begin{bmatrix} b_1 & b_2 & \dots & b_q \end{bmatrix} = b^T P_u b \quad (5.34)$$

If one neglects the end effects in Equation (5.30) and (5.31), which is legitimate for long data sets, P_u is of the same form as Equation (5.31). In that case, if P_Φ is positive definite, then $b^T P_u b$ is positive for all b . *q.e.d.*

Theorem 5.2 gives explicitly the condition for any regressor to be persistently exciting. The question arises what input signals are in general persistently exciting. A few typical input signals are analyzed in the following, using Theorem 5.2.

Quite often in system identification, the input sequence to the system is of random structure. The randomness of the input prohibits its prediction and therefore the summation in Equation (5.32) does not vanish. Thus a random signal is persistently exciting. Using the pulse function as an input, Equation (5.33) indicates that P_u becomes zero, and thus proves that the pulse function is not persistently exciting.

5.4 Numerical Example

For the numerical example, the beam-like structure introduced in Section 2.4.2 is being used. The measurement is performed such that all the states are represented in the output vector. As addressed in the previous section, the identifiability question is reduced to the convergence problem of the estimate. To show this numerically, the F-Norm of the error covariance $P_{\hat{\theta}}$ is computed for increasing data lengths. Two sets of simulation were performed. The first one includes the system where a constant gain state feedback controller enhances the damping of the overall system. The other case involves the same system but no controller. The damping ratios and natural frequencies of the two systems are given in Table 5.1

Table 5.1: System Characteristics with and without Controller

Frequencies of uncompensated System	Damping Ratios of uncompensated System	Frequencies of compensated System	Damping Ratios of compensated System
5.457	0.0064	8.707	0.848
5.457	0.0064	8.707	0.848
14.91	0.0101	15.08	0.246
14.91	0.0101	15.08	0.246
20.36	0.0130	20.16	0.111
20.36	0.0130	20.16	0.111

The simulation were performed using a process and measurement noise variance of 5% and for the construction of the information matrix Φ an ARX model order of $q = 3$. The results are given in Figure 5.1. It is clearly to recognize the trend of

$$\lim_{l \rightarrow \infty} \|P_{\hat{\theta}}\|_F = \lim_{l \rightarrow \infty} \left\| \frac{\sigma^2}{l} \left(\frac{1}{l} \Phi^T \Phi \right)^{-1} \right\|_F = 0 \quad (5.35)$$

which is equivalent to the statement of Equation (5.24). The consistency of the estimation

is shown, and therefore the identifiability of the parameters of the system exists. An interesting observation can be made if the compensated and uncompensated system are compared. The magnitude of the norm of the covariance decreases much more rapidly for the controlled system. Since the error covariance directly influences the quality of the estimation of the ARX parameters, it is expected that the results of a system identification experiment, using the above data is greatly influenced. This is done for the data sets of both systems using a data length of $l = 1000$. The results are given in Figure 5.2 - 5.5. Figure 5.2 and 5.3 show the open-loop Markov parameters for both systems as well as the identified, the true and the Markov parameters composed of the ARX model. For the uncompensated system, the difference between the Markov parameters of the true and the identified system is much larger than for the identification results of the compensated system. For the compensated system, the identified and the Markov parameters composed from the ARX model agree very closely, which indicates that the system identification procedure introduces very little error. The responses of both systems are given in Figure 5.4 and Figure 5.5.

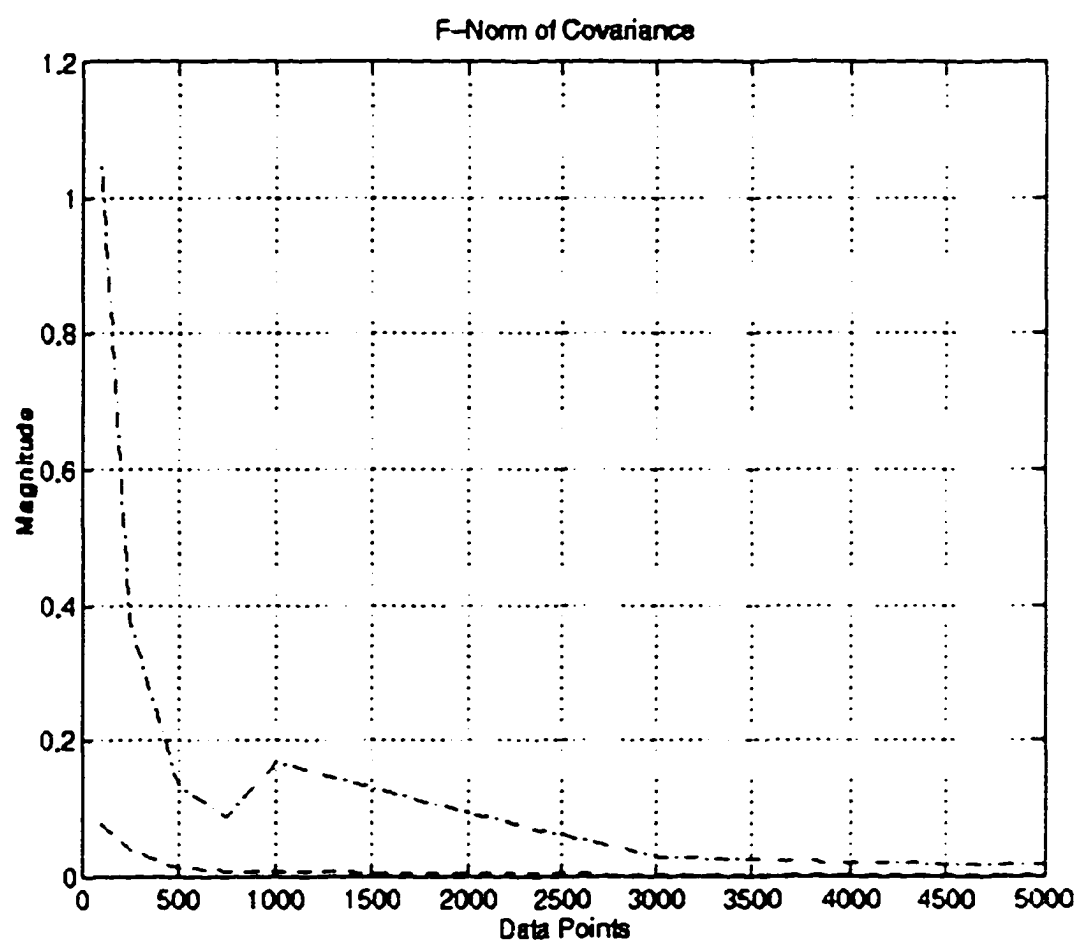


Figure 5.1 F-Norm of error covariance for compensated (dashed line) and uncompensated (dot-dashed line).

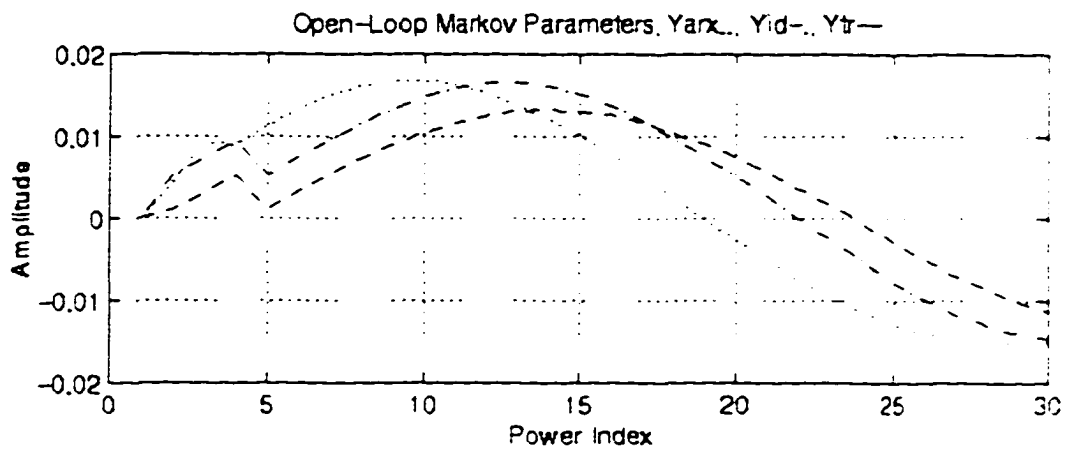


Figure 5.2 Open-loop Markov parameters of uncompensated system. Markov parameters computed from ARX model in dotted line, true Markov parameters are plotted in dashed line and identified Markov parameter are given in dot-dashed line.

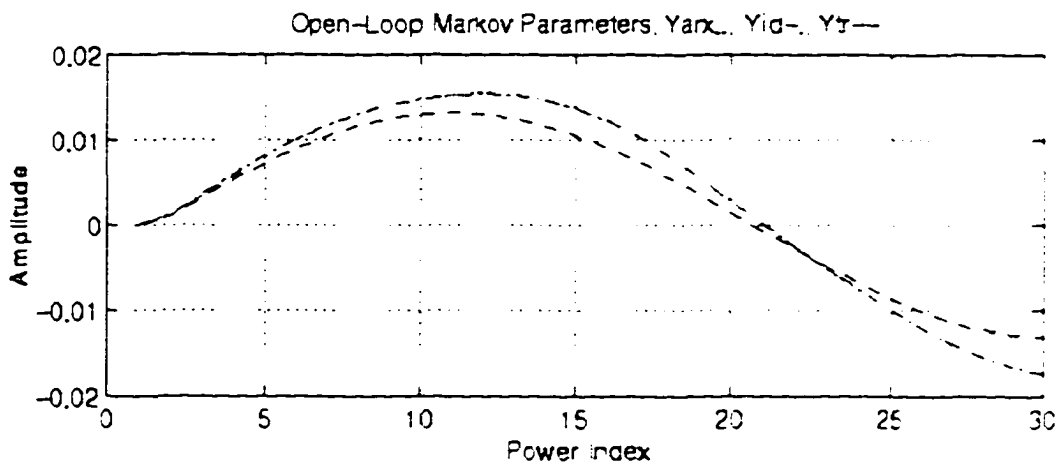


Figure 5.3 Open-loop Markov parameters of compensated system. Markov parameters computed from ARX model in dotted line, true Markov parameters are plotted in dashed line and identified Markov parameter are given in dot-dashed line.

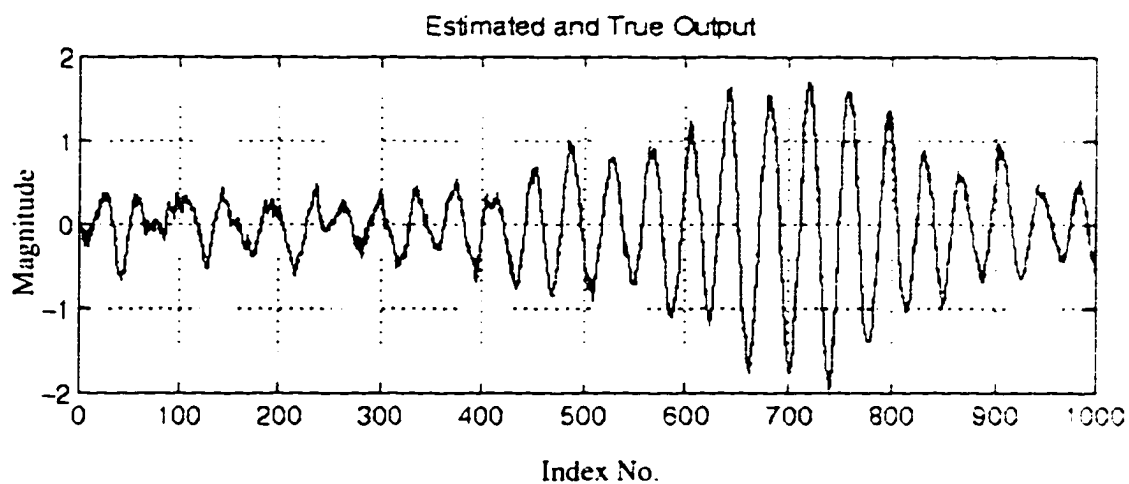


Figure 5.4 Estimated and true output of the first state for uncompensated system.

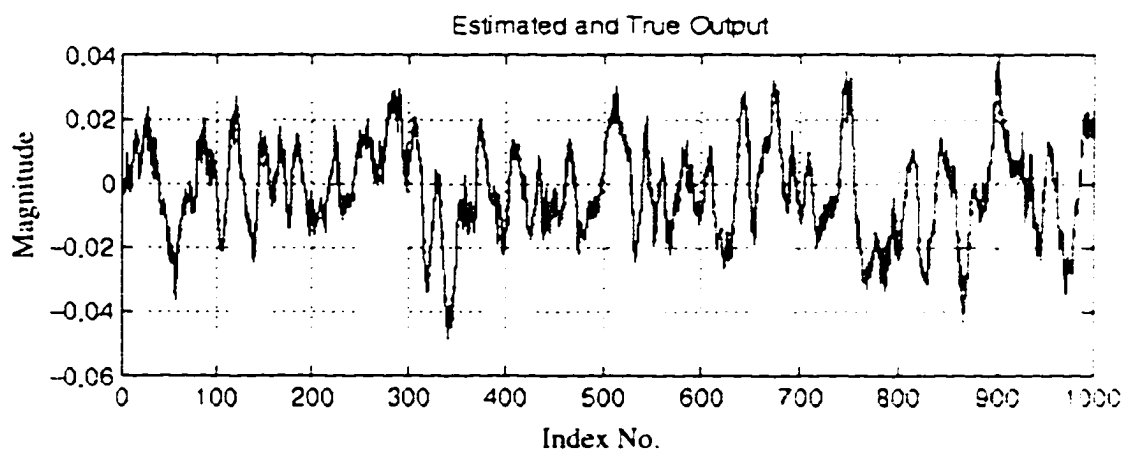


Figure 5.5 Estimated and true output of the first state for uncompensated system.

CHAPTER VI

COMPARISON BETWEEN DIRECT AND INDIRECT SYSTEM IDENTIFICATION

6.1 Introduction

The objective of this chapter is to compare two identification methods based on the theory presented in the previous two chapters. In the first section, the methods are compared based on the identifiability condition established in Chapter V. The input signal is subjected to a specified constraint and the error of the open-loop Markov parameters as well as the magnitude of the error covariance matrices are compared. In the second part, a special problematic is given for deterministic systems described by a low ARX model order and a simple controller. The problem arrives due to the constant gain feedback, which can in some instances cancel some portion of the reference input and cause the information matrix to become singular. The third part of this chapter compares the two method directly based on the data length and noise level. Stable and unstable systems from various disciplines are being used to perform the simulations.

6.2 Identification with Constraint Reference Input

System Identification is applied in the most various fields in science and technology. One distinction can be drawn by classifying the operating mode of the system identification. The operating mode can be on-line or off-line. Off-line identification is often used to get an overall system characterization and model description of the plant under investigation. The presented system identification methods in Chapter III are developed for off-line system identification. On-line system identification methods can be used to adapt the system model to the current changes in its physical nature. Often, the controller designed to regulate the plant under investigation, is updated by using the new system

characteristics obtained from the on-line identification. On-line system identification differs from the off-line system identification method in that point, that continuously new data are supplied and the system parameters, in this case the ARX model parameters, are continuously estimated. Since the computational speed is essential to keep up with the changes of the system and therefore controller update, the estimation methods used in on-line identification uses often fewer data points and delivers less accurate estimations. An alternative estimation technique for computing the ARX model parameters is the sequential least-squares estimation technique, which is a recursive solution to the estimation problem. The advantage is that the estimates are being updated continuously without repeating the matrix inversion of Equation (5.18). On-line system identification methods and the related estimation problem are investigated in ^{77,78,79} among others.

In this section, the on-line system identification process is simulated with the off-line system identification methods introduced in Chapter III. The conditions for such an assumption is that the system characteristics do not change rapidly with time, i.e. the computation of the new system characteristics takes much less time than the system dynamics changes. As a matter of fact, for the simulation in this work, only time invariant systems are being used, since the goal of this study is to investigate the applicability of the two system identification methods to situations where the system under investigation is in normal operating mode, and no special excitation signals can be applied to the system. This situation occurs in on-line system identification processes, when a plant is in production, and therefore the states of the system is in steady state. Consider for example the human lung model introduced in Chapter II. The input to the system is the fraction of CO₂ in inspired gas. If one tries to excite the system, which is in normal operating mode, by changing the CO₂ content in inspired gas, the person could be harmed if a high percentage of CO₂ is used and his condition does not allow any additional stress to his respiratory system. In the worst case, from the system identification point of view, the input to the system is a constant. From Chapter V, it is obvious that a constant reference input does not excite the system modes (does not fulfill the identifiability condition), and therefore, the indirect system identification method is not capable of producing any results. In the first part of this section, the possibility of using the direct system identification method for this situation is

investigated. Figure 6.1 depicts the situation. Assuming a stochastic environment, some of the measurement and process noise of the system is being fed back into the closed-loop and along with the control input compared with the constant reference input. The recycled noise carried by the control signal has random characteristics. The question tried to be numerically answered here is, if the noise suffice to excite the system, such that the identifiability condition is satisfied and if so, system identification yields good results.

For the simulation, the beam-like structure introduced in Chapter II was used. The states of this system are all assumed to be measured directly, that is the C matrix is an identity matrix. The ARX model order was set to be seven and the number of data points was chosen to be 4000 for every simulation. Since the norm of the error covariance matrix depends on the size of the matrix, the numerical results for this system cannot be compared with a different system, though it indicates the applicability of the method. Figure 6.2 depicts the norm of the error covariance as a function of the process and measurement noise. The Magnitude of the norm indicates that the ARX model order can be estimated, that is, identifiability exists. In Figure 6.3 the error percentage of the 30 first open-loop Markov parameters are plotted against the process and measurement noise. The error is too high for an acceptable system identification. Which indicates that the ARX model parameters were possible to estimate, but the estimation error lead to a large system identification error. Simulations with the human lung model resulted in similar results.

A less restrictive situation can be defined if the reference input has to fulfill some constraint, defined by the system weakness or process dynamics. This can be a power limitation on the reference input due to the actuators, or as mentioned above for the lung model, a range limitation, among others. This topic has been studied intensively since ever its introduction by Levin⁸⁰ and is generally in the field of optimum input signals^{81,82}. In parameter estimation, one seeks the input which yields the most accurate estimates. The input causing the error to be minimum is called the optimum input signal. The error covariance was defined in Equation (5.21) as

$$P_{\hat{\theta}} = \sigma^2(\Phi^T \Phi)^{-1} \quad (6.1)$$

From Equation (6.1), one can conclude that the estimation error of the parameter is somehow related to the magnitude of the error covariance matrix. In the above simulations the

F-norm of the error covariance matrix was chosen to represent the magnitude. Another approach is to look at each element of this matrix, and one can conclude that the magnitude of $P_{\hat{\theta}}$ increases or decreases with the increase or decrease of the magnitude of (y_i, r_i) . That implies that high signal-to-noise ratio at the input and/or output of the system delivers more accurate estimation results. The limitation of the signal-to-noise ratio is given by the actuator and the system itself (for the outputs). Once the constraints of the actuator and/or system are known, the optimal input signal design becomes a constraint optimum problem. In the following, the restriction, that the reference input is a constant input is loosened such that r is limited to a specific percentage of its normal magnitude. The simulation were performed using both methods, the indirect and the direct system identification method. Figure 6.4 depicts the error percentage of the open-loop Markov parameters for a variable process and measurement noise, and a variable amplitude percentage of the reference input. As one would expect, the error for a constant reference input goes to infinity (in the graph, the error was limited to be less or equal to 1000%). Though as soon as the reference input carries some randomness, the error drops dramatically. In comparison to the direct method, Figure 6.5 indicates the indirect method produces identification results with lower error percentages, especially for high noise levels. Figure 6.6 shows the magnitude of $P_{\hat{\theta}}$. The indirect method gives slightly lower values compared with the direct method. This implies that the error is given to some extent already in the estimation, and therefore in the ARX-model representation. Since for computing the error covariance matrix for the direct method only the input data is different, one can assume that the controller behaves like a filter, and reduces the randomness of the input signal somewhat, which causes the slightly less accurate estimation compared to the indirect method. Though, to perform system identification with the indirect method produces slightly better results, except if the reference input is constraint to have no or very little randomness.

6.3 Loss of Identifiability due to Feedback

The attention in this short section is given to a specific problem encountered for simple systems represented by ARX models of low order operating in a deterministic environment⁸³. For example, a system described by

$$y_k = a_1 y_{k-1} + b_1 u_{k-1} + \varepsilon_k \quad (6.2)$$

where the ARX model order is one. If one employs a constant feedback gain of the form

$$u_k = -Gx_k \quad (6.3)$$

and $Gx_k = gy_k$

where $G = gC$

The parameter estimation problem can then be solved by reformulating Equation (6.3) as follows

$$\begin{aligned} pu_{k-1} + pg y_{k-1} &= 0 \\ y_k &= a_1 y_{k-1} + b_1 u_{k-1} + \varepsilon_k + pu_{k-1} + pg y_{k-1} \\ y_k &= (a_1 + pg)y_{k-1} + (b_1 + p)u_{k-1} + \varepsilon_k \end{aligned} \quad (6.4)$$

and the estimates of the parameters have to satisfy the following equations:

$$\hat{a}_1 = a_1 + pg \quad (6.5)$$

$$\hat{b}_1 = b_1 + p \quad (6.6)$$

The cost function defined in Equation (5.17) yields the same value for the estimated parameters in Equation (6.5) and (6.6), regardless of the value of g . Thus, the identified parameters are not unique and therefore identifiability does not exist. This problem occurs only for the direct system identification method and does not exist for the indirect method, since the input data for the later method is the reference input, where no feedback term is included.

6.4 Data Length Comparison for different Systems

In the following, several different systems are used to determine numerically the system identification error given a specific data length. The results are used to compare the two methods in regard of their efficiency and accuracy. The data length along with the noise level of the measurement and process, were varied, to compute the error percentage of the deviation of the Markov parameters. The noise levels were selected at 5%, 10% and 15% noise variance. The number of data points were chosen to be 1000, 2500 and 5000. The ARX model order was determined according to the system under investigation. For most of the systems, constant gain feedback and LQR controller were designed such that the closed-loop system has its damping ratios in the interval of 0.4 - 0.8. The simulation

contained one single set of data for each comparison at a given noise level and data length, such that the randomness of the noise is eliminated in the results. The measure is solely based on the error percentage of the 30 first open-loop Markov parameters of the identified and true system.

The large angle magnetic suspension test facility introduced in Chapter II, is an unstable system. The controller used is a dynamic output feedback controller. For the simulation, an ARX model order of 14 indicated to produce the best results. This was determined by the contour plot given in Figure 6.7. The controller used is given in the appendix. Figure 6.8 depicts the simulation results for the two methods. The error percentages for the simulations with the indirect method show marginally lower values over the whole region. The average error percentage over the whole region is 98.75% for the direct method and 97.22% for the indirect method. Good identification results are obtained when 2500 data points or less over the entire noise interval are used. A contour plot of the error percentage of the open-loop Markov parameters with changing noise variance and number of data points is given in Figure 6.9. One can detect an increasing error with higher noise values and lower data points.

The same approach was taken for the spring-mass system. This system is marginal stable, and the comparison includes the direct and indirect method with control input, and the direct method without controller presence. The ARX model order was set equal to five, which was determined by the contour plot given in Figure 6.10. The contour plot was generated using the direct method and a LQR controller while keeping the noise variance constant for all simulations at 5%. The results of the comparison between the two methods is given in Figure 6.11. The upper surface represents the error percentages yield by using the direct method to the system which has no controller. The middle surface is the error surface for system identification with the direct method to the system including the controller, while the error surface with the lowest values represents the results from the indirect method. The average error percentages for the three cases are: direct method without controller 25.96%, direct method with controller 14.87% and indirect method with controller 12.78%. These results indicate that the controller can have a rather large impact on the data length in respect of noise sensitivity and furthermore, the indirect method seems to produce more accurate results than the direct method.

Though the macro economy model in Chapter II was introduced as a deterministic model, the same simulation strategy was applied, that is, the noise level of the process and measurement was ranged, and the number of data points was varied as well, to generate the error percentage surfaces of the two identification methods. The ARX model order was selected to be five. The controller is a constant gain output feedback controller. Figure 6.12 depicts the three cases. The upper surface represents the error resulting by using the direct method to a system with controller (average error percentage: 28.17%), the middle surface is error for the same system but using indirect system identification method (average error percentage: 25.1%). The surface on the bottom is representing the error of the results for the direct system identification to a system without a controller (average error percentage: 3.28%). The figure indicates the same findings as for the two previous cases, though the controller does not help to improve the accuracy of the system identification. The results of the direct method to a system without controlled input are much better than to a system with control input.

The lung model was equipped with a similar constant gain feedback controller and the same simulations were performed as in the previous case. The results can be seen in Figure 6.13. The error surfaces are similar to the ones for the spring-mass system. The averaged error percentages are for the direct method without controller: 25.96%, direct method with controller: 14.87% and indirect method with controller: 12.78%. The controller enhances the system identification accuracy and the indirect method indicates to yield better results.

For the heat and mass transfer system, the lyophilisation model, a controller design was not successful, such that reasonable system identification results could be obtained. The simulations were performed without a controller, and with a measurement and process noise variance of 5%. Only the direct method was used and the number of data points was selected in the range of 1000 to 10000. Figure 6.14 depicts the results. The error percentage of the open-loop Markov parameter decays with increasing data length.

As a last system, the time delay system introduced in Chapter II is used. The identification did not yield any reasonable results when the time delay was included to the system. Therefore, the model given in Equation 2.2 was altered to include only A_0 as system matrix. The results given in Figure 6.15 present the error surface for the direct method.

where no controller is being used and the direct and indirect method with controller interaction. The controller is comprised by an LQR controller design and is given in the appendix given. For this example, the controller has no real advantage, and the direct and indirect method yield qualitatively similar results (the average error percentages are for the direct method without controller: 13.05%, direct method with controller: 12.57%, and indirect method with controller: 12.15%).

The simulations indicate that the controller design is crucial for accurate system identification. Using an appropriate controller, the indirect method yields better results than the direct method in terms of the error percentage. This can be used in reducing the data length for the indirect method in order to achieve the same accuracy as the direct method with larger data length.

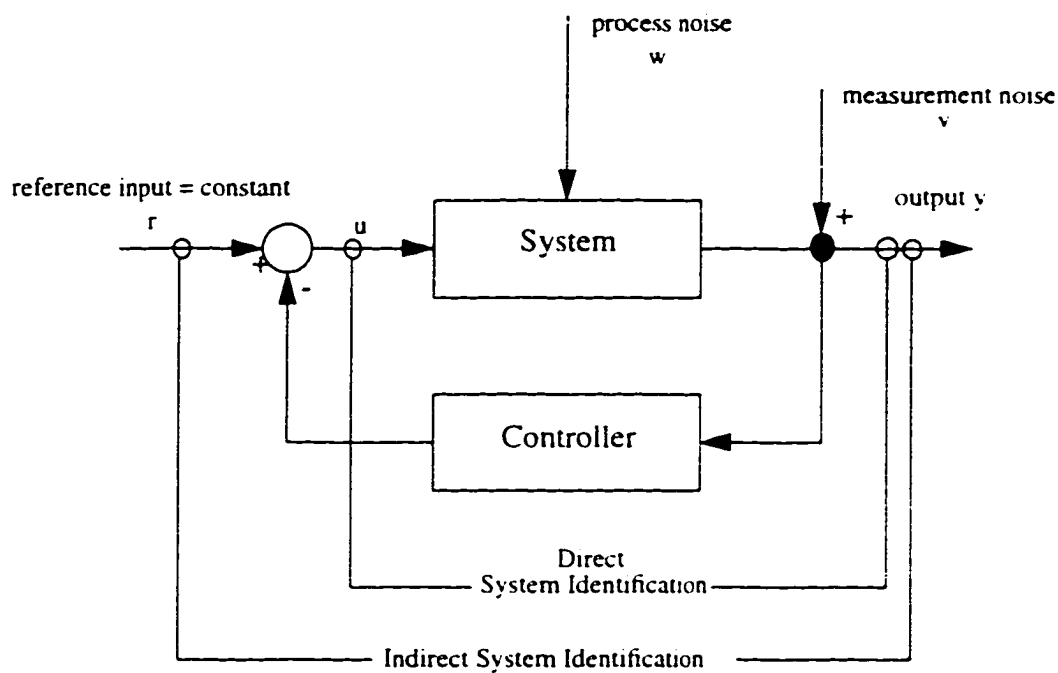


Figure 6.1 Situation for identification with constant reference input.

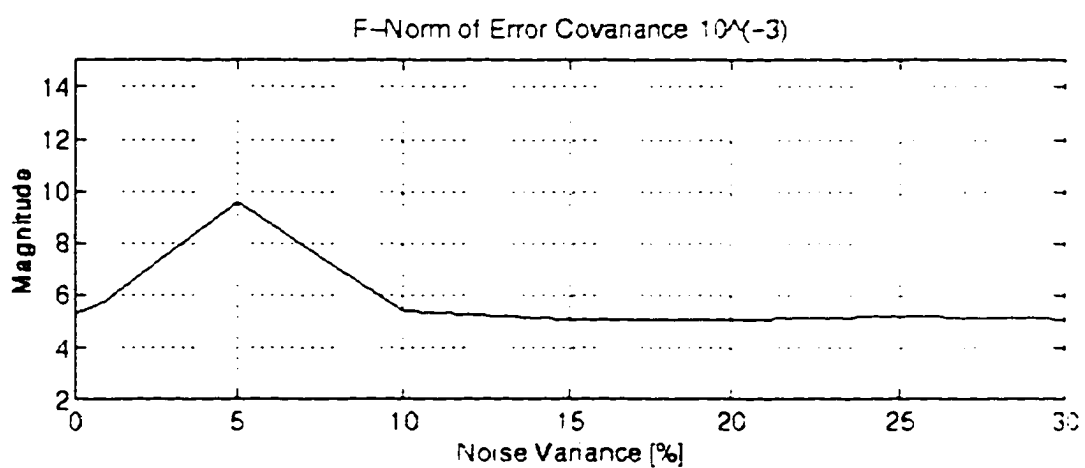


Figure 6.2 Magnitude of the norm of the error covariance vs. noise level.

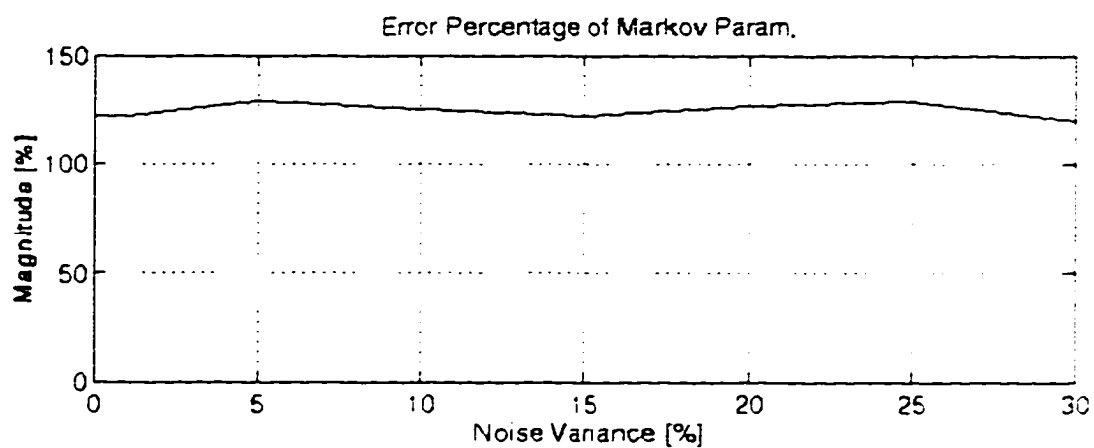


Figure 6.3 Error percentage of the open-loop Markov parameters vs. noise level.

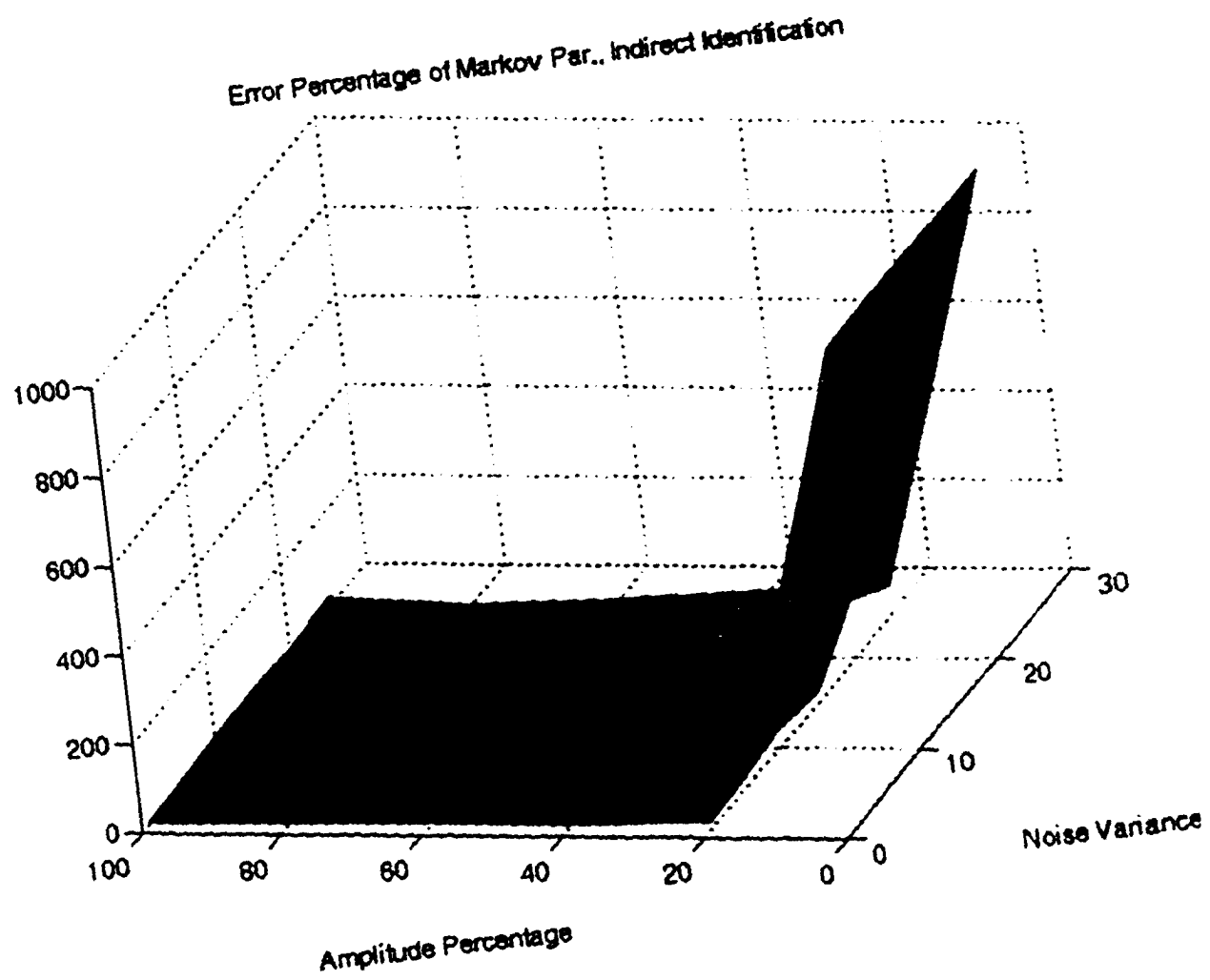


Figure 6.4 Error percentage of open-loop Markov parameters for the indirect identification

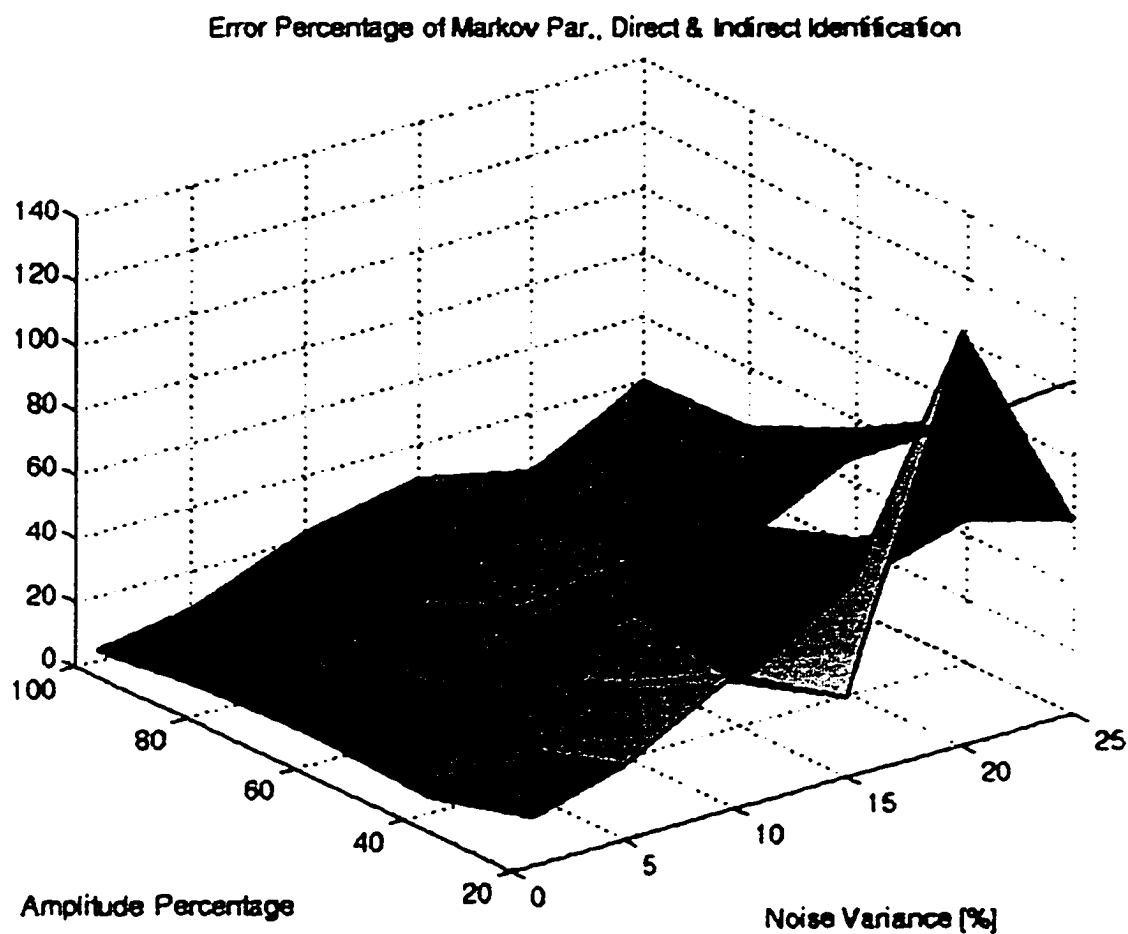


Figure 6.5 Error percentage of Markov parameters for the direct and indirect identification

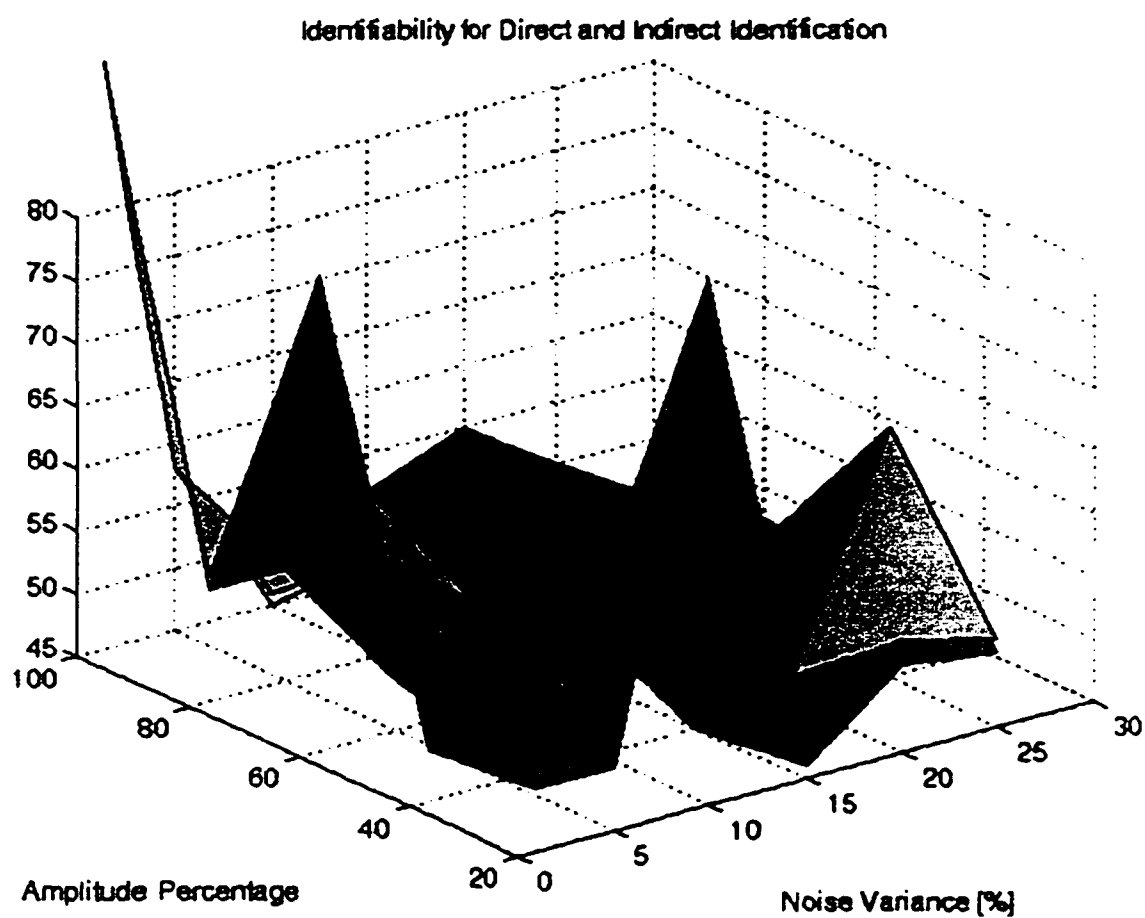


Figure 6.6 Magnitude of error covariance for the direct and indirect identification.

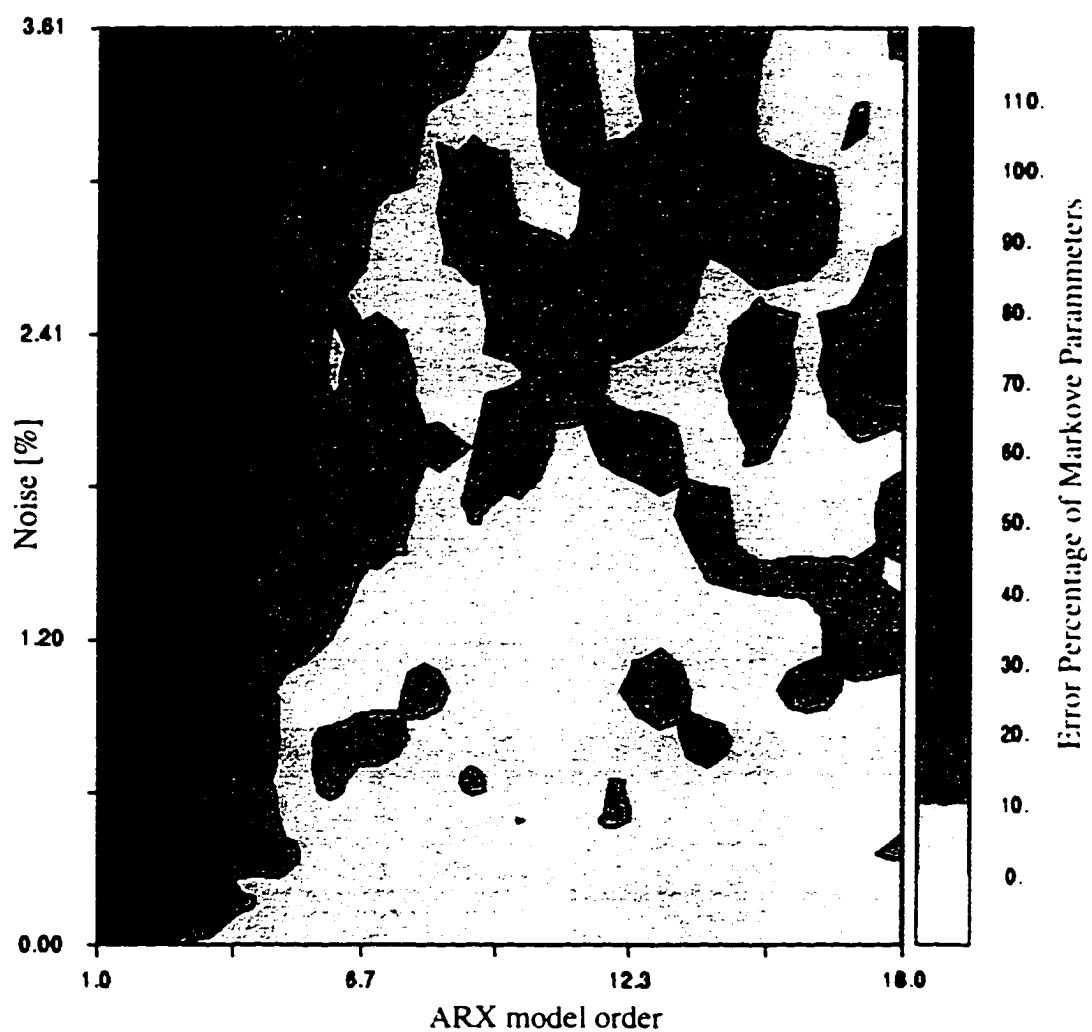


Figure 6.7 Magnitude of the percentage of error deviation of the open-loop system Markov parameters in relation to the ARX model order and the noise level.

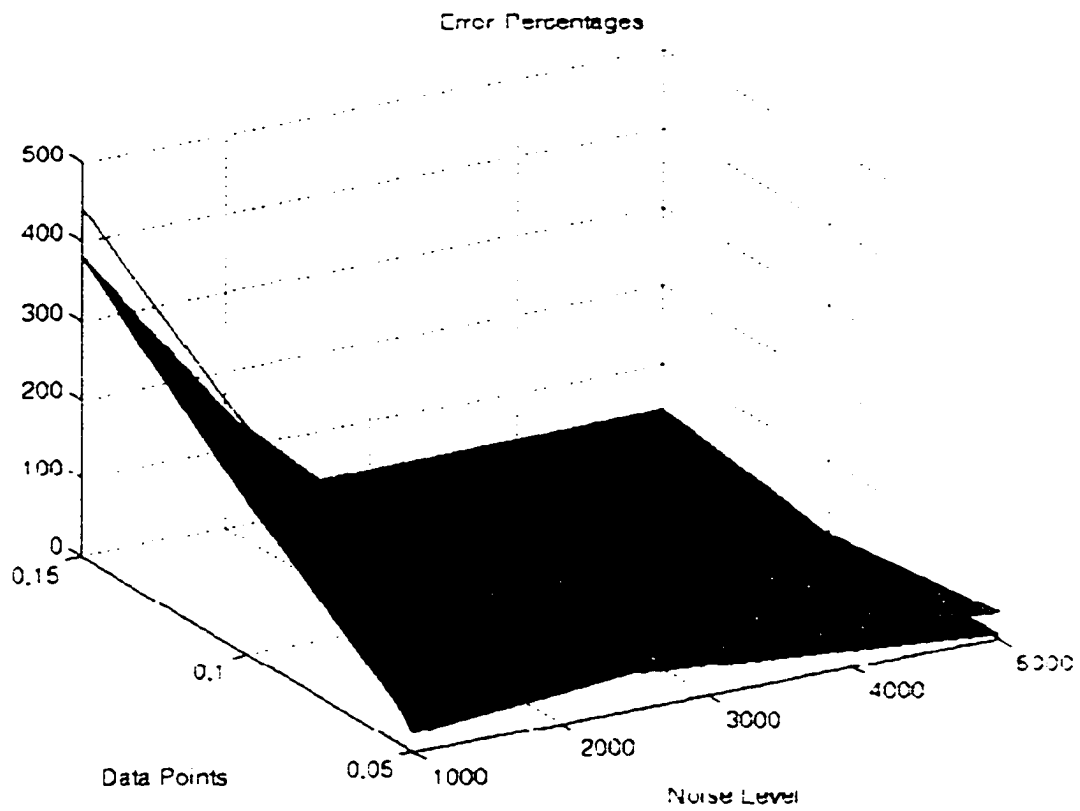


Figure 6.8 Error percentages of the 30 first open-loop Markov parameters for the direct and indirect system identification method.

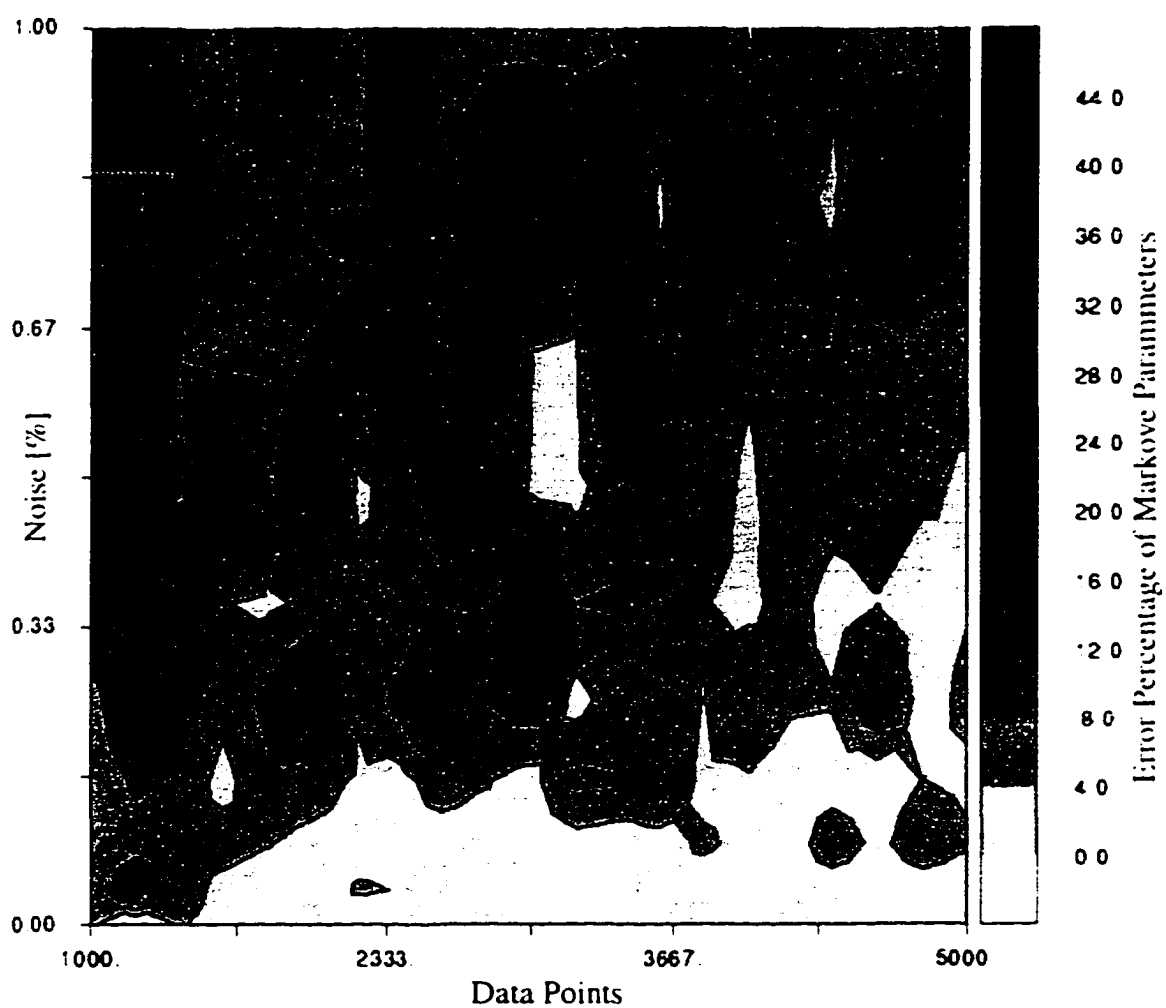


Figure 6.9 Magnitude of the percentage of error deviation of the open-loop system Markov parameters in relation to the number of data points and the noise level.

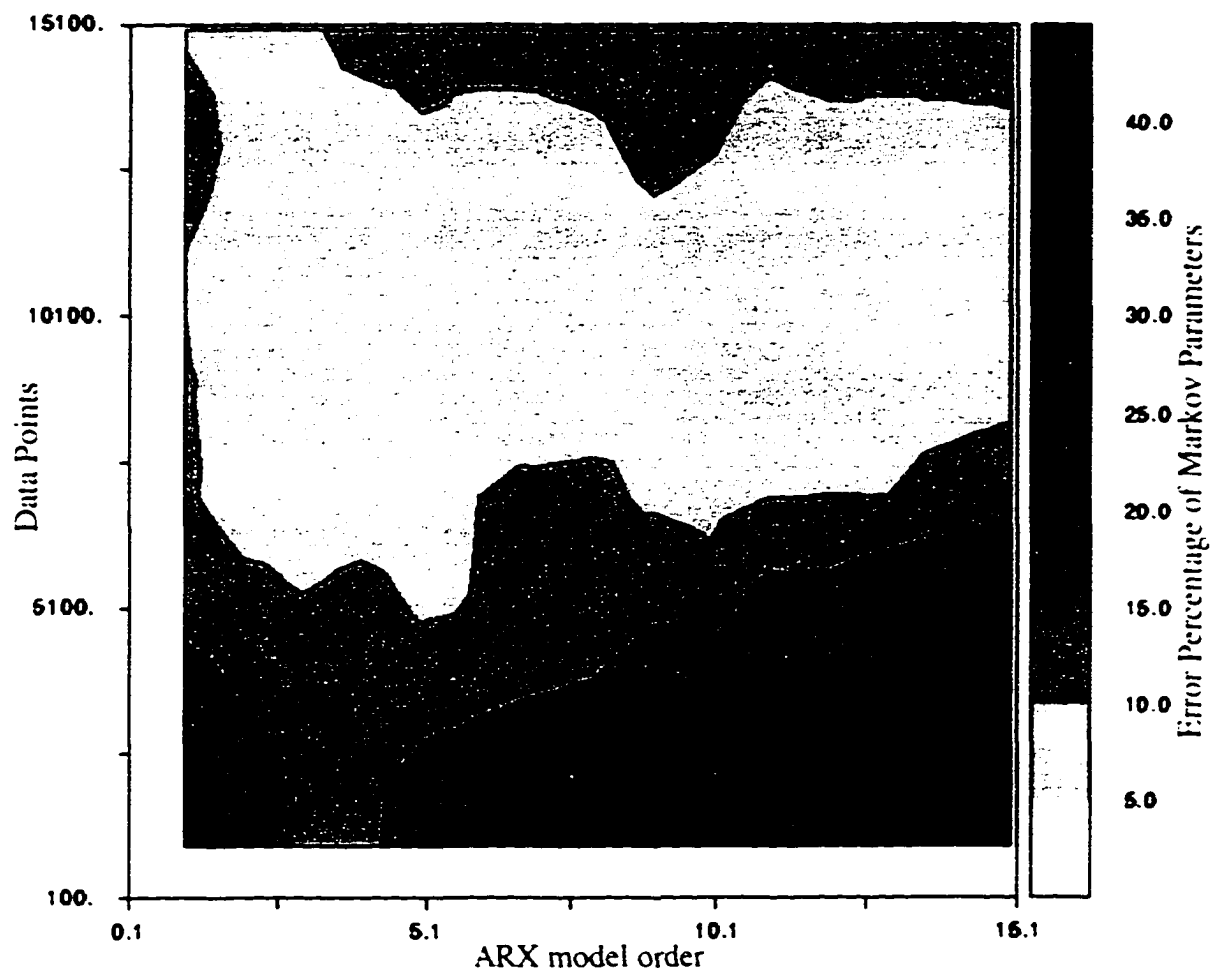


Figure 6.10 Magnitude of the percentage of error deviation of the open-loop system Markov parameters in relation to the ARX model order and the data length.

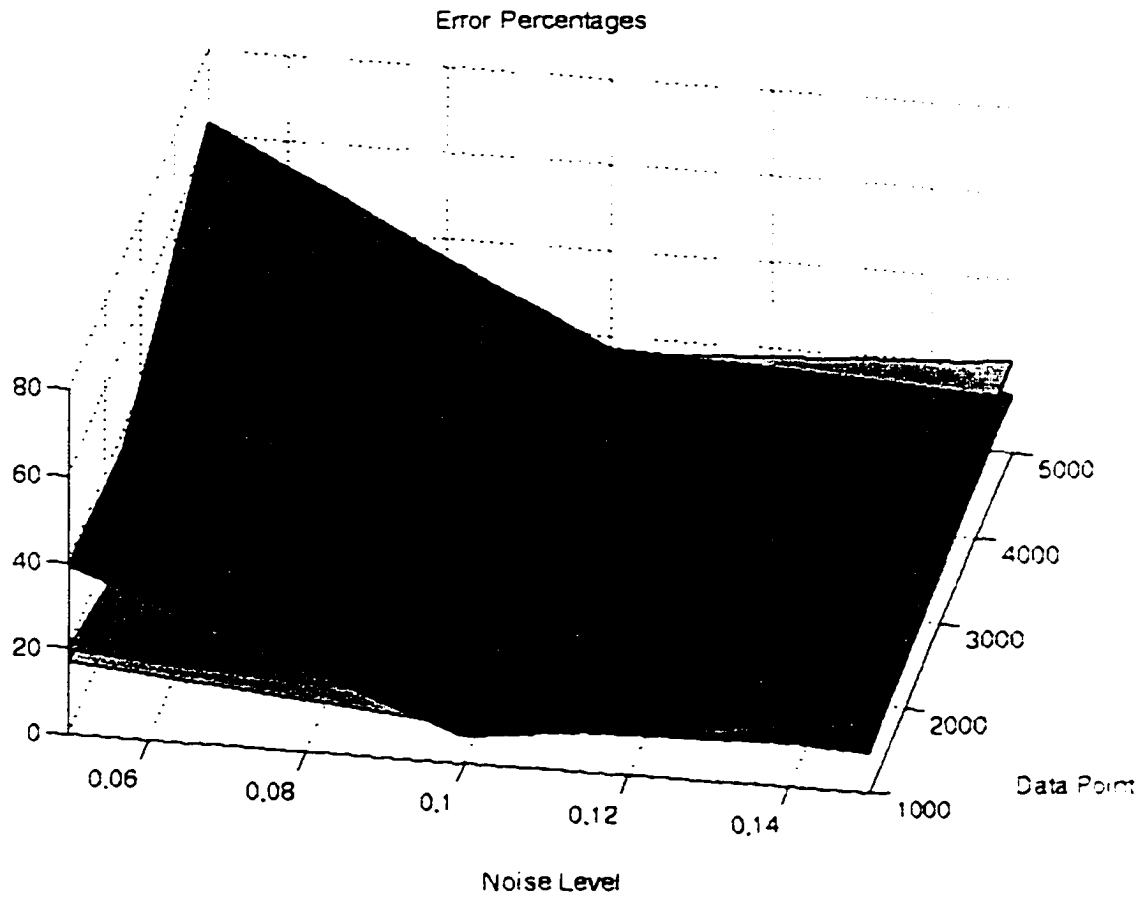


Figure 6.11 Error percentages of the 30 first open-loop Markov parameters for the direct and indirect system identification method.

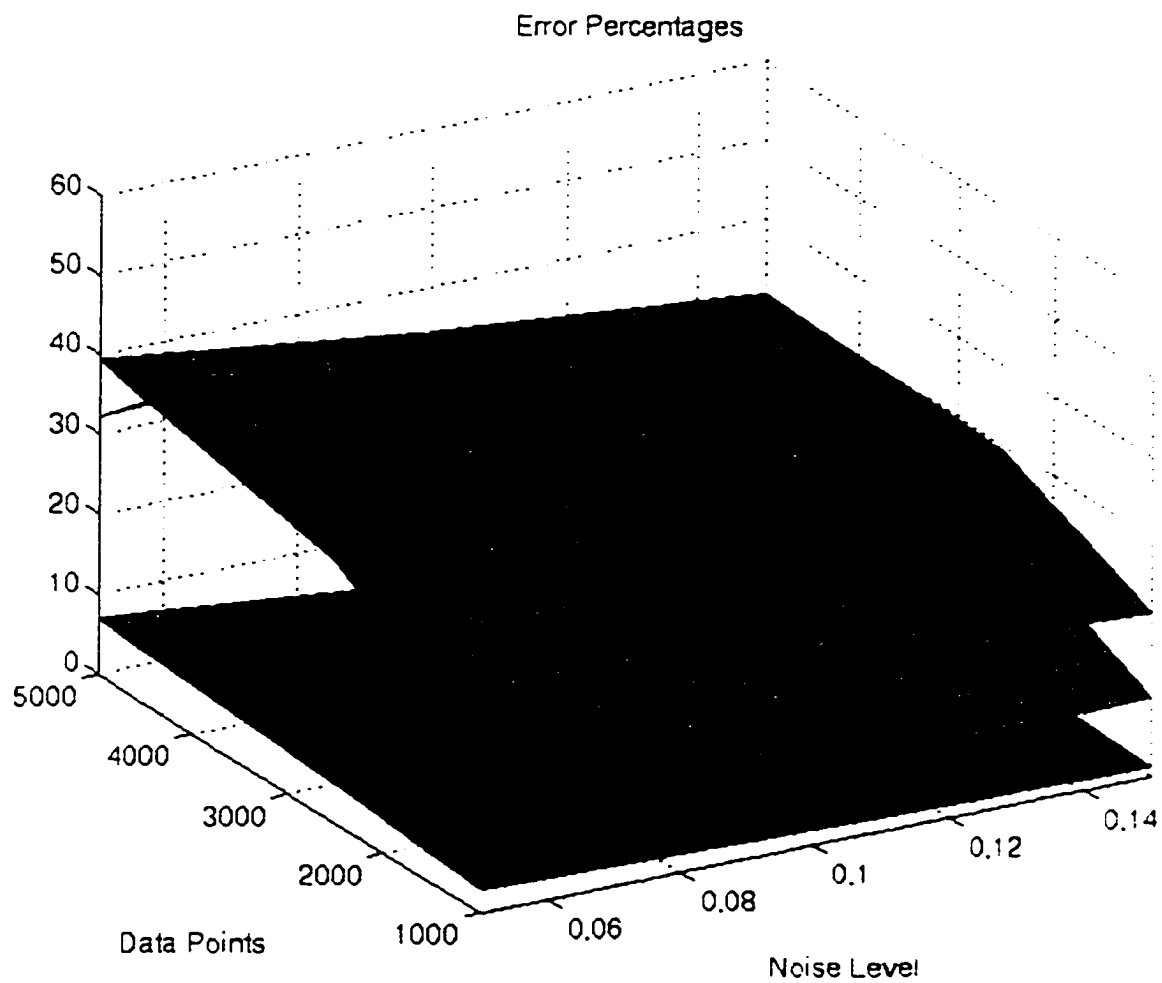


Figure 6.12 Error percentages of the 30 first open-loop Markov parameters for the direct and indirect system identification method.

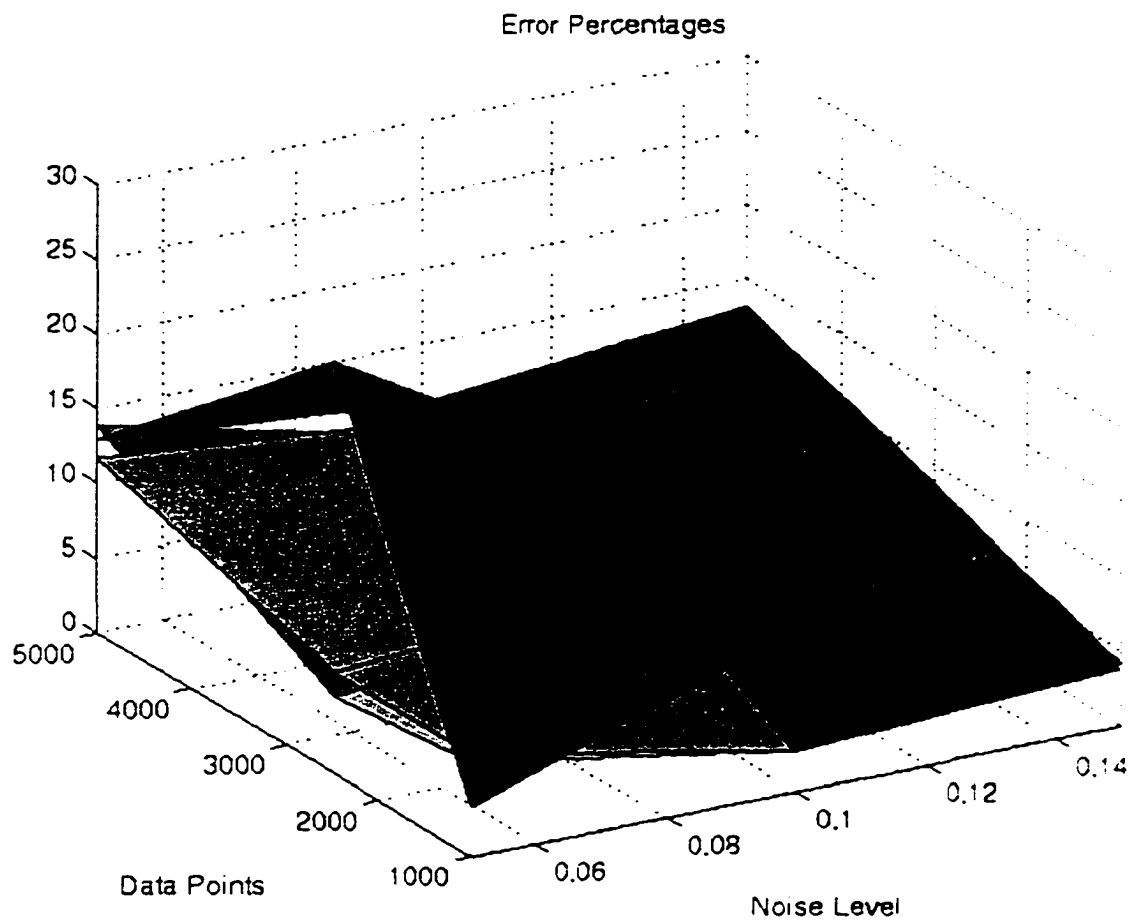


Figure 6.13 Error percentages of the 30 first open-loop Markov parameters for the direct and indirect system identification method.

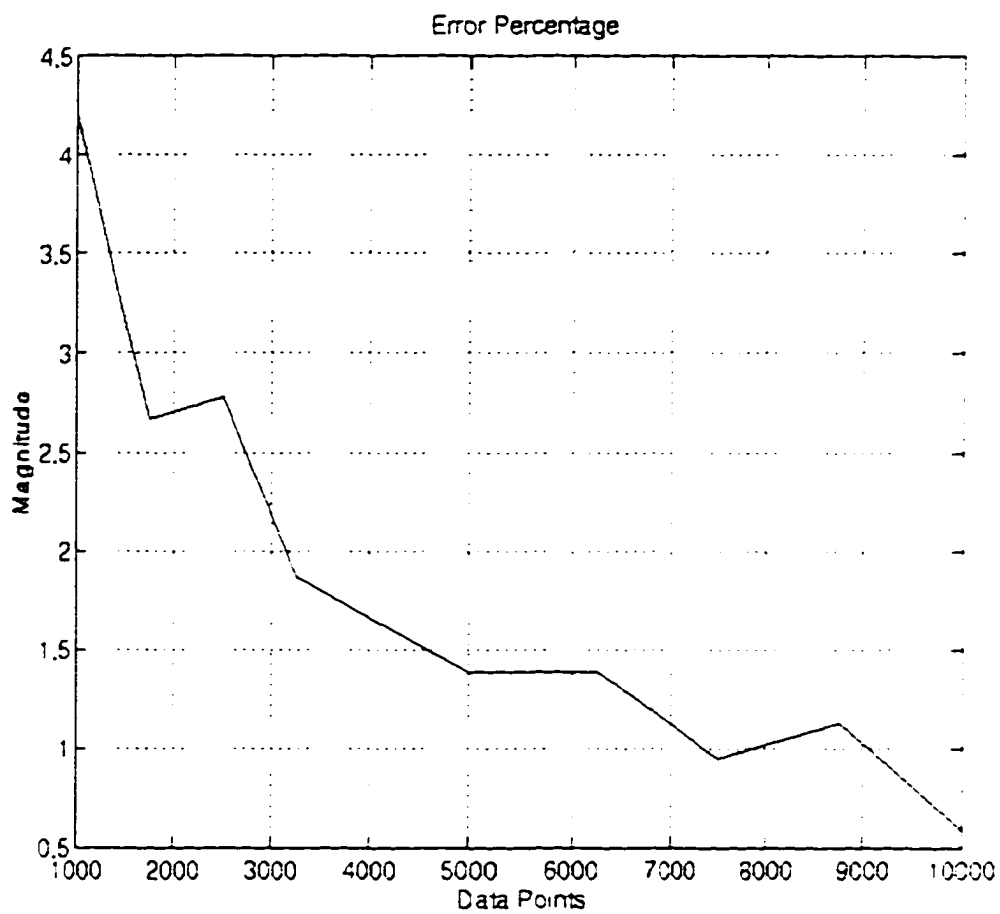


Figure 6.14 Error percentages of the 30 first open-loop Markov parameters for the direct system identification method.

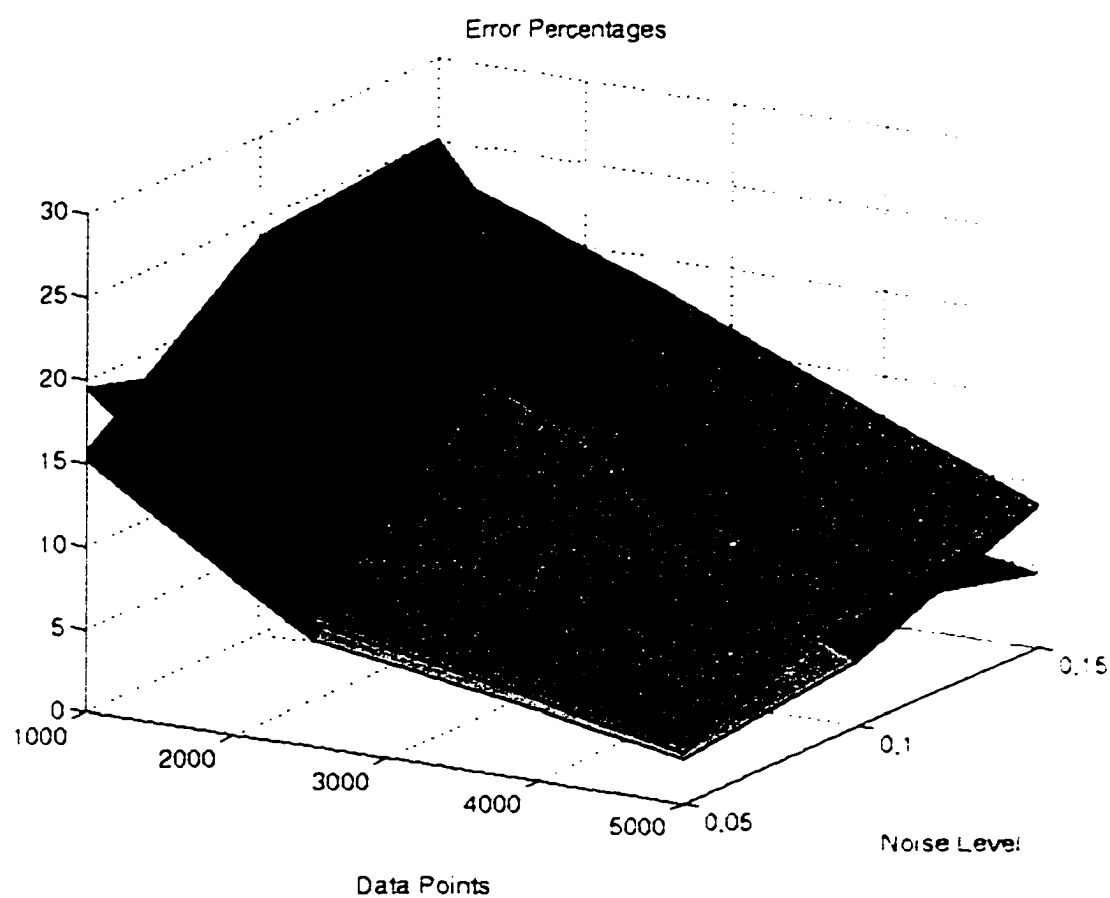


Figure 6.15 Error percentages of the 30 first open-loop Markov parameters for the direct and indirect system identification method.

CHAPTER VII

INPUT DESIGN FOR SYSTEMS UNDER IDENTIFICATION

7.1 Introduction

In the previous three chapters, the problematic of applied system identification is considered, in particular, the contents of Chapter IV indicates that the ARX model representation of the system by its input/output data is mainly responsible for the quality and accuracy of the identified system description. In Chapter V, one finds that the input data is highly relevant for the identifiability, of a given observable and controllable system. Chapter VI indicated that a suitable controller can improve the system identification accuracy and efficiency. That is, all of the above mentioned problems are defined and influenced by the selection of the input, which can be done by using a suitable controller. The purpose of this Chapter is to address the above mentioned issues by developing an input design such that the identification results are improved. In the following a new input design is proposed based on input/output data gathered from random excitation.

7.2 Input Design for ARX Model Representation

Equation (4.7) represents the ARX model for a finite-dimensional system. If one considers each summation of the finite ARX model series as a contributor for the current estimate of the output, the ARX model of an open-loop system can be represented in matrix format as follows:

$$\begin{bmatrix} \bar{y}_{k_1} \\ \bar{y}_{k_2} \\ \bar{y}_{k_3} \\ \dots \\ \bar{y}_{k_q} \end{bmatrix} = \begin{bmatrix} a_1 & 0 & 0 & \dots & 0 \\ 0 & a_2 & 0 & \dots & 0 \\ 0 & 0 & a_3 & \dots & 0 \\ \dots & \dots & \dots & \dots & \dots \\ 0 & 0 & 0 & \dots & a_q \end{bmatrix} \begin{bmatrix} y_{k-1} \\ y_{k-2} \\ y_{k-3} \\ \dots \\ y_{k-q} \end{bmatrix} + \begin{bmatrix} b_1 & 0 & 0 & \dots & 0 \\ 0 & b_2 & 0 & \dots & 0 \\ 0 & 0 & b_3 & \dots & 0 \\ \dots & \dots & \dots & \dots & \dots \\ 0 & 0 & 0 & \dots & b_q \end{bmatrix} \begin{bmatrix} u_{k-1} \\ u_{k-2} \\ u_{k-3} \\ \dots \\ u_{k-q} \end{bmatrix} + \epsilon_k \quad (7.1)$$

where

$$\hat{y}_k = \sum_{i=1}^q \bar{y}_{k_i} \quad (7.2)$$

If one wants to design a new input sequence to yield a new ARX model with $q_2 < q$ model order, one can first ignore ε_k in Equation (7.1) and have

$$\begin{bmatrix} \bar{y}_{k_{q_2+1}} \\ \bar{y}_{k_{q_2+2}} \\ \bar{y}_{k_{q_2+3}} \\ \dots \\ \bar{y}_{k_q} \end{bmatrix} = \begin{bmatrix} a_{q_2+1} & 0 & 0 & \dots & 0 \\ 0 & a_{q_2+2} & 0 & \dots & 0 \\ 0 & 0 & a_{q_2+3} & \dots & 0 \\ \dots & \dots & \dots & \dots & \dots \\ 0 & 0 & 0 & \dots & a_q \end{bmatrix} \begin{bmatrix} y_{k-q_2-1} \\ y_{k-q_2-2} \\ y_{k-q_2-3} \\ \dots \\ y_{k-q} \end{bmatrix} + \begin{bmatrix} b_{q_2+1} & 0 & 0 & \dots & 0 \\ 0 & b_{q_2+2} & 0 & \dots & 0 \\ 0 & 0 & b_{q_2+3} & \dots & 0 \\ \dots & \dots & \dots & \dots & \dots \\ 0 & 0 & 0 & \dots & b_q \end{bmatrix} \begin{bmatrix} u_{k-q_2-1} \\ u_{k-q_2-2} \\ u_{k-q_2-3} \\ \dots \\ u_{k-q} \end{bmatrix} \quad (7.3)$$

or in short:

$$\gamma = \Lambda \underline{y} + \Omega \bar{u} \quad (7.4)$$

$$\text{where } \gamma = \begin{bmatrix} \bar{y}_{k_{q_2+1}} \\ \bar{y}_{k_{q_2+2}} \\ \bar{y}_{k_{q_2+3}} \\ \dots \\ \bar{y}_{k_q} \end{bmatrix}, \quad \Lambda = \begin{bmatrix} a_{q_2+1} & 0 & 0 & \dots & 0 \\ 0 & a_{q_2+2} & 0 & \dots & 0 \\ 0 & 0 & a_{q_2+3} & \dots & 0 \\ \dots & \dots & \dots & \dots & \dots \\ 0 & 0 & 0 & \dots & a_q \end{bmatrix}, \quad \underline{y} = \begin{bmatrix} y_{k-q_2-1} \\ y_{k-q_2-2} \\ y_{k-q_2-3} \\ \dots \\ y_{k-q} \end{bmatrix}$$

$$\Omega = \begin{bmatrix} b_{q_2+1} & 0 & 0 & \dots & 0 \\ 0 & b_{q_2+2} & 0 & \dots & 0 \\ 0 & 0 & b_{q_2+3} & \dots & 0 \\ \dots & \dots & \dots & \dots & \dots \\ 0 & 0 & 0 & \dots & b_q \end{bmatrix} \text{ and } \bar{u} = \begin{bmatrix} u_{k-q_2-1} \\ u_{k-q_2-2} \\ u_{k-q_2-3} \\ \dots \\ u_{k-q} \end{bmatrix}$$

It is noted that the coefficients a_i and b_i of the ARX model are matrices for multiple input and multiple output systems. Since each element of Equation (7.4) represents a contribution to the current output, the influence of these summation can be minimized by

setting

$$\gamma = 0 \quad (7.5)$$

For a time-invariant system, the matrices Λ and Ω are constant. If Λ and Ω are known and Ω is invertible, one can solve for the input which satisfies Equation (7.5)

$$\bar{u} = -\Omega^{-1} \Lambda \underline{y} \text{ or } \bar{u}_{k-q_2-j} = -b_{q_2+j}^{-1} a_{q_2+j} y_{k-q_2-j} \quad (7.6)$$

where $\Delta q = q - q_2$.

From Equation (4.7) the ARX model coefficient are accordingly given as

$$a_i = C\bar{A}^{i-1}AK \text{ and } b_i = C\bar{A}^{i-1}B \text{ for } i=1, \dots, q \quad (7.7)$$

Rewriting Ω and Λ in Equation (7.4)

$$\Lambda = \begin{bmatrix} C\bar{A}^{-q_2}AK & 0 & 0 & \dots & 0 \\ 0 & C\bar{A}^{-q_2+1}AK & 0 & \dots & 0 \\ 0 & 0 & C\bar{A}^{-q_2+2}AK & \dots & 0 \\ \dots & \dots & \dots & \dots & \dots \\ 0 & 0 & 0 & \dots & C\bar{A}^{-q-1}AK \end{bmatrix} \quad (7.8)$$

$$\Omega = \begin{bmatrix} C\bar{A}^{-q_2}B & 0 & 0 & \dots & 0 \\ 0 & C\bar{A}^{-q_2+1}B & 0 & \dots & 0 \\ 0 & 0 & C\bar{A}^{-q_2+2}B & \dots & 0 \\ \dots & \dots & \dots & \dots & \dots \\ 0 & 0 & 0 & \dots & C\bar{A}^{-q-1}B \end{bmatrix} \quad (7.9)$$

If $|\Omega|$ is invertible, then

$$\Omega^{-1} = \begin{bmatrix} (C\bar{A}^{-q_2}B)^{-1} & 0 & 0 & \dots & 0 \\ 0 & (C\bar{A}^{-q_2+1}B)^{-1} & 0 & \dots & 0 \\ 0 & 0 & (C\bar{A}^{-q_2+2}B)^{-1} & \dots & 0 \\ \dots & \dots & \dots & \dots & \dots \\ 0 & 0 & 0 & \dots & (C\bar{A}^{-q-1}B)^{-1} \end{bmatrix} \quad (7.10)$$

From Equation (7.6), the revised input \tilde{u} can be written as

$$u_{k-q_2-j} = -(C\bar{A}^{q_2+j}B)^{-1}C\bar{A}^{q_2+j}AKy_{k-q_2-j} \text{ for } j = 1, 2, \dots, \Delta q \quad (7.11)$$

If $C \in R^{n_o \times n}$, $B \in R^{n \times n_i}$ and $n_o = n_i = n$

$$u_{k-q_2-j} = -B^{-1}AKy_{k-q_2-j} \quad (7.12)$$

It is proposed to use this new input in a second identification experiment as outlined in the following. The schematic of such an identification process is given in Figure 7.1. In the first step, the system is excited by a random input and the input/output data is recorded. From that data, the corrected input is computed and used for a second identification experiment of the system. In Figure 7.2, the input design is depicted for the first simulation. The original input is windowed q data points at a time, and q_2 data points are substituted by the newly computed values. The simulations were done with the spring-mass system given in Chapter II. A total of 2500 data points were used for the simulation, the ARX model order q was set to be 10 and q_2 was set to be 7. The noise level of the process and measurement was 5% (variance). For the following simulation, a LQR controller was used to enhance the stability and damping ratio of the system. The error percentage of the thirty first open-loop Markov parameters from the identification without input design was 107.019%. The input was computed according to the above formula, and feed to the system for a second identification. The error percentage reduced to 4.905%. Figure 7.3 shows the original output of the system for the first step of the identification and the new output for the second step of the identification. One clearly recognizes the random characteristic of the output from the first identification, and the oscillatory behavior of the output from the second identification. Also noted is a dramatic increase in magnitude for the second identification. Figure 7.4 depicts the input for the first identification step and the input for the second identification step. The corrected and original input show similar characterizes and magnitude. The human lung model introduced in Chapter II was used, using no feedback controller, and identification was performed also in two steps, normal identification with random input and identification with input design. The ARX model order was chosen to be 15, and q_2 was set to be 10. The measurement noise and process noise was 1% (variance). A total of 2500 data points were used for each simulation. For the first

identification, the error percentage of the open-loop Markov parameters was 5.71%, the error percentage for the identification with input design was 0.162%. Figure 7.5 shows the original input and the corrected input. The characteristic of the corrected input signal indicates much less randomness and a much larger magnitude than for the original input. The large input is due to the corrected signals.

The rather large magnitude required for the input from the human lung model simulation lead to the following alteration of the input design. Only the first q_2 input data are newly computed, and thereafter, the input data is kept random. The simulation for this case were performed with the spring-mass system, using a LQR feedback controller. The noise level was set to be 30% measurement and process noise (variance). The ARX model order q is 4 and q_2 is equal to 3. The error percentage of open-loop Markov parameters for the simulation without input design is 112.72%, while the error percentage of open-loop Markov parameters for the simulation with input design is 7.97%. Figure 7.6 gives the graph of the two outputs, for the simulation without input design and the output with input design. The output of the second simulation with the corrected input shows again an oscillatory characteristic with much larger magnitude as the for the output without input design. Figure 7.7 depicts the original input and the corrected input. Both seem to have the same randomness and magnitude. Simulation with the lung model resulted in similar outcomes. The dominant poles are identified quite accurately, though the less dominant poles of the system show some inaccuracies. By changing only the first q_2 inputs of the original input, the system is excited at its modes and produces high signal to noise ratios, which yields somewhat more accurate identification results than using the original input but does not required the magnitude of the input to change.

Figure 7.8 and 7.9 depict the error percentages of the open-loop Markov parameters for the simulation results using input design and normal random input for the min-mast system. For both simulation the noise level of the process and measurement were varied between 0% and 50% (variance). The number of data points used for the identification was in all cases 2500, and the ARX model order q was set to 4 and q_2 equal to 3. For the results depicted in Figure 7.8, the system was operated in open-loop, while the results shown in Figure 7.9 were obtained by exciting a closed-loop system. The dashed lines

represent the error percentage level for the identification results using input design. In both cases and over the whole interval of the noise level, the results with an alternating input design are much more accurate, especially for high noise levels. Figure 7.9 depicts also the results for different ARX model orders (dash dotted line is for $q=15$, and dotted line is for $q=3$), using input design. The results are similar to the ones for $q=4$.

In the following, the effects of this input design to the ARX model representation is analyzed for a specific case, that is $q = 3$, $q_2 = 2$.

From Equation (4.7), the new output after applying \bar{u} at $k=1$ becomes

$$\begin{aligned}\bar{y}_1 &= \sum_{i=1}^q C\bar{A}^{i-1}AK\bar{y}_{k-i} + \sum_{i=1}^q C\bar{A}^{i-1}B\bar{u}_{k-i} + \varepsilon_k \\ \bar{y}_1 &= CAK\bar{y}_0 + CB\bar{u}_0 + \varepsilon_1\end{aligned}\quad (7.13)$$

$$\text{but } \bar{y}_0 = 0 \text{ and } \bar{u}_0 = 0, \text{ so } \bar{y}_1 = \varepsilon_1 \quad (7.14)$$

$$\bar{y}_2 = CAK\bar{y}_1 + CB\bar{u}_1 + \varepsilon_2$$

but $\bar{u}_1 = -B^{-1}AKy_1$ and using Equation (7.14),

$$\bar{y}_2 = CAK\varepsilon_1 - CAKy_1 + \varepsilon_2$$

the output y_1 , on the other hand is given by Equation (4.7) and can be given as

$$y_1 = CAKy_0 + CBu_0 + \varepsilon_1$$

and therefore

$$\bar{y}_2 = \varepsilon_2 \quad (7.15)$$

Continuing with the same methodology:

$$\begin{aligned}\bar{y}_3 &= CAK\bar{y}_2 + C\bar{A}AK\bar{y}_1 + C\bar{A}^2AK\bar{y}_0 + CB\bar{u}_2 + C\bar{A}B\bar{u}_1 + C\bar{A}^2B\bar{u}_0 + \varepsilon_3 \\ &= CAK\varepsilon_2 + C\bar{A}AK\varepsilon_1 - CAKy_2 - C\bar{A}AKy_1 + \varepsilon_3\end{aligned}$$

$$\text{but } y_2 = CAKy_1 + C\bar{A}AKy_0 + CBu_1 + C\bar{A}Bu_0 + \varepsilon_2 = CAK\varepsilon_1 + CBu_1 + \varepsilon_2$$

therefore

$$\bar{y}_3 = -CAKCAK\varepsilon_1 - CAKCBu_1 + \varepsilon_3 \quad (7.16)$$

$$\bar{y}_4 = CAK\bar{y}_3 + C\bar{A}AK\bar{y}_2 + C\bar{A}^2AK\bar{y}_1 +$$

$$\begin{aligned}
& + CB\bar{u}_3 + C\bar{A}B\bar{u}_2 + C\bar{A}^2\bar{u}_1 + \varepsilon_4 \\
\bar{y}_4 = & -CA^2KCAK\varepsilon_1 + CAK\varepsilon_3 + \varepsilon_4 - CA^2KCBu_1 + CBu_3 \\
\end{aligned} \tag{7.17}$$

$$\begin{aligned}
\bar{y}_5 = & CAK\bar{y}_4 + C\bar{A}AK\bar{y}_3 + C\bar{A}^2AK\bar{y}_2 + \\
& + CB\bar{u}_4 + C\bar{A}B\bar{u}_3 + C\bar{A}^2\bar{u}_2 + \varepsilon_5 \\
\bar{y}_5 = & -CA^3KCAK\varepsilon_1 + CA^2K\varepsilon_3 + CAK\varepsilon_4 + \varepsilon_5 + \\
& - CA^3KCBu_1 + CABu_3 + CBu_4 \\
\end{aligned} \tag{7.18}$$

$$\begin{aligned}
\bar{y}_6 = & -(CA^4K - C\bar{A}^3AK)CAK\varepsilon_1 + CA^3K\varepsilon_3 + CA^2K\varepsilon_4 + CAK\varepsilon_5 + \varepsilon_6 \\
& - (CA^4K - C\bar{A}^3AK)CBu_1 + CA^2Bu_3 + CABu_4 + CBu_5 \\
\end{aligned} \tag{7.19}$$

If continued in this fashion, the output is described by a series of observer gain Markov parameters times the residual, plus a series consistent with the open-loop system Markov parameters times the input. The terms for ε_1 and u_1 depend on the selection of q and q_2 . From Chapter IV, we know that the residual is quit small, and therefore the new output is described by the convolution of the original input and the open-loop Markov parameters. Simulations indicate that the term involving u_1 is small compared with the summation of the other contributors. Therefore by using the described input design, one can excite the system modes directly and achieve a high signal to noise ratio, which leads to very accurate identification results.

7.3 Feedback Controller Design Criteria for System under Identification

The input design can be implemented into a controller design by using Hsiao's approach of iterative LQG controller design, or simple LQR controller design. Hsiao points out that for good identification results the closed-loop system should have damping ratios of 0.4 - 0.7. These requirements sometimes do not agree with the system performance requirements. In general, controllers are designed such that a particular system characteristic can be established. System identification, on the other hand uses random

input data, or at least binary random sequences, to excite the system. This is a broad based approach, since with the random input data, one wants to make sure that all the significant system frequencies are excited and can be detected by the system identification algorithm. The newly developed input design is capable of concentrating onto the system modes, which leads partially to a non random input. Since this method does not require a lot of substitutions, this can be done periodically during the system identification process, while the ARX model parameters are updated and the input is improved. Figure 7.10 outlines such an approach.

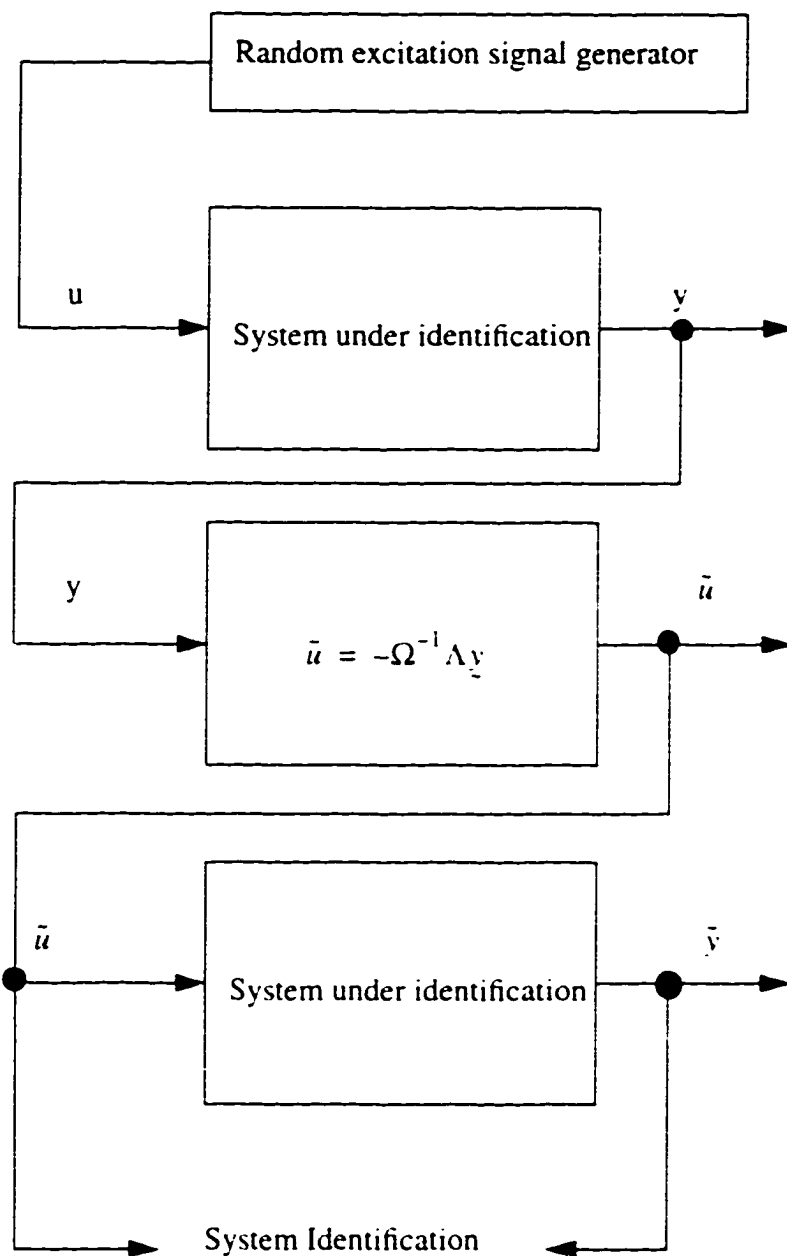


Figure 7.1 Two-step system identification with proposed input design.

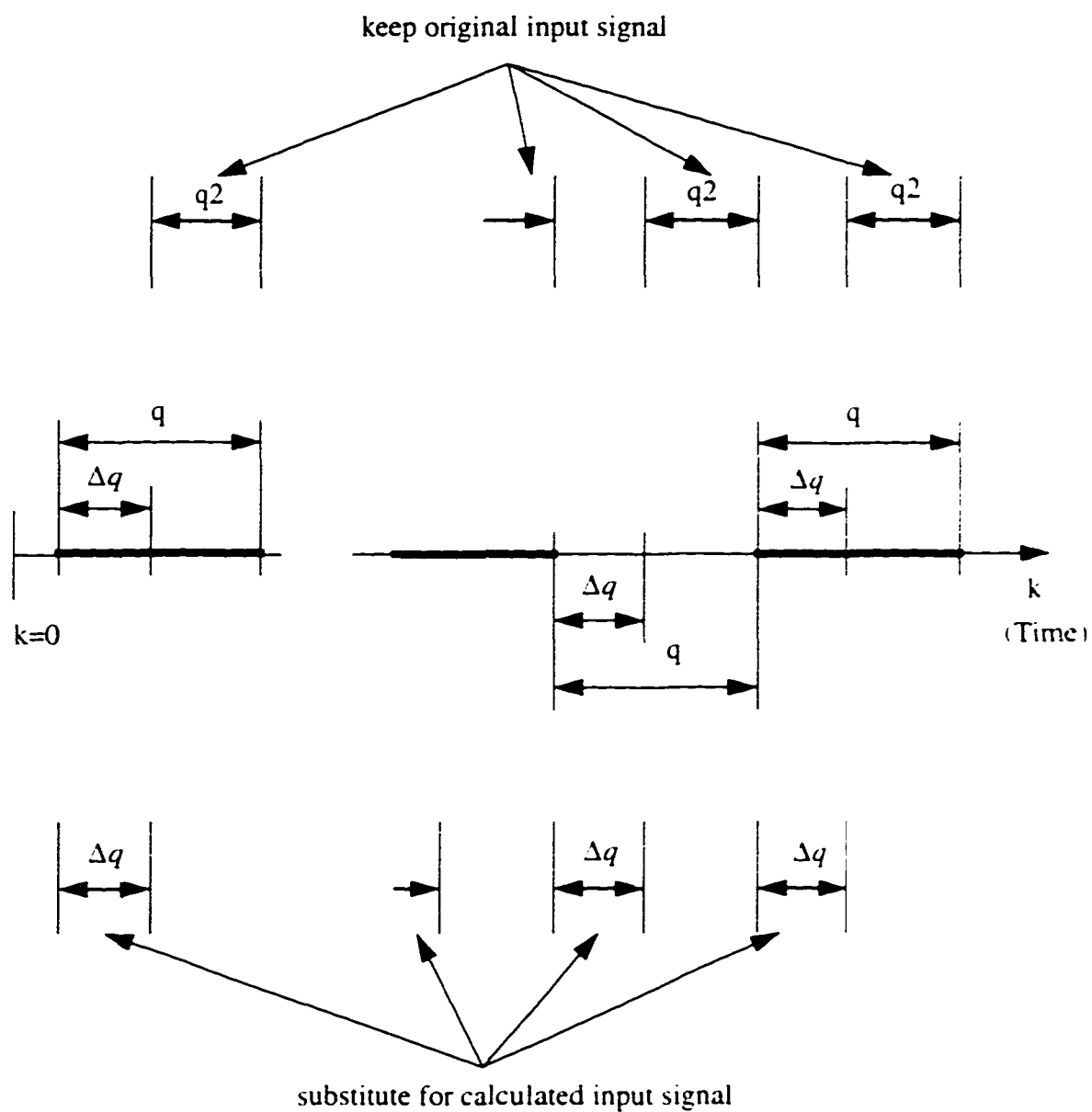


Figure 7.2 Input signal design with repeated substitution of new input data.

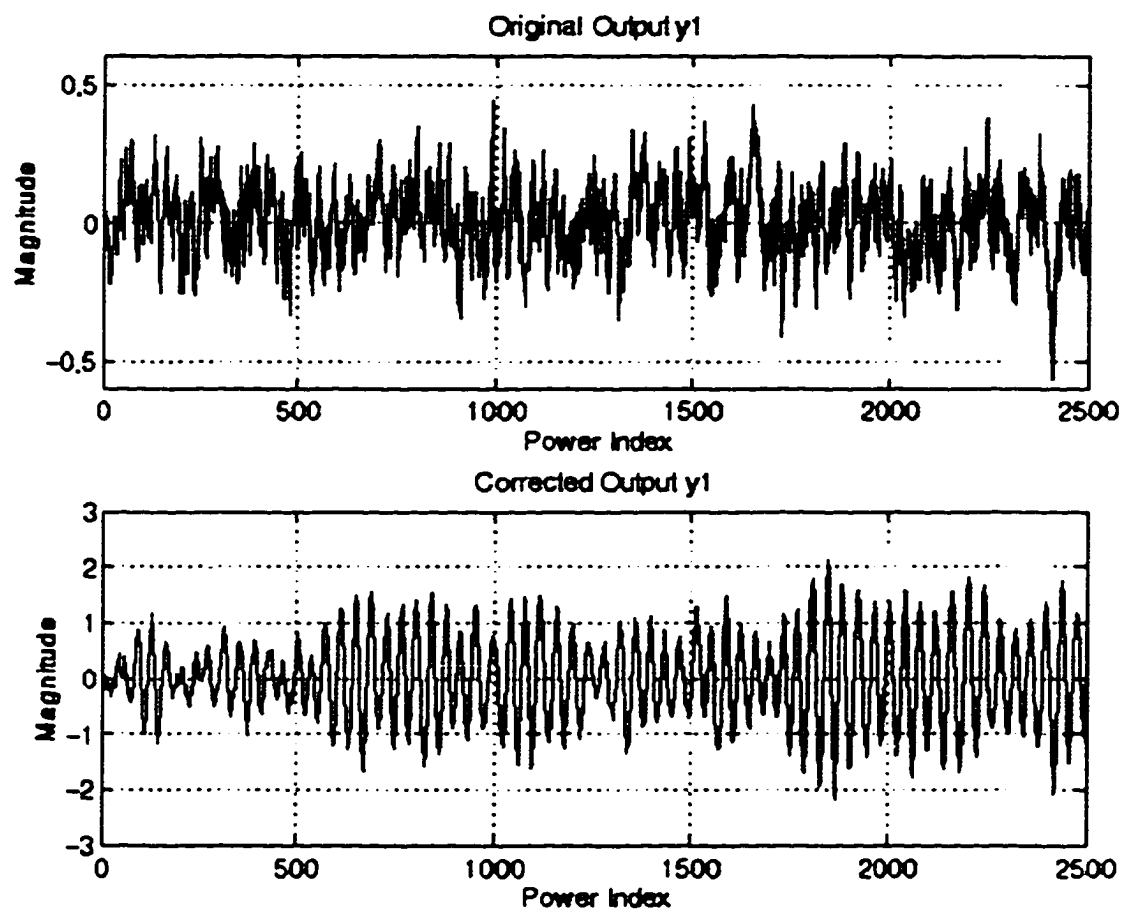


Figure 7.3 System output of original simulation and simulation with input design.

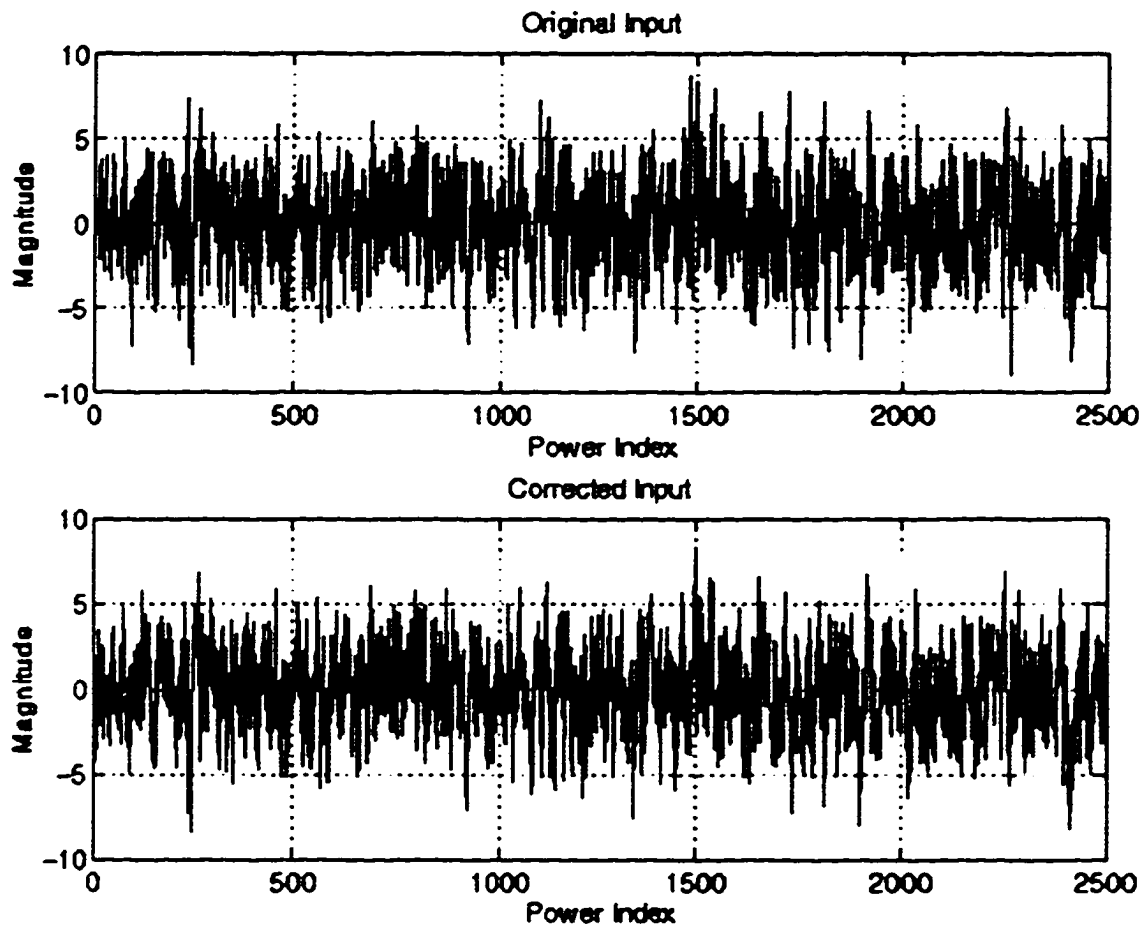


Figure 7.4 System input of original simulation and simulation with input design.

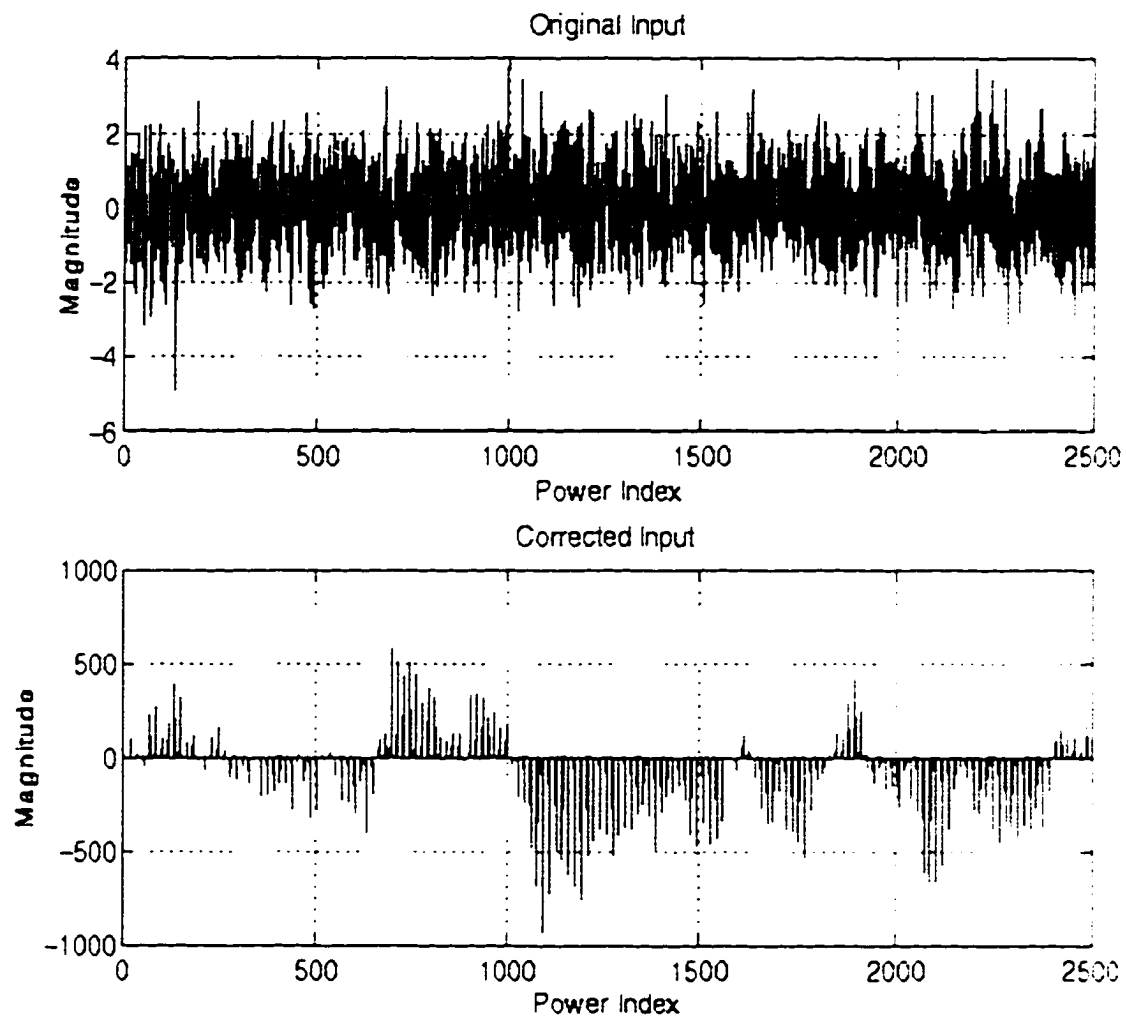


Figure 7.5 Original system input and corrected input for respiratory system.

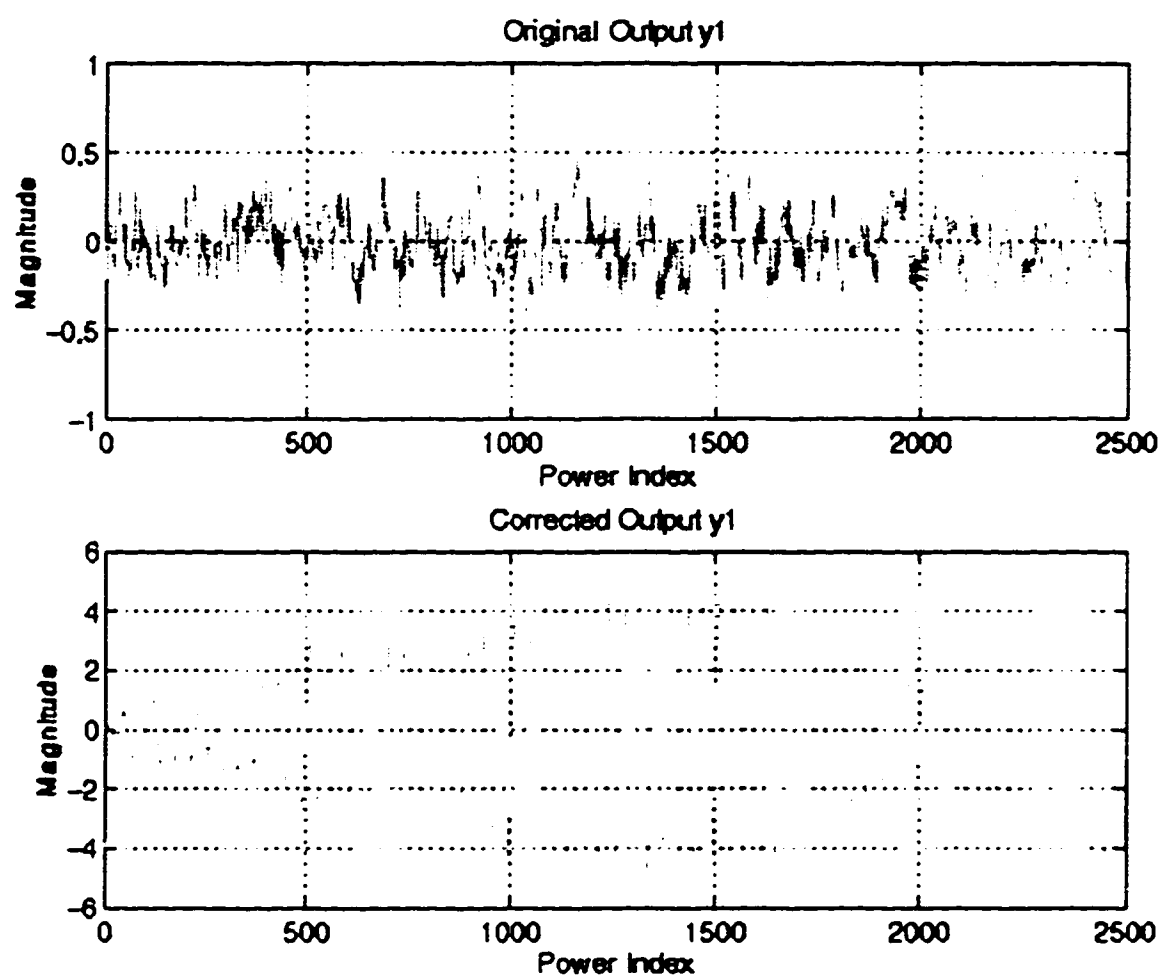


Figure 7.6 System output of original simulation and simulation with input design.

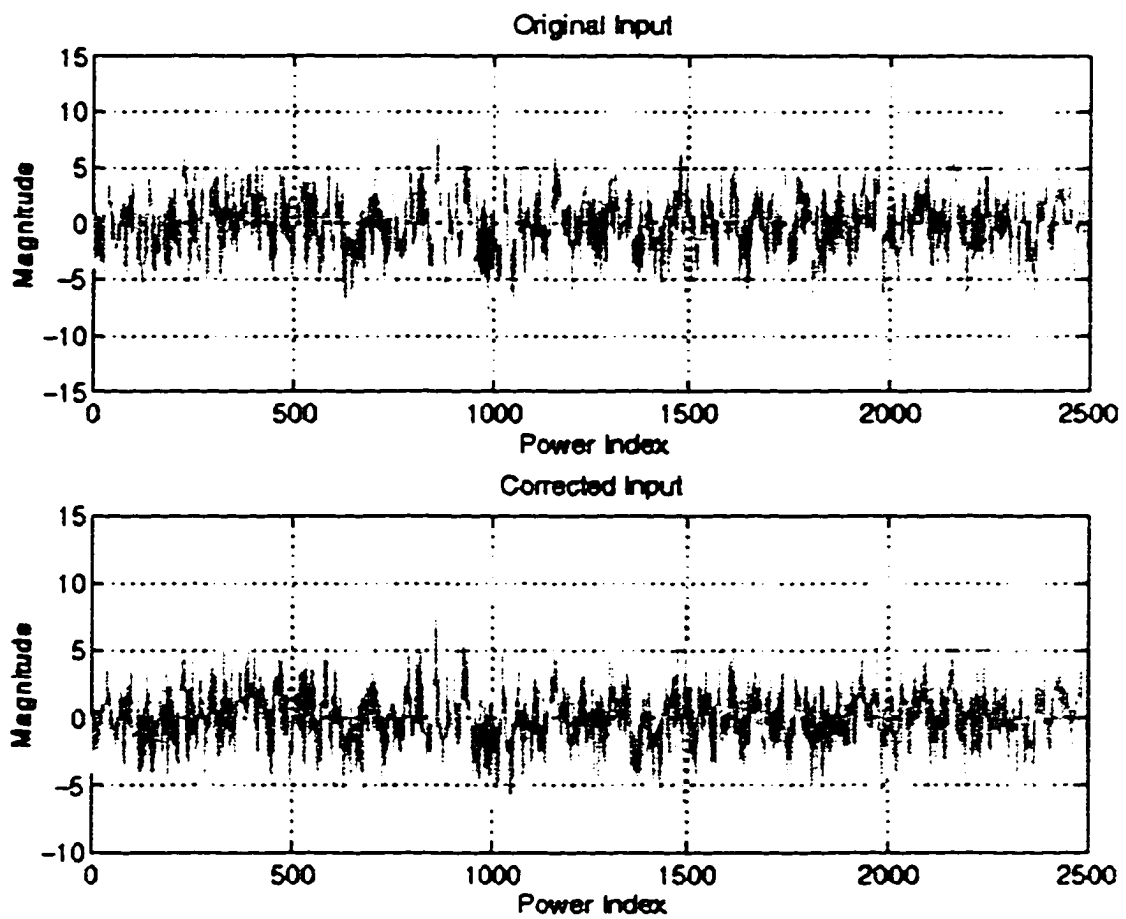


Figure 7.7 System input of original simulation and simulation with input design.

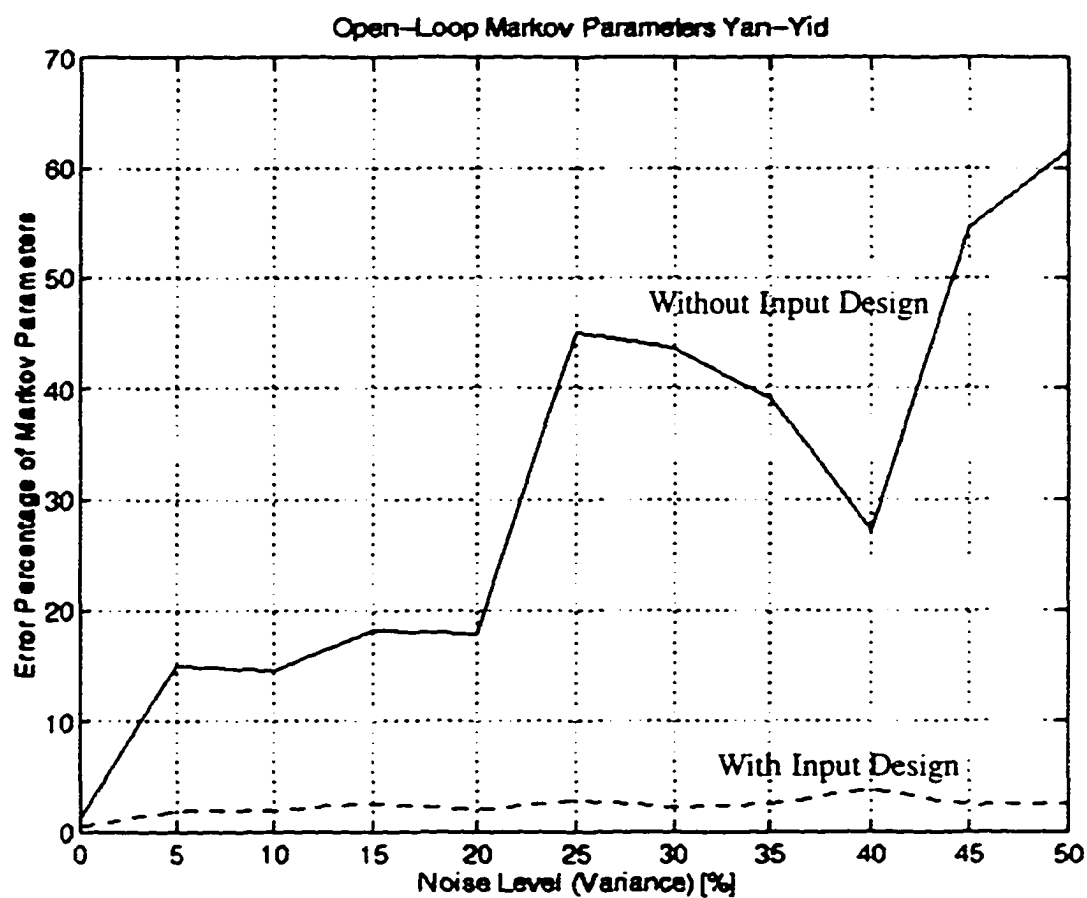


Figure 7.8 Error percentages of open-loop Markov parameters for identification of the system operating in open-loop, with and without input design and different noise levels.

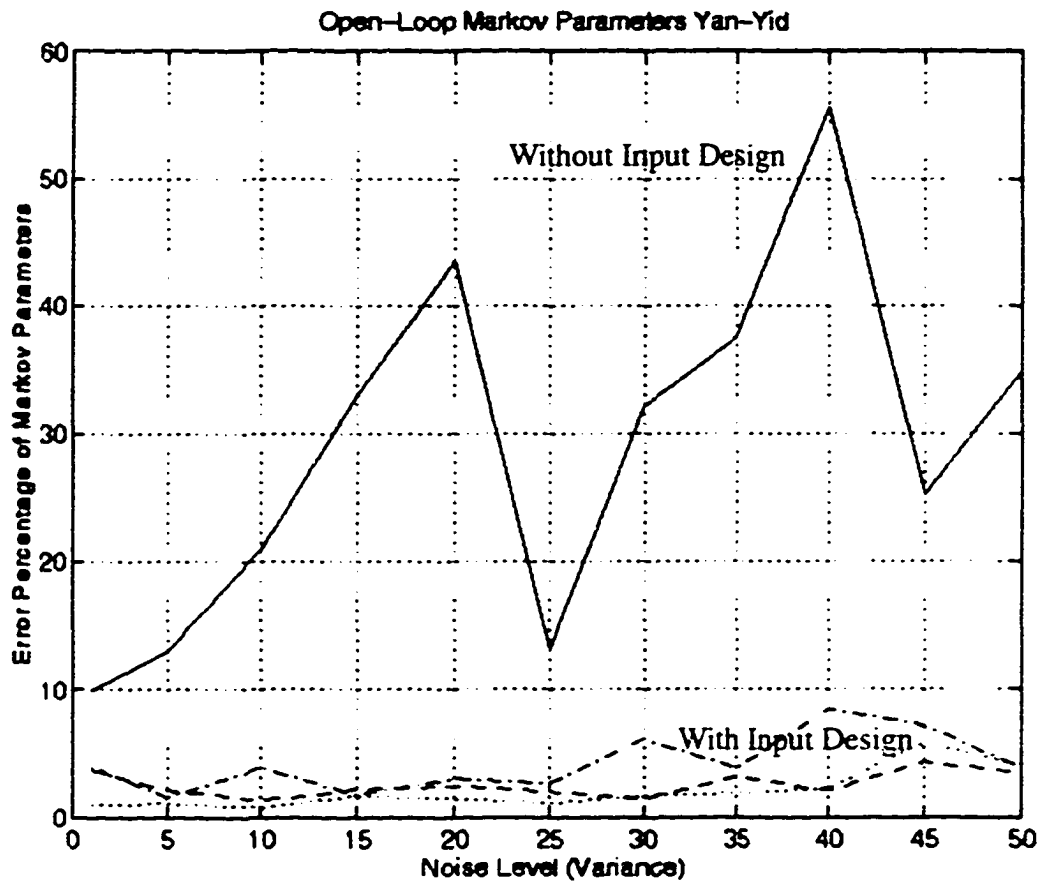


Figure 7.9 Error percentages of open-loop Markov parameters for identification of the system operating in closed-loop, with and without input design and different noise levels

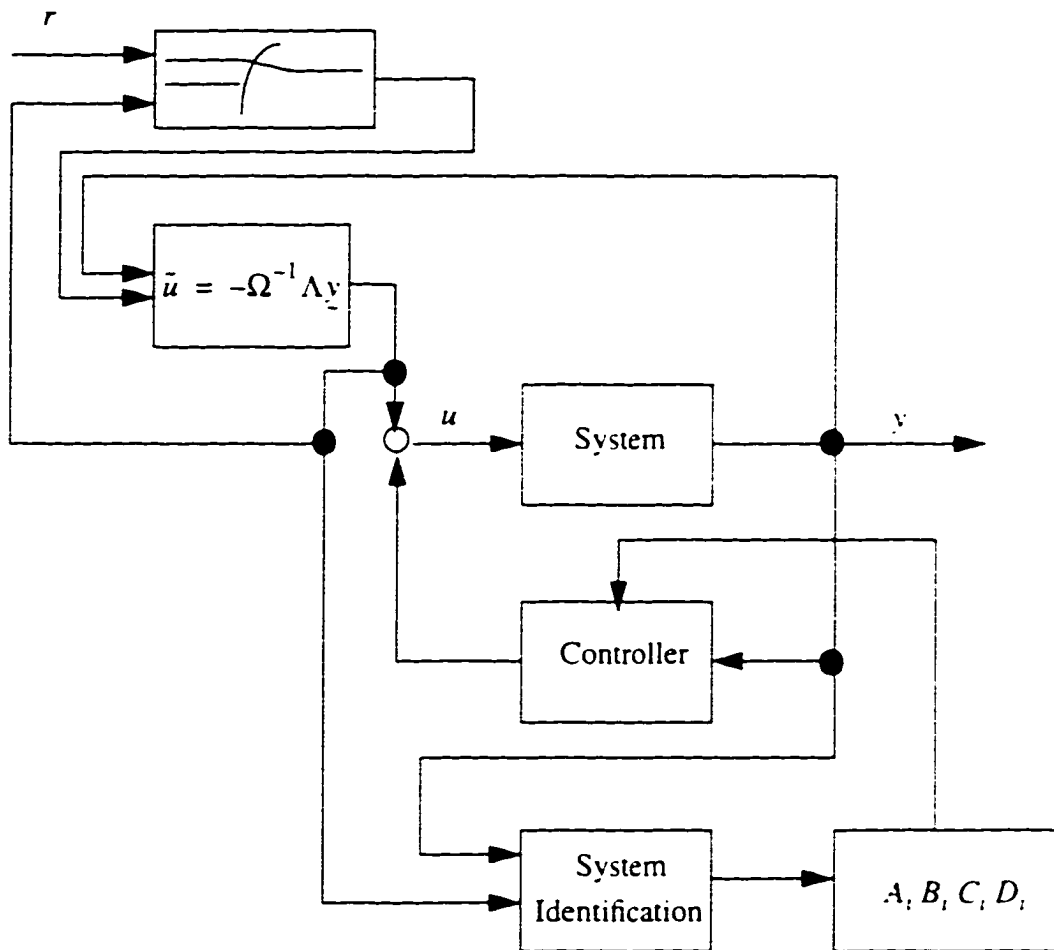


Figure 7.10 Possible iterative controller design schematic with input design.

CHAPTER VIII

CONCLUSIONS

8.1 Contributions

A new input design has been proposed for system identification using direct or indirect methods. The input is calculated according to the estimated model parameters and fed back along with the partially substituted original input to the system, where new output data is produced. This new input/output data is used for the system identification.

Existing identification methods, such as Open-Loop Kalman filter Identification (OKID) and Closed-Loop Identification (CLID), use random input signals to excite the unknown or partially known system. The randomness of the input signal is assuring that all system modes are stimulated. Also a benefit of the random, or binary random signal, is to satisfy the identifiability condition for the model parameters. However, there is a lot of energy wasted on composing an input signal with frequencies which do not correspond to the system frequencies. Another problematic of standard system identification methods is the truncation of an infinite model approximation of the physical system. In particular, ARX models are reduced to finite length and along with the truncation some of the system characteristics is being cut off. A relatively unknown factor to the accuracy and/or data length requirement of system identification is the role of the controller. The controller is believed to have similar effects as a state observer to the system identification process, where a lot of information can be condensed into a relatively short data length. Though, the corrected input from the controller to the system may not guarantee identifiability.

The truncation error stemming from the finite ARX model is being investigated along with any possible other error source which may occur during the system identification process. The computation of the identified state-space description of the system under investigation does not include noticeable error sources. The major error is introduced by the truncation of the infinite ARX model series into a finite model. Compared to the

innovation, this error clearly dominates. This error occurs for both system identification methods, regardless of the employment of a state or output feedback controller. The effect of the process noise to the system identification is also determined. The controller does have no influence on limiting the influence of the process noise for the ARX model representation.

The identifiability problem is reduced to the consistency parameter estimation problem and experimental conditions are developed from it. These conditions are given by the input/output data which makes it very practical to use. In case one has to identify the system from early stage of the experiment, the role of the initial condition to the identifiability problem is explored. The initial conditions of the system must excite all system modes in order that the system is identifiable.

Several different example systems are used to investigate the influence of the controller to the system identification process. The numerical examples include a human respiratory system, a structural system, a magnetic suspension system, a heat-mass transfer system, and a macro economical system. The indirect system identification method indicates to have a slight advantage over the direct system identification method in terms of accuracy and/or data length, if the feedback controller is well designed.

The proposed input design uses some of the information obtained from the first part of the identification to update the input and concentrate more on the system modes. The results indicate a much higher signal to noise ratio, which makes the identification less sensible to process and/or measurement noise. The newly computed input for stable systems shows to have about the same magnitude, though for marginally stable systems, the input may saturate the actuators and the input design may not work. Given the new input design in input/output representation, the output can be described by a convolution involving the residual and the observer gain Markov parameters and a convolution involving the new input and the open-loop system Markov parameters. Since the residual is very small, the output is dominated by the amplified open-loop system Markov parameters. Simulation using the structural system and the human lung system indicate very accurate identification results compared with the normal identification results, especially for high noise levels where the identification is capable of inferring the system characteristics quite well.

8.2 Further Extension of the Research

Since the indirect system identification showed that it is capable of delivering slightly more accurate results than the direct method, the role of the controller poles should be investigated at greater depth. This knowledge will enable one to place the closed-loop poles at a certain location to improve the identification results.

A natural extension of the input design is its implementation into a controller design. Developing a controller design schematic which results in a controller to produce the same input as obtained from the input design, one would make the proposed system identification process more efficient.

Naturally, a physical validation of the proposed input design is highly desirable. For this, almost any stable system could be used and the identification process could be partitioned into two steps to make it most convenient. Another interesting point would be a mathematical proof of the input designs perform better than the normal excitation used in the system identification.

The stated input design could be implemented into the computational algorithm of the closed-loop or open-loop system identification methods. This would enable one to reduce the time necessary to perform the computation for the system identification process and may lead to simplification of the derivation.

BIBLIOGRAPHY

- 1 Ljung L., *System Identification - Theory for the User*, Prentice-Hall, Inc., Englewood Cliffs, New Jersey, 1987.
- 2 Juang, J.-N., *Applied System Identification*, PRT Prentice-Hall, Inc., Englewood Cliffs, New Jersey, 1994.
- 3 Gustavsson I., Ljung L., and Soderstrom T., "Survey Paper: Identification of Processes in Closed-Loop-Identifiability and Accuracy Aspects," *Automatica*, Vol. 13, pp. 59-75, 1977.
- 4 Phan, M., Horta, L. G., Juang, J.-N., and Longman, R. W., "Improvement of Observer/Kalman Filter Identification by Residual Whitening," *Proceedings of Eight VPI & SU Symposium*, edited by L. Meirovitch, Blacksburg, Virginia, May, 1991, pp. 467-478.
- 5 Chen, C.W., Huang, J.-K., and Juang, J.-N., "Identification of Linear Stochastic Systems Through Projection Filters," *Proceedings of the AIAA Structures, Structural Dynamics and Materials Conference*, Dallas, TX, 1992, pp.2330-2340.
- 6 Chen C. W., Lee, G., and Juang, J.-n., "Several Recursive Techniques for Observer/Kalman Filter System Identification From Data," *Paper No. 92-4386, Proceedings of AIAA Guidance, Navigation and Control Conference*, Hilton Head, SC, August 1992.
- 7 Juang, J.-N., and Phan, M., "Linear System Identification via Backward Observer Models," *NASA Technical Memorandum TM-107632*, May 1992.
- 8 Huang, J.K., Juang, J.-N. and Chen, C. W., "Single-Mode Projection Filters for Modal Parameter Identification for Flexible Structures," *AIAA Journal of Guidance, Control and Dynamics*, Vol. 12, No. 4, July-August 1989, pp. 568-576.
- 9 Chen, C. W., Juang, J.-N., and Huang, J.-K., "Adaptive Linear Identification and State Estimation," in *Control and Dynamic Systems: Advances in Theory and Applications*, Vol. 57, *Multidisciplinary Engineering Systems: Design and Optimization Techniques and Their Application*, edited by C.T. Leondes, New York: Academic Press, Inc., 1993, pp. 331-368.
- 10 Juang, J.N., Phan, M., "Identification of System, Observer, and Controller form Closed-Loop Experimental Data," *Journal of Guidance, Control, and Dynamics*, Vol 17, No. 1, 1994, pp. 91-96.
- 11 Hu, A., and Martin, D., "System Identification of Unstable Manipulators Using ERA Methods," *Proc. of the AIAA Guidance, Navigation and Control Conference*, 1993, pp. 1264-1270.

- 12 Huang, J.-K., Hsiao, M.-H., and Cox D.E., "Identification of Linear Stochastic Systems from Closed-Loop Data with known Feedback Dynamics," *Proc. AIAA Structures, Structural Dynamics and Materials Conference*, Hiltonb Head SC., pp. 1619-1627, 1994.
- 13 Phadke, M.S., and Wu, S.M., "Identification of Multi-Input-Multi-Output Transfer function and Noise Model of a Blast Furnace from Closed-Loop Data," *IEEE Trans. AC-19*, 1974, pp. 944-951.
- 14 Mehra R.K., *Trends and Progress in System Identification* by Eykhoff, editor, pp. 305-366, Netherlands, 1981.
- 15 Chen, C.W., Huang, J.-K., Phan, M., and Juang, J.-N., "Integrated System Identification and Modal State Estimation for Control of Flexible Space Structures," *Journal of Guidance, Control and Dynamics*, Vol. 15, No. 1, 1992, pp. 88-95.
- 16 Phan, M., Juang, J.-N., and Longman, R. W., "Identification of Linear Multivariable Systems form a Single Set of Data by Identification of Observers with Assigned Real Eigenvalues," *Journal of Astronautical Science*, Vol. 40, No. 2, 1992, pp. 261-279.
- 17 Phan, M., Horta, L.G., Juang, J.-N., and Longman, R. W., "Linear System Identification via Asymptotically Stable Observer," *Proc. of the AIAA Guidance, Navigation and Control Conference, New Orleans, LA, Aug. 12-14, 1991*, pp. 1180-1194. Also to appear in *Journal of Optimization and Application*.
- 18 Ljung L., Gustavsson I., and Soederstroem T., "Identification of Linear Multivariable Systems Operating under Linear Feedback Control," *IEEE, Transaction on Automatic Control*, Vol. AC-19, No.6, pp. 836 - 840, Dec. 1974.
- 19 Tse E., and Anton J., "On the Identifiability of Parameters," *IEEE Transactions on Automatic Control*, Vol. AC-17, No. 5, pp. 637-646, October 1972.
- 20 Gustavsson I., "Survey of Application of Identification in Chemical and Physical Processes," *Automatica*, Vol. 11, pp. 3-24, 1975.
- 21 Maudsley D., and Anderson J. S., "A Practical Investigation of Statistical Modelling Techniques," *Reprints 5th UKAC Control Convention on Modelling and Simulation for Applied Control Systems*, Bath, England, 1973.
- 22 Williams T. J. and Otto R. E., "A Generalized Chemical Processing Model for the Investigation of Computer Control," *Transaction of the American Institute of Electrical Engineeris*, Vol. 79, No. 11, pp. 458-473, 1960.
- 23 Ross D. W., "Controller Design for Time Lag Systems via a Quadratic Criterion," *IEEE Transaction on Automatic Control*, Vol. AC-16, No. 6, pp. 664-672, Dec. 1971.

- 24 Schoen M. P., Braxton B.K., Gatlin L.A., and Jefferis III, R.P., "A Simulation Model for the Primary Drying Phase of the Freeze-Drying Cycle," *International Journal of Pharmaceutics*, Vo. 114, pp. 159-170, 1995.
- 25 Joshi S. M., *Lectures Notes in Control and Information Science: Control of Large Flexible Space Structures*, Springer Verlag, 1989.
- 26 Uhl, R.R. and F.J. Lewis, "Digital computer calculations of human pulmonary mechanics using a least squares fit technique," *Computers and Biomedical Research*, 7, pp. 489-495, 1974.
- 27 Ferguson, D.R., Mills, R.J., Moran F., Murray-Smith D.J. and Pack A.I., *Estimation of the parameters of the lung model with clinical applications*, Eikhoff P., ed., Identification and System Parameter Estimation. Proc 3rd IFAC Symp., North Holland/American Elsevier Publishing Co., Amsterdam, 1973.
- 28 Grodins F.S., John S., Gray K. R., Schroeder A. L., Noris and Richard W.J., "Respiratory Response to CO₂ Inhalation. A Theoretical Study of a Nonlinear Biological Regulator," *Journal of Applied Physiology*, Vol. 7, pp. 283-308, 1954.
- 29 Horgan J. D., and Lange R. L., "A model of the respiratory control system which includes the effects of cerebrospinal fluid and brain tissue," *Proc. 17th Ann. Conf. on Engineering in Med. and Biol.*, Cleveland, Ohio. 1964, pp. 10.
- 30 Milhorn Howard T.Jr., Benton R., Ross R. and Guyton A. C., "A Mathematical Model of the Human Respiratory Control System," *Biophysical Journal*, Vol. 5, pp. 27-46, 1965.
- 31 Grodins F. S., Buell J., and Bart J., "Mathematical analysis and digital simulation of the respiratory control system," *J. Appl. Physiol.* Vol. 22 (2), pp. 260-276, 1967.
- 32 Sano A., and Kikucki M., "Adaptive control of arterial oxygen pressure of newborn infants under incubator oxygen treatments," *IEEE Proc.*, Vol. 132, Pt.D. No. 5, pp. 205-211, Sept. 1985.
- 33 Allen, R.G.D., *Macro-economic Theory*, Macmillan, 1968.
- 34 Noton, A.R.M., and Ho D.C.C., "A Study of Alternative Policies in the Control of a National Economy via Dynamic Programming," *Economica*, May 1972.
- 35 Desai M., and Henry S.G.B., *Fiscal Policy Simulation for the UK Economy*, The Econometric Study of the United Kingdom, Macmillan, 1970.
- 36 Livesey D.A., "Optimising Short Term Policy," *Economic Journal*, pp. 525-546, 1971.

- 37 Klein L.R., and Goldberger A.S., *An Econometric Model of the United States 1929-1952*, North-Holland, 1955.
- 38 Mahmoud M.S., *Hierarchical Control Policies for Macroeconomic Systems Stabilization*, Simulation of Distributed Parameter and Large-Scale Systems, North-Holland, 1980.
- 39 Zahdeh L. A., "From circuit theory to system theory," *Proc. IRE* 50, pp. 856-865, 1962.
- 40 Yule G.U., "On a method of investigating periodicities in disturbed series, with special reference to Woelfe's sunspot numbers," *Phil. Trans. Royal Soc. (London)*, Vol. A226, 1927, pp. 267-298.
- 41 Sorenson H.W., *Parameter Estimation*, Marcel Dekker Inc., New York, 1980.
- 42 Haykin S., *Adaptive Filter Theory*, Second Edition, Prentice-Hall, Englewood Cliffs, New Jersey, 1991.
- 43 Goodwin, G. C., and Sin, K. S., *Adaptive Filtering, Prediction and Control*, Prentice Hall, Englewood Cliffs, New Jersey, 1984.
- 44 Groom, N. J., Britcher, C.P., "A Description of a Laboratory Model Magnetic Suspension Test Fixture with Large Angular Capability," *Proc. of the IEEE Conference on Control Applications*, Vol. 1, pp. 454, 1992.
- 45 Gunnarsson S., "Frequency Domain accuracy of recursively identified ARX model," *International Journal of Controls*, Vol. 54, No. 2, pp. 465-480, 1991.
- 46 Millnert M., "Identification of ARX models with markovian parameters," *International Journal of Control*, Vol. 45, No. 6, pp. 2045-2058, 1987.
- 47 Karaboyas S., Kalouptsidis N., and Caroubalos C., "Efficient ARX Identification Algorithms with Full Parallelism," *IEEE Trans. on Acoustics, Speech and Signal Processing*, Vol. 38, No. 11, pp. 1902-1913, Nov. 1990.
- 48 Karaboyas S., Kalouptsidis N., "Efficient Adaptive Algorithms for ARX Identification," *IEEE Trans. on Signal Processing*, Vol. 39, No. 3, pp. 571-582, March 1991.
- 49 Mosca E., Zappa G., "ARX Modeling of controller ARMAX Plants and LQ Adaptive Controllers," *IEEE Automatic Control*, Vol. 34, No. 2, pp. 240-242, 1989
- 50 McGraw G. A., Gustafson C. L., Gillis J.T., "Conditions for the Equivalence of ARMAX and ARX Systems," *IEEE Trans. on Automatic Control*, Vol. 38, No. 4, pp. 632-636, April 1993.

- 51 Grewald M. S., and Glover K., "Identifiability of linear and non-linear dynamical systems," *IEEE*, Vol. AC-21, pp. 833-837, 1976.
- 52 Sontag E. D., "On the observability of polynomial systems, I: finite-time problems," *SIAM Journal of Control and Optimization*, Vol. 17, pp. 139-151, 1979.
- 53 Sontag E. D., "On the length of inputs necessary to identify a deterministic linear system," *IEEE*, Vol. AC-25, pp. 120-121, 1980.
- 54 Kalman R. E., *Identifiability and modeling in econometrics*, In Krishnaiah P. R. (Ed.), *Developments in Statistics*, Vol. 4, pp. 97-136. Academic Press, New York, 1983.
- 55 Chen C. T., *Techniques for identification of linear time-invariant multivariable systems*, In C. T. Leondes (Ed.), *Control and Dynamic Systems*, Vol. 26, pp. 1-34. Academic Press, New York, 1987.
- 56 Heij C., "System Identifiability from Finite Time Series," *Automatica*, Vol. 29, No. 4, pp. 1065-1077, 1993.
- 57 Heij C., "Exact Modeling and Identifiability of Linear Systems," *Automatica*, Vol. 28, No. 2, pp. 325-344, 1992.
- 58 Staley R. M. and Yue P. C., "On System Parameter Identifiability," *Information Sciences*, Vol. 2, pp. 127-138, 1970.
- 59 Bellman R., and Astroem K. J., "On Structural Identifiability," *Mathematical Biosciences*, Vol. 7, pp. 329-339, 1970.
- 60 Tse E., and Anton J., "On the Identifiability of Parameters," *IEEE Transactions on Automatic Control*, Vol. AC-17, No. 5, pp. 637-646, October 1972.
- 61 Glover K., and Willems J. C., "Parametrization of Linear Dynamical Systems: Canonical Forms and Identifiability," *IEEE Transactions on Automatic Control*, Vol. AC-19, No. 6, pp. 640-645, December 1974.
- 62 Soederstroem T. Gustavsson I. and Ljung L., "Identifiability conditions for linear systems operating in closed-loop," *International Journal of Control*, Vol. 21, No. 2, pp. 243-255, 1975.
- 63 Correa G. O., and Glover K., "Pseudo-canonical Forms, Identifiable Parametrization and Simple Parameter Estimation for Linear Multivariable Systems: Input-Output Models," *Automatica*, Vol. 20, No. 4, pp. 429-442, 1984.
- 64 Correa G. O., and Glover K., "Pseudo-canonical Forms, Identifiable Parametrization and Simple Parameter Estimation for Linear Multivariable Systems: Parameter Estimation," *Automatica*, Vol. 20, No. 4, pp. 443-452, 1984.

- 65 Gevers M., and Wertz V., "Uniquely Identifiable State-Space and ARMA Parametrization for Multivariable Systems," *Automatica*, Vol. 20, No. 3, pp. 333-347, 1984.
- 66 Swami A., and Mendel J. M., "Identifiability of the AR Parameters of an ARMA Process Using Cumulants," *IEEE Transactions on Automatic Control*, Vol. 37, No.2, pp. 268-273, 1992.
- 67 Von Den Hof P. J., De Vries D. K., and Schoen P., "Delay Structure Conditions for Identifiability of Closed Loop Systems," *Automatica*, Vol. 28, No. 5, pp. 1047-1050, 1992.
- 68 Ljung L., Glad T., "On Global Identifiability for Arbitrary Model Parametrization," *Automatica*, Vol. 30, No. 2, pp. 265-276, 1994.
- 69 Fisher F. M., *The Identification Problem in Econometrics*, McGraw-Hill, New York, 1966.
- 70 Mayne D. Q., "A canonical model for identification of multivariable linear systems," *IEEE Transaction on Automatic Control*, Vol. AC-17, pp. 728-729, 1972.
- 71 Denham M. J., "Canonical forms for the identification of multivariable linear systems," *IEEE Trans. Aut. Control*, AC-19, pp. 646, 1974.
- 72 Hsiao C., *Identification*. In Z. Griliches and M. D. Intriligator (Eds.), *Handbook of Econometrics*, Vol. 1, pp. 223-283. North-Holland, Amsterdam, 1983.
- 73 Gevers M., and Wertz V., *Techniques for the selection of identifiable parameterization for multivariable linear systems*. In C. T. Leondes (Ed.), *Control and Dynamic Systems*, Vol. 26, pp. 35-86. Academic Press, New York, 1987.
- 74 Hannan E. J., and Deistler M., *The Statistical Theory of Linear Systems*, Wiley, New York, 1989.
- 75 Lee R. C. K., *Optimal Estimation, Identification, and Control*, M.I. T. Press, Cambridge, Massachusetts, 1964.
- 76 Hsia T. C., *System Identification: Least-Squares Methods*, Lexington Books, 1977.
- 77 Isermann R., Baur U., Bamberger W., Kneppo P., and Siebert H. "Comparison and Evaluation of six On-line Identification and Parameter Estimation Methods with three simulated Processes," *Proceedings of the 3rd IFAC Symposium on Identification and System Parameter Estimation*, The Hague/Delft, Netherlands, pp. 1081-1102, June, 1973.

- 78 Baur U., Iserman R., "On-Line Identification of a Steam Heat Exchanger with a Process Computer," *Proceedings of the 4th IFAC Symposium on Identification and System Parameter Estimation*, Tbilisi, USSR, pp. 252-293, 1976.
- 79 Abbosh F.G., "Application of Stochastic Approximation to the On-Line Estimation of the Parameters of Noisy Processes," *Proceedings of the 3rd IFAC Symposium on Identification and System Parameter Estimation*, The Hague/Delft, Netherlands, pp. 281-284, June, 1973.
- 80 Levin M. J., "Optimum Estimation of Impulse Response in the Presence of Noise," *IRE Transactions on Circuit Theory*, Vol. CT-7, pp. 50-56, Mar. 1960.
- 81 Goodwin G. C., Murdock J.C., and Payne R.L., "Optimal Test Signal Design for Linear Single-input Single-output System Identification," *International Journal of Control*, Vol. 17, No. 1, pp. 45-55, 1973.
- 82 Mehra R. K., "Optimal Input Signals for Parameter Estimation in Dynamic Systems - Survey and New Results," *IEEE Transaction on Automatic Control*, Vol. AC-19, pp. 753-768, Dec. 1974.
- 83 Astrom K.J., and Wittenmark B., *Adaptive Control*, Addison Wesley, Reading Massachusetts, 1989.

APPENDIX

Selected Matlab Programs for System Identification

```
% ***** sysok.m *****
%
%           November 26. 1996. Marco Schoen
%
%-----
%function [y,u]=sysok(A,B,C,D);
%function [y,u]=sysok(A,B,C,D);
% generate input/output data for okid
% x(k+1)=Ax(k)+Bu(k)
% y(k)=Cx(k)+Du(k)
%load dmodel2.mat;%C=[1 0 1 0 1 0];D=[0];
%C=eye(6);D=zeros(6,1);
%
%-----
%load model.mat:[A,B]=c2d(A1,B1,TS);C=C1:[no,n2]=size(C);n3=0;
%load lung.mat:[A,B]=c2d(A1,B1,TS);C=C1:[no,n2]=size(C);n3=0;
%[n2,ni]=size(B);[no,n2]=size(C);[A1,B1]=d2c(A,B,TS);
%Q=diag([750 750 1000 750 2250
750]);R=eye(ni);[F,S,poll]=lqrd(A1,B1,Q,R,TS);pol=poll';n3=0;
%F=zeros(no,n2);
%
%-----
load dmodel2.mat:[A1,B1]=d2c(A,B,TS);[no,n2]=size(C);
%load lung.mat:[A,B]=c2d(A,B,TS);D1=D;
[n2,ni]=size(B);n1=1:n=n2/2;%C=[1 0 1 0 1 0;2 0 2 0 2 0];[no,n2]=size(C);
%D=[0;0];
%C=eye(n2);[no,n2]=size(C);D=zeros(no,ni);
n3=0;nnc=n2+n3;
%pol=[.9543+.0573i .9543-.0573i .9467+.064i .9467-.064i .9391+.0706i .9391-.0706i];
pol=[.9856+.1628i .9856-.1628i .8976+.4305i .8976-.4305i .8127+.569i .8127-.569i];%
for no controller
%F=zeros(ni,n2);F=place(A,B,pol);
Q=diag([750 750 1000 750 2250
750]);R=eye(ni);[F,S,poll]=lqrd(A1,B1,Q,R,TS);pol=poll';
%
%-----
Ac=[A-B*F];Bc=B;%X=dlyap(Ac,Bc*Bc');X=X(1:n2,1:n2);
X=dlyap(A,B*B');M=sqrt(diag(C*X*C'));%X=sqrt(X);%X=sqrt(diag(X));
Mo=eig(A1);Mc=log(eig(Ac))/TS;%M=sqrt(C*X*C');
M=sqrt(diag(C*X*C'));X=sqrt(diag(X));
[zz,zi]=size(Mc);dam=zeros(zz,1);fre=zeros(zz,1);for i=1:zz;
freq(i,1)=((imag(Mc(i,1))^2)+(real(Mc(i,1))^2))^.5;
```

```

dam(i,1)=cos(atan(imag(Mc(i,1))/real(Mc(i,1)))));end
disp(' cl - roots   frequency [Hz]   damping ratio');
disp([Mc freq dam]);
input('number of data points =');nd=ans;
input('variance of process noise [.01] =');pn=sqrt(ans);pnn=pn*X;
input('variance of measurement noise [.01] =');mn=sqrt(ans);mnn=mn*M;
%input('ARX model order=');q=ans;
x=zeros(n2,nd+1);y=zeros(no,nd);ry=y;rx=x;r=zeros(ni,nd);u=r;
yrr=zeros(no,nd);xrr=x;
for i=1:nd
    ry(:,i)=randn(no,1).*mnn;y(:,i)=C*x(:,i)+ry(:,i);yrr(:,i)=C*xrr(:,i);
    r(:,i)=randn(ni,1);u(:,i)=r(:,i)-F*x(:,i);
    rx(:,i)=randn(n2,1).*pnn;x(:,i+1)=A*x(:,i)+B*u(:,i)+rx(:,i);
    xrr(:,i+1)=x(:,i+1)-rx(:,i);
end;
save datnoise n3 r;
nni=ni*100;i=ni;H=zeros(no,nni);H(:,1:ni)=zeros(no,ni);i=ni;for iw=1:nni
    ini=i+ni;H(:,i+1:i+ni)=C*(A^(iw))*B;i=ini;
end;H=H(:,1:i);
h=0;for k=1:no;for j=1:i;h=h+H(k,j)*H(k,j);end;end;nd1=nd-1;
%okid

% ***** clsysdoc.m *****
%
%           March 24th, 1996, Marco Schoen
%
% -----
% Data generation for the LAM6DOF system, using David Coxe's controller
% design and model(ls_mod6.mat and lqgi_6.mat) and sensor to position
% conversion matrix s2p (s2p.mat), to compare Markov Parameters and
% ARX model parameter.
% -----

load dmodel2.mat;[A1,B1]=d2c(A,B,TS);
[n2,ni]=size(B);n1=1;n=n2/2;C=eye(n2);[no,n2]=size(C);
n3=0;nnc=n2+n3;
pol=[.9543+.0573i .9543-.0573i .9467+.064i .9467-.064i .9391+.0706i .9391-.0706i];
F=zeros(ni,n2);F=place(A,B,pol);
%Q=diag([750 750 1000 750 2250
750]);R=eye(ni);[F,S,poll]=lqrd(A1,B1,Q,R,TS);pol=poll';
Ac=[A-B*F];Bc=B;X=dlyap(Ac,Bc*Bc');X=X(1:n2,1:n2);
Mo=eig(A1);Mc=log(eig(Ac))/TS;M=sqrt(diag(C*X*C'));X=sqrt(diag(X));
[zz,zi]=size(Mc);dam=zeros(zz,1);fre=zeros(zz,1);for i=1:zz;
    freq(i,1)=((imag(Mc(i,1))^2)+(real(Mc(i,1))^2))^0.5;
    dam(i,1)=cos(atan(imag(Mc(i,1))/real(Mc(i,1)))));end
disp(' cl - roots   frequency [Hz]   damping ratio');

```

```

disp([Mc freq dam]);
input('number of data points ='):nd=ans;
input('variance of process noise [.01] ='):pn=sqrt(ans);pnn=pn*X;
input('variance of measurement noise [.01] ='):mn=sqrt(ans);mnn=mn*M;
input('ARX model order='):q=ans;
x=zeros(n2,nd+1);y=zeros(no,nd);ry=y;rx=x;r=zeros(n1,nd);u=r;
Cc=eye(n2);ex=zeros(n2,nd);yrr=zeros(no,nd);xrr=x;
K=zeros(n2,no*nd+2);etha=zeros(n2+n3,nd+1);
for i=1:nd
    ry(:,i)=randn(no,1).*mnn;y(:,i)=C*x(:,i)+ry(:,i);yrr(:,i)=C*xrr(:,i);
    r(:,i)=randn(n1,1);u(:,i)=r(:,i)-F*x(:,i);
    rx(:,i)=randn(n2,1).*pnn;x(:,i+1)=A*x(:,i)+B*u(:,i)+rx(:,i);
    xrr(:,i+1)=x(:,i+1)-rx(:,i);
end;
Q=diag(diag(rx(:,1)*rx(:,1)'));R=diag(diag(ry(:,1)*ry(:,1)'));
P=Q;ex(:,1)=zeros(n2,1);nnu=1;
AcKc=zeros(nnc,no*nd);Abar=zeros(nnc,(nnc)*nd);for i=2:nd;
    P=A*(P-P*(C')*(inv(C*P*(C')+R))*C*P)*A'+Q;
    K(:,nnu:nnu+no-1)=P*C'*(inv(C*P*(C')+R));
    ex(:,i)=(A-A*K(:,nnu:nnu+no-1)*C)*ex(:,i-1)+B*u(:,i-1)+A*K(:,nnu:nnu+no-1)*y(:,i-1);%nnu=nnu+no;
    etha(:,i)=[ex(:,i)];
    AcKc(:,(i-2)*no+1:(i-1)*no)=[A*K(:,nnu:nnu+no-1)-B*F];
    Abar(:,(i-2)*(nnc)+1:(i-1)*(nnc))=[Ac-A*K(:,nnu:nnu+no-1)*C];nnu=nnu+no;
end;Kk=K(:,nnu-no:nnu-1);
figure(1);subplot(3,1,1);mar=nd-999:1:nd;plot(mar,x(1,mar),'-');grid;
title('True state x1');subplot(3,1,2);mar=1:1:nd;plot(mar,ex(1,mar),'-');
grid;title('Estimated State ex1');
subplot(3,1,3);mar=1:no:no*nd;plot(mar,K(1,mar),'-');grid;
title('Kalman Gain');
%figure(2);for j=1:7;subplot(4,2,j);
% mar=1+j:no:(no-1)*nd+j;plot(mar,K(:,mar));grid;end;
%hold;mar=1:no:no*nd;plot(mar,Kk(1,1),'-');hold;
[ba1,ba2]=size(Cc*Abar(:,1:nnc)*AcKc(:,1:no));aclm=zeros(ba1,q*ba2);
[bb1,bb2]=size(Cc*Abar(:,1:nnc)*Bc);bclm=zeros(bb1,q*bb2);
%for k=1:q+1
% aclm(:,(k-1)*ba2+1:k*ba2)=Cc*(Abar(:,(k-1)*(n3+n2)+1:k*(n3+n2))^(k-1))*AcKc(:,(k-1)*no+1:k*no);
% bclm(:,(k-1)*bb2+1:k*bb2)=Cc*(Abar(:,(k-1)*(n3+n2)+1:k*(n3+n2))^(k-1))*Bc;
%end;

AcKck=[A*Kk-B*F];Abark=[Ac-A*Kk*C];
[ba1,ba2]=size(Cc*Abark*AcKck);aclm=zeros(ba1,q*ba2);
[bb1,bb2]=size(Cc*Abark*Bc);bclm=zeros(bb1,q*bb2);
for k=1:q+1
    aclm(:,(k-1)*ba2+1:k*ba2)=Cc*(Abark^(k-1))*AcKck;

```

```

    bclm(:,(k-1)*bb2+1:(k)*bb2)=Cc*(Abark^(k-1))*Bc;
end;
figure(2);
for j=1:no
    subplot(3,3,j);mar=1:1:nd;plot(mar,y(j,mar),' ');grid;xlabel('k');end;
nni=ni*30;i=ni;H=zeros(no,nni);H(:,1:ni)=zeros(no,ni);i=ni;
for iw=1:nni;ini=i+ni;H(:,i+1:i+ni)=C*(A^(iw))*B;i=ini;
end;H=H(:,1:i);
he=0;for k=1:no,for j=1:i,he=he+H(k,j)*H(k,j);end;end;
%Ak=eye(size(a));h=zeros(ni,no*101);h(:,1:no)=d;
%for i=no:no:100*no,h(:,i+1:i+no)=c*Ak*b;Ak=a*Ak;end;
dy=sqrt(diag(ry*ry')/diag(y*y'));dx=sqrt(diag(rx*rx')/diag(x*x'));
yarx=zeros(no,nd);yarxi=zeros(no,nd);
for k=1+q:nd
    for i=1:q
        yarx(:,k)=Cc*(Abark^(i-1))*AcKck*y(:,k-i)+Cc*(Abark^(i-1))*Bc*r(:,k-i);
        yarx(:,k)=yarx(:,k)+yarxi(:,k);
    end;
end;figure(3);
%
plot([q+1:nd],[yarx(1,q+1:nd)],'c-',[q+1:nd],[yrr(1,q+1:nd)],'y');grid;
[cnr,cnr]=size(Cc);Aterm=zeros(cnr,nd+1);
for k=nd:-1:q+1
    for i=1:q
        yarxi(:,k)=aclm(:,(i-1)*ba2+1:i*ba2)*y(:,k-i)+bclm(:,(i-1)*bb2+1:i*bb2)*r(:,k-i);
        yarx(:,k)=yarx(:,k)+yarxi(:,k);
    end;
    Aterm(:,k)=Cc*(Abark^(q))*etha(:,k-q);
end;
figure(4);for j=1:no;subplot(4,2,j);
plot([nd-500:nd],[yarx(j,nd-500:nd)],'c-',[nd-500:nd],[yrr(j,nd-500:nd)],'y--');
grid;end;subplot(4,2,1);title('yarx - & yrr --, no noise');
figure(5);for j=1:no;subplot(4,2,j);
plot([nd-500:nd],[(yarx(j,nd-500:nd)-yrr(j,nd-500:nd))]);grid;end;
subplot(4,2,1);title('yarx-yrr, no noise');
figure(6);for j=1:no;subplot(4,2,j);
plot([nd-500:nd],[(yarx(j,nd-500:nd)-y(j,nd-500:nd))]);grid;end;
subplot(4,2,1);title('yarx-y, with noise');
save dsys A B C Mo Mc TS H y r dy dx Abar rx ry aclm bclm
%tmarco%cliddfc
% y = Cx+v
% yrr = C*xrr xrr=Ax+Bu
% yarx = yarx analytical
% yiarx = y from data

```

```

% ***** okid.m *****
%
% Version December 14, 1995, Marco Schoen
%
% Using okid.m in connection with sys.m to identify LAM6DOF
% System with generated data using constant feedback gain
% controller.
% true state space matrices A B C D, sampling time TS
% true Markov parameters H(no,ni*n);
% N=number of data points
% output data y(no,N); no=number of outputs
% input data u(ni,N); ni=number of inputs
%
% if exist('y')==0,load dsys;end;% use if real data exists
[ni,N]=size(u);[no,N]=size(y);p=no+ni;p1=p-1;
input('order of ARX mode=(0=skip)');
if ans~=0,
    q=ans;input('identify D?(1=yes,0=no)');
    th=arx_bat(y,u,q,ans);
end;
input('number of Markov parameters for ERA=(0=skip)');
if ans~=0
    n=ans;
    np1=n+1;ni1=ni-1;nni=np1*ni;nom1=no-1;nno=np1*no;
    Y11=zeros(no,nni);Y12=zeros(no,nno);
    for i=1:q+1
        i1=i-1;n1=i1*ni+1;n2=n1+ni1; n3=i1*no+1;n4=n3+nom1;
        n11=i1*p+1;n12=n11+ni1;n21=n11+ni;n22=n21+nom1;
        Y11(:,n1:n2)=th(1:no,n11:n12);
        Y12(:,n3:n4)=th(1:no,n21:n22);
    end;
    Y11=markov(Y11,Y12,0,n);Y12=markov(Y12,Y12,1,n);
    if exist('H')==1
        [n1,n2]=size(H);if n2>nni,n2=nni;end;
    else
        subplot(2,1,1)
        hold
    end;
end;
[Ai,Bi,Ci,Di]=eram(Y11,ni,q);
% Ytr... True Markov Parameters, Y11... ARX Markov Parameters,
% Yid... Identified Markov Parameters
Ytr=zeros(n1,ni*30+1);Yi=zeros(n1,ni*30+1);n22=1+ni;for j=1:q;
    Ytr(:,n22:n22+ni1)=C*A^(j-1)*B;Yid(:,n22:n22+ni1)=Ci*A^(j-1)*Bi;n22=n22+ni;
end;
%figure(4);

```

```
%plot([1:q],[Y11(1,1:ni:q*ni)],'y:',[1:q],[Yid(1,1:ni:q*ni)],'c-
',[1:q],[Ytr(1,1:ni:q*ni)],'m--');grid;
%title('Open Loop System Markov Parameters Yarx ..., Yi ..., Ytr --');
```

```
mo=log(eig(Ai))/TS;Mo=log(eig(A))/TS;Ki=kalman(Ai,Ci,Y12,n);
disp('true OL poles      id OL poles');disp([Mo mo]);
err5;
```

```
% ***** clmarco.m *****
```

```
%
```

```
%      December 8., 1995, Marco Schoen
```

```
%
```

```
% Identification of LAM6DOF with a dynamic output feedback controller
% (LQG-Controller), plotting the closed and open loop Markov Parameters
% derived from the ARX model and the ones from the analytical model.
% true state space matrices A B C D and Mo Mc
% sampling time TS
% output data y(no,N); no=number of outputs
% input data r(ni,N); ni=number of inputs
% N=number of data points
```

```
%
```

```
[ni,N]=size(r);[no,N]=size(y);p=no+ni;n3=0;nspm=n3;%[n3,n3]=size(a);no=7;
```

```
input('order of ARX mode=(0=skip)');
```

```
if ans~=0,
```

```
    q=ans;input('identify D(1=yes,0=no)');
```

```
    th=arx_bat(y,r,q,ans);
```

```
end;
```

```
input('number of Markov parameters for ERA=(0=skip)');
```

```
if ans~=0
```

```
    n=ans;
```

```
    np1=n+1;no1=no+1;ni1=ni+1;nom1=no-1;nni=np1*ni;nno=np1*no;
```

```
    Y=zeros(no,nni);N=zeros(no,nno);
```

```
    for i=1:q+1
```

```
        il=i-1;n1=il*ni+1;n2=n1+ni1; n3=il*no+1;n4=n3+nom1;
```

```
        n11=il*p+1;n12=n11+ni1;n21=n11+ni;n22=n21+nom1;
```

```
        Y(:,n1:n2)=th(1:no,n11:n12); N(:,n3:n4)=th(1:no,n21:n22);
```

```
    end;
```

```
    Y=markov(Y,N,0,n);YM1=Y; N=markov(N,N,1,n);NM1=N;
```

```
    [Y,E]=clmarkov(Y,h,n,N);YM2=Y;
```

```
end;
```

```
[Ai,Bi,Ci,Di]=era(Y,ni,q);Ki=kalman(Ai,Ci,E,n);%[Ai,Bi,Ci,Di]=era(Y,no,q);
```

```
mo=log(eig(Ai))/TS;
```

```
if exist('H')~=0
```

```
    [n1,n2]=size(H);Yi=zeros(n1,n2);Ak=eye(size(Ai));Akt=Ak;
```

```
    Yi(:,1:ni)=Di(1:no,1:ni);Ytr=zeros(n1,n2);%Ytr(:,1:ni)=D(1:no,1:ni);
```

```

n2n=n2/ni-1;for i=1:n2n,n3=i*ni+1;Yi(:,n3:n3+ni1)=Ci*Ak*Bi;Ak=Ai*Ak;
Ytr(:,n3:n3+ni1)=C*Akt*B;Akt=A*Akt;end;
Ye=Yi-H;Ye=Ye*Ye'/(H*H');
% figure(1);subplot(2,2,2)
% plot([0:n2n],[Yi(1,1:ni:n2);H(1,1:ni:n2)]');grid;
end;
mo=log(eig(Ai))/TS;disp('true OL poles      id OL poles');
disp([Mo mo]);
% Open loop System Markov Parameters:
% Ytr = analytical M.P., Yi = from identification, YM2 = from ARX derived.
%figure(6);
%plot([1:30],[YM2(1,1:ni:240)],'y',[1:30],[Yi(1,1:ni:240)],'c-
',[1:30],[Ytr(1,1:ni:240)],'m--');grid;
%title('Open Loop System Markov Parameters Yarx ... Yi __, Ytr --');
[ba1,ba2]=size(Cc*Ac*AcKc(:,1:no));
aclm2=zeros(ba1,(q+1)*ba2);bclm2=zeros(bb1,(q+1)*bb2);Ack1=eye(size(Ac));
% Closed Loop System Markov Parameters:
% True Markov Parameters, aclm2=cl. controller Markov Parameters, bclm2=cl. system
M.P.:
for k=1:q
    aclm2(:,(k)*ba2+1:(k+1)*ba2)=Cc*(Ack1)*AcKck;%AcKc(:,(k-1)*no+1:(k)*no);
    Ack1=Ac*Ack1;
    bclm2(:,(k)*bb2+1:(k+1)*bb2)=Cc*(Ac^(k-1))*Bc;
end;aclm2(:,1:ba2)=eye(no);
bclm2(:,1:bb2)=zeros(bb1,bb2);load s2p;
% Identified Markov Parameters:
[aA,bB]=d2c(Ai,Bi,TS);
cC=s2p*Ci;
p=[cC;cC*aA];
Amc=p*aA/p;
Bmc=p*bB;
Cm1=cC/p;Cm=pinv(s2p)*Cm1;Cci=[Cm zeros(no,nspm)];
[Am,Bm]=c2d(Amc,Bmc,TS);
Aci=[Am+Bm*d*Cm Bm*c;b*Cm a];Bci=[Bm;zeros(nspm,ni)];
% calculate AcKc accurately for identified System.
aclmii=zeros(ba1,(q+1)*ba2);bclmii=zeros(bb1,(q+1)*bb2);Ack1=eye(size(Ac));
for k=1:q
    aclmii(:,(k)*ba2+1:(k+1)*ba2)=Cci*(Ack1)*AcKck;%AcKc(:,(k-1)*no+1:(k)*no);
    Ack1=Aci*Ack1;
    bclmii(:,(k)*bb2+1:(k+1)*bb2)=Cci*(Aci^(k-1))*Bci;
end;aclmii(:,1:ba2)=eye(7);
bclmii(:,1:bb2)=zeros(bb1,bb2);
figure(7);
subplot(2,1,1);plot([1:12],[bclm2(1,1:8:96)],'m--
',[1:12],[YM1(1,1:8:96)],'g',[1:12],[bclmii(1,1:8:96)],'c-');grid;
title('Closed Loop System Markov Parameters Yd an. --, Yd dat. ... Yd id. _ ');

```

```

%subplot(2,1,2);plot([1:12],[ac1m2(1,1:7:84)],'m--
',[1:12],[NM1(1,1:7:84)],'g:',[1:12],[ac1mii(1,1:7:84)],'c-.');grid;
%title('Closed Loop Kalman Markov Parameters Nd an. --, Nd dat. ..., Nd id. _');
err3;%figure(5);
%for j=1:ba1;
% for i=1:ba2+1
% subplot(ba1,ba2+1,j*i);plot([1:12],[ac1m2(j,i:7:83+i)]);grid
% end;
%end;
yiarx=zeros(no,nd);yiarxi=zeros(no,nd);
for k=nd:-1:q+1:babab=0;
    for i=1:q
        yiarxi(:,k)=th(:,babab+1:babab+bb2)*r(:,k-
i)+th(:,babab+bb2+1:babab+bb2+ba2)*y(:,k-i);
        yiarx(:,k)=yiarx(:,k)+yiarxi(:,k);babab=babab+ba2+bb2;
    end;
end;
%figure(8);for j=1:no;subplot(4,2,j);
%plot([nd-500:nd],[yiarx(j,nd-500:nd)],'c--',[nd-500:nd],[yrr(j,nd-500:nd)],'y:');
%grid;end;subplot(4,2,1);title('yiarx -- & yrr ..');
% Checking the identified system, by applying same input
[n2,n2]=size(Am);[n3,n3]=size(a);
xii=zeros(n2,nd+1);yi=zeros(no,nd);ui=r;zi=zeros(n3,1);
for i=1:nd
    yi(:,i)=Cm*xii(:,i);
    xii(:,i+1)=Am*xii(:,i)+Bm*u(:,i);
end;
%figure(13);for j=1:no;subplot(4,2,j);
%plot([q+1:100],[yiarx(j,q+1:100)],'r--
',[q+1:100],[yarx(j,q+1:100)],'y:',[q+1:100],[y(j,q+1:100)],'b-.');
%grid;end;subplot(4,2,1);title('yiarx --, yarx .. y _');
epsilon=y-C*ex;
%figure(14);for j=1:no;subplot(4,2,j);
%plot([q+1:nd],[Aterm(j,q+1:nd)],'m:',[q+1:nd],[epsilon(j,q+1:nd)],'c-.');
%grid;end;subplot(4,2,1);title('Aterm ..., Eps _');
%plot([q+1:100],[yiarx(j,q+1:100)],'c-
',[q+1:100],[yarx(j,q+1:100)],'y:',[q+1:100],[yi(j,q+1:100)],'r:',[q+1:100],[y(j,q+1:100)],
'b--');
%grid;end;subplot(4,2,1);title('yiarx -, yarx .. yi o');
if yarx=100%, what is the percent error deviation of yarx-yiarx
% F-Norm:
%[col,row]=size(yarx);nume=0;denu=0:error=0;
%for k=1:col;
% for t=row-100:row
% nume=nume+(yarx(k,t)-yiarx(k,t))*(yarx(k,t)-yiarx(k,t));
% denu=denu+(yarx(k,t)*yarx(k,t));

```

```

% end;
%end;
%error=sqrt(num)/sqrt(denu)*100;
% 2-Norm:
%num=0;den=0;error2=0;
%num=norm((yax(:,row-100:row)-yiarx(:,row-100:row)),2);den=norm((yax(:,row-
100:row)),2);
%error2=num/den*100;
%disp(sprintf('Percentage of error dev. of y(arx) and y(i,arx), F-Norm: =%g',error));
%disp(sprintf('Percentage of error dev. of y(arx) and y(i,arx), 2-Norm: =%g',error2));
% if y anal. = 100%, what is the percent error deviation of y-yiarx
% F-Norm:
%[col,row]=size(yax);num=0;denu=0;error=0;
%for k=1:col;
% for t=row-100:row
%  num=num+(y(k,t)-yiarx(k,t))*(y(k,t)-yiarx(k,t));
%  denu=denu+(y(k,t)*y(k,t));
% end;
%end;
%error=sqrt(num)/sqrt(denu)*100;
% 2-Norm:
%num=0;den=0;error2=0;
%num=norm((y(:,row-100:row)-yiarx(:,row-100:row)),2);den=norm((y(:,row-
100:row)),2);
%error2=num/den*100;
%disp(sprintf('Percentage of error dev. of y and y(i,arx), F-Norm: =%g',error));
%disp(sprintf('Percentage of error dev. of y and y(i,arx), 2-Norm: =%g',error2));

% if y anal. = 100%, what is the percent error deviation of y-yarx
% F-Norm:
%[col,row]=size(yax);num=0;denu=0;error=0;
%for k=1:col;
% for t=row-100:row
%  num=num+(y(k,t)-yarx(k,t))*(y(k,t)-yarx(k,t));
%  denu=denu+(y(k,t)*y(k,t));
% end;
%end;
%error=sqrt(num)/sqrt(denu)*100;
% 2-Norm:
%num=0;den=0;error2=0;
%num=norm((y(:,row-100:row)-yarx(:,row-100:row)),2);den=norm((y(:,row-
100:row)),2);
%error2=num/den*100;
%disp(sprintf('Percentage of error dev. of y and y(arx), F-Norm: =%g',error));
%disp(sprintf('Percentage of error dev. of y and y(arx), 2-Norm: =%g',error2));
% error of the mean:

```

```

% statistics about y
%mty=mean(mean(y'));%sty=std(y');
%disp(sprintf('Mean of y: =%g',mty));
% statistics about yarx
%mtyarx=mean(mean(yarx'));%styarx=std(yarx');
%disp(sprintf('Mean of yarx: =%g',mtyarx));
% statistics about yiarx
%mtyiarx=mean(mean(yiarx'));%styiarx=std(yiarx');
%disp(sprintf('Mean of yiarx: =%g',mtyiarx));
%for i=1:no
% for j=1:no
%   y_yiarxv=corrcoef(y(j,:),yiarx(i,:));y_yiarx(j,i)=y_yiarxv(1,2);
%   y_yarxv=corrcoef(y(j,:),yarx(i,:));y_yarx(j,i)=y_yarxv(1,2);
%   y_yrrv=corrcoef(y(j,:),yrr(i,:));y_yrr(j,i)=y_yrrv(1,2);
%   yarx_yiarxv=corrcoef(yarx(j,:),yiarx(i,:));yarx_yiarx(j,i)=yarx_yiarxv(1,2);
% end;
%end;
%yyiarx=diag(y_yiarx);
%yyarx=diag(y_yarx);
%yyrr=diag(y_yrr);
%yarxyiarx=diag(yarx_yiarx);
%disp('correlation of y,yiarx, y1-yiarx1, y2-yiarx1...');
%disp([yyiarx]);
%figure(15);for j=1:ni:subplot(4,2,j);
% psd(r(j,:),256,1/TS,hanning(256),128,'none');
%grid;ylabel(' ');xlabel(' ');grid;end;subplot(4,2,1);
%title('Power Spectrum Estimate of r');

```

```

% ***** ides.m *****
%
%           February 20, 1997 Marco P. Schoen
%
%

```

```

% Iterative ARX modeling for improved system identification.
% 1. estimated ARX model coefficient {ai,bi}
% 2. Form parameter matrices Av and Om
% 3. Load y old
% 4. Computer vk=-Om^-1*Av*w
% 5. at t=k-q-1: uk-3, .. uk-q=f(Om, Av, yk-2,...,yk-q)
% 6. used data obtained in step 5 to perform new SI: {ai, bi}=f(u,y)
%

```

```

% 1. Data generation and System identification
clsysdocar;
okidar;
th=arx_bat(y,u,q,0);figure(1);uorg=u;yorg=y;
% 2. Parameter formation Av and Om
Avl=zeros(no*q,no*q);Oml=zeros(no*q,ni*q);
for k=nd:-1:q+1:babab=0;
    for i=1:q
        Avl((i-1)*ba2+1:i*ba2,(i-1)*ba2+1:i*ba2)=th(:,babab+bb2+1:babab+bb2+ba2);
        Oml((i-1)*ba2+1:i*ba2,(i-1)*bb2+1:i*bb2)=th(:,babab+1:babab+bb2);
        babab=babab+ba2+bb2;
    end;
end;
input('New ARX model order =');q2=ans;
Av=Avl((q2)*no+1:q*no,(q2)*no+1:q*no);
Om=Oml((q2)*no+1:q*no,(q2)*ni+1:q*ni);

% 3. Load original output and determine what input it should be
wyl=zeros(no*q,1);vul=zeros(ni*q,1);%vu2=zeros(ni*nd,1);%u2=u;
for i=nd:-q:q+1;%nd-fix(nd/q)*(q-1)+1;
    for p=1:q
        wyl(((p-1)*no+1):(p*no),:)=y(:,i-p);
        vul((p-1)*ni+1:p*ni,1)=u(:,i-p);
    end;
wy=wyl(q2*no+1:q*no,1);
%vu(q2*ni+1:q*ni,1)=-pinv(Om)*Av*wy;
vu=-pinv(Om)*Av*wy;
vu2=[vul(1:q2,:);vu];
for p=1:q
    u2(:,i-p)=vu2((p-1)*ni+1:p*ni,1);
end;
%vu2(i-q*ni+1:i,1)=[vul(1:q2*ni,1);vu(q2*ni+1:q*ni,1)];
end;uorg=u;

% 4. Estimate new ARX model parameters and check goodness
%u3=u2;
clsysdocar3;
okidar2;
th=arx_bat(y,u,q,0);
figure(2);%for j=1:no;subplot(2,1,j);
subplot(2,1,1);
plot([1:nd],[yorg(1,:)]);% 'c--',[nd-500:nd],[y(j,nd-500:nd)],'y-');
grid;title('Original Output y');
xlabel('Time index k');
ylabel('Magnitude');
subplot(2,1,2);

```

```

plot([1:nd],[y(1,:)]);
grid;title('Corrected Output y');
xlabel('Time index k');
ylabel('Magnitude');
figure(3);%for j=1:no:subplot(2,1,j):
subplot(2,1,1);
plot([1:nd],[uorg(1,:)]);% 'c--',[nd-500:nd],[y(j,nd-500:nd)],'y-');
grid;title('Original Input u');
xlabel('Time index k');
ylabel('Magnitude');
subplot(2,1,2);
plot([1:nd],[u(1,:)]);
grid;title('Corrected Input u');
xlabel('Time index k');
ylabel('Magnitude');

```